



**This electronic thesis or dissertation has been
downloaded from Explore Bristol Research,
<http://research-information.bristol.ac.uk>**

Author:

Ockenden, Amy R O

Title:

Investigating The Effects Of Titanium Nanoparticles On Freshwater Benthic Algae

General rights

Access to the thesis is subject to the Creative Commons Attribution - NonCommercial-No Derivatives 4.0 International Public License. A copy of this may be found at <https://creativecommons.org/licenses/by-nc-nd/4.0/legalcode>. This license sets out your rights and the restrictions that apply to your access to the thesis so it is important you read this before proceeding.

Take down policy

Some pages of this thesis may have been removed for copyright restrictions prior to having it been deposited in Explore Bristol Research. However, if you have discovered material within the thesis that you consider to be unlawful e.g. breaches of copyright (either yours or that of a third party) or any other law, including but not limited to those relating to patent, trademark, confidentiality, data protection, obscenity, defamation, libel, then please contact collections-metadata@bristol.ac.uk and include the following information in your message:

- Your contact details
- Bibliographic details for the item, including a URL
- An outline nature of the complaint

Your claim will be investigated and, where appropriate, the item in question will be removed from public view as soon as possible.

Investigating The Effects Of Titanium Nanoparticles On Freshwater Benthic Algae

Amy Ockenden



Online graphic illustration of a variety of diatoms (not scientifically accurate) by Amy Ockenden

A dissertation submitted to the University of Bristol in accordance with the requirements for award of the degree of Masters by Research in the Faculty of Life Sciences, School of Biological Sciences, 2019.

Word count: c., 28,500

Abstract

Background

Titanium dioxide nanoparticles (n-TiO₂s) possess a range of unique physico-chemical properties, which makes them differ greatly from their bulk counterparts. These unique properties make them highly desirable, and they are used in a broad range of cosmetic, textile and medical products. Increasing consumer demands are expected to drive worldwide production up to 2.5 million tonnes/year by 2025. The amount of n-TiO₂s entering freshwater bodies is increasing, causing concerns about the potential toxic impacts on freshwater biota, including microalgae. Previous studies have shown that freshwater algae are negatively affected by the presence of n-TiO₂s, however, most of this research has focused on the effects on green, planktonic algal species. Due to the high sedimentation rate of n-TiO₂s, the benthic sediment may be a temporary repository, and benthic algae may be more at risk of n-TiO₂ exposure.

Aims and Methods

The main aim of this thesis was to investigate the impacts of n-TiO₂ on benthic freshwater algae. The two main objectives were **i)** to quantify the impacts of n-TiO₂s on the growth and photophysiology on a single species benthic diatom, *Nitzschia palea* and **ii)** to quantify the impacts of n-TiO₂s on the biomass, photophysiology and species composition of whole benthic biofilm communities in outdoor artificial mesocosms using river water from the River Frome (Dorset, UK).

Results

Increasing n-TiO₂ concentration exerted an acute toxic effect on benthic algae. Exposure to n-TiO₂ negatively impacted the growth and photophysiology of *N. palea* in the laboratory and negatively impacted the photophysiology and pigment concentration of biofilm communities in the field. Negative impacts were more pronounced in the field, as biofilms were impacted by lower n-TiO₂ concentrations, suggesting *N. palea* may be a relatively tolerant species. Negative effects, both in the laboratory and field, were less pronounced after 72 hours.

Implications

This research confirms that n-TiO₂s negatively impact benthic algal communities and highlights the need for extensive testing of n-TiO₂ on benthic species. The use of mesocosm experiments in nanotoxicology is vital for understanding the toxicity impacts in the field, which may be under-estimated in the laboratory due to field conditions potentially altering the toxicity of n-TiO₂s. Due to the variability in algal response to n-TiO₂ throughout the literature, future research should consider how methodological variations can change the toxicity profile of n-TiO₂s, leading to the production non-comparable and non-reproducible data.

Dedication and Acknowledgements

I would like to dedicate this research to the following people and organisations...

To my primary supervisor, **Professor Marian Yallop** - I would like to emphasize my sincere appreciation for your supervision throughout this masters. You have taught me new scientific techniques, provided excellent feedback and advice, and most importantly, you have inspired a future in freshwater ecotoxicology.

To my mum, **Claire** - thank you for making this research all possible. Your emotional and financial support throughout this masters has been incredible. You have always made me feel relaxed at home when I have needed a break from my studies, and from Bristol. Your positive outlook on life has reflected in my studies, and I am so grateful.

To my grandparents, **Barbara** and **Rodney** - thank you for always showing massive amounts of interest in my work, and always offering to read through sections of my thesis, and giving me advice on spelling and grammar! Your interest in my research has filled me with joy and confidence. Thank you also for letting me use your beautiful home as a writing retreat.

To my younger brother, **Toby** - thank you for making me smile and laugh throughout the last year and a half, your happiness and jokes has made writing up this thesis so much easier.

To my dad, **Keith** - thank you for supporting me throughout University, your help and support throughout my undergraduate degree, allowed me to progress into research.

To my secondary supervisor, **Professor Gary Barker** - thank you for always providing me with help and advice when I needed it.

To the **Freshwater Biological Association (FBA)** - thank you for allowing me to use your on-site resources for field work.

To members in my lab group, **Dr Kelly Atkins** and **Dan Fagan** - thank you both for all your support and providing me with all the relevant training I needed to complete this research.

To my friends, - Thank you to **all my friends** that have supported me and made sure I took a healthy number of breaks when writing up. Specifically, thank you too **Laura Case**, **Kelly-Louise Ray**, **Lizzie Senior**, **Jacob Povey** and **Jonathan Girt** for being amazing friends, and allowing me to escape the thesis from time to time.

To **Sam Smithers** and **Sam Huguet** - thank you for allowing me to stay with you whilst writing up, the surrounding environment has been so much nicer with you guys around. It has been so much easier being able to write up here in Bristol, and I am so grateful for your kindness.

To my best friends, **Benito Wainwright**, **Sam South** and **Tom Timberlake** - thank you

for always boosting my confidence during setbacks, dealing with my negativity from time to time, reading my thesis endlessly, and just being amazing people. So much love.

Last but definitely not least, I would like to thank my doggo, **Jack** - for providing me with love and cuddles throughout.

This research was partly supported by the NERC grant, (NE/N006518/1): 'Multimodal characterization of nanoparticles in the environment.'

Author's Declaration

I declare that the work in this dissertation was carried out in accordance with the requirements of the University's Regulations and Code of Practice for Research Degree Programmes and that it has not been submitted for any other academic award. Except where indicated by specific reference in the text, the work is the candidate's own work. Work done in collaboration with, or with the assistance of, others, is indicated as such. Any views expressed in the dissertation are those of the author.

SIGNED: DATE:.....

Contents

1	Introduction	1
1.1	Types of engineered nanoparticles (ENPs)	2
1.2	Titanium dioxide nanoparticles (n-TiO ₂ s)	3
1.2.1	Particle Size	3
1.2.2	Crystalline Structure	4
1.3	Fate of ENPs in the environment	4
1.3.1	The entry of ENPs into the aquatic environment	4
1.3.2	Fate and behaviour of ENPs in the aquatic environment	5
1.3.3	The influence of pH on the properties and behaviour of titanium dioxide nanoparticles in aqueous media	5
1.3.4	The influence of ionic strength (IS) on the properties and behaviour of titanium dioxide nanoparticles in aqueous media	6
1.3.5	The influence of natural organic matter (NOM) on the properties and behaviour of titanium dioxide nanoparticles in aqueous media	7
1.3.6	The influence of extracellular polymeric substances (EPS) on the properties and behaviour of titanium dioxide nanoparticles in aqueous media	7
1.4	Regulations for the production, toxicity testing and evaluation of ENPs	8
1.5	Variation in toxicity testing protocols for microalgae	9
1.6	Evidence of toxicity of n-TiO ₂ s to freshwater microalgae	11
1.6.1	Particle Composition and Size	12
1.6.2	Growth Medium	12
1.7	Freshwater benthic biofilms and their uses as bio-indicators of water quality	15

1.7.1	The importance of biofilms and benthic diatoms in water quality assessment	15
1.7.2	Freshwater biofilms for measuring the impacts of ENPs	16
1.8	Knowledge gaps and aims of thesis	17
1.8.1	Knowledge gaps	17
1.8.2	Aims of thesis	18
1.9	Thesis Outline	18
2	The impacts of n-TiO₂ on freshwater benthic diatom <i>Nitzschia palea</i>	20
2.1	Introduction	21
2.1.1	The importance of testing the impacts of ENPs on benthic diatoms . .	21
2.1.2	The impacts of ENPs on benthic diatoms	22
2.1.3	The OECD Freshwater Alga and Cyanobacteria Growth Inhibition Test: A guide for ENP toxicity testing	22
2.1.4	The rationale for selecting <i>Nitzschia palea</i> as a possible test species for evaluating n-TiO ₂ toxicity on benthic diatoms	25
2.2	Aims of study	25
2.3	Methods	26
2.3.1	Specimen collection and maintenance	26
2.3.2	Titanium dioxide nanoparticle (n-TiO ₂) characterization	28
2.3.3	Preparation of the titanium dioxide nanoparticles (n-TiO ₂ s)	28
2.3.4	Experimental set-up	29
2.3.5	Cell growth analysis	29
2.3.6	Pulse amplitude modulated (PAM) fluorometry	31
2.3.7	Imaging Diatom Cells	32
2.3.8	Statistical analysis	32
2.4	Results	33
2.4.1	Titanium dioxide nanoparticle (n-TiO ₂) characteristics	33
2.4.2	The impact of an increasing n-TiO ₂ exposure concentration on the the growth of <i>Nitzschia palea</i>	35

2.4.3	The impact of an increasing n-TiO ₂ exposure concentration on the photophysiology of <i>Nitzschia palea</i>	38
2.4.4	Imaging diatom cells using light microscopy	45
2.4.5	Summary of results	45
2.5	Discussion	46
2.5.1	The effect of n-TiO ₂ exposure on the growth of the freshwater diatom, <i>Nitzschia palea</i>	46
2.5.2	The effect of n-TiO ₂ on the photophysiology of <i>Nitzschia palea</i>	50
2.5.3	Limitations and caveats of study	52
2.5.4	Conclusion	52
3	The impacts of n-TiO₂ on riverine biofilm assemblages	54
3.1	Introduction	55
3.1.1	The roles of benthic biofilms in freshwater ecosystems	55
3.1.2	The diatom fraction of freshwater biofilms	55
3.1.3	The use of artificial mesocosms to study biofilm functioning in freshwater environments	56
3.1.4	The impact of titanium dioxide nanoparticles (n-TiO ₂ s) on freshwater biofilms	57
3.2	Aims of study	58
3.3	Methods	59
3.3.1	Study site and environmental data	59
3.3.2	Experimental design	60
3.3.3	Experimental set-up	62
3.3.4	Mesocosm water properties	62
3.3.5	Biofilm sampling	63
3.3.6	Chlorophyll pigment extraction	63
3.3.7	Dry mass	65
3.3.8	Pulse amplitude modulated (PAM) fluorometry	65
3.3.9	Diatom cleaning and species identification	65

3.3.10	Statistical analysis	66
3.4	Results	67
3.4.1	Mesocosm water properties and local weather data	67
3.4.2	Changes in the periphytic biomass of benthic biofilms following the application of n-TiO ₂	68
3.4.3	Diatom species composition	71
3.4.4	Changes in the photophysiology of riverine biofilms following n-TiO ₂ exposure	74
3.4.5	Summary of results	81
3.5	Discussion	81
3.5.1	The effects of n-TiO ₂ on the biomass of riverine biofilm assemblages .	81
3.5.2	The effects of n-TiO ₂ on the diatom species composition of riverine biofilm assemblages	83
3.5.3	The effects of n-TiO ₂ on the photophysiology of riverine biofilm as- semblages	85
3.5.4	Limitations and caveats of study	86
3.5.5	Conclusion	87
4	Synthesis and future recommendations	88
4.1	Do results from investigating n-TiO ₂ impacts on a single species diatoms, <i>N. palea</i> , tell a similar story to the results from investigating the impacts of n-TiO ₂ on whole riverine biofilm assemblages in the field?	89
4.2	Problems with evaluating the impacts of ENPs using the OECD Freshwater Alga and Cyanobacteria Growth Inhibition Test	91
4.3	Future recommendations for testing the impacts of n-TiO ₂ s in the field	93
4.4	The larger scale impacts of n-TiO ₂ pollution on the world's water bodies . . .	94

List of Figures

1.1	The classification of nanoobjects	2
1.2	The effect of increased ionic strength on nanoparticle homoaggregation	6
2.1	Raman spectra of n-TiO ₂	33
2.2	EDS element phase map of n-TiO ₂ sample	34
2.3	Growth curve of <i>Nitzschia palea</i> exposed to n-TiO ₂ over a period of 72 hours	35
2.4	Average growth rate inhibition (GI%) of <i>Nitzschia palea</i> exposed to n-TiO ₂ over a 72-hour period	37
2.5	Rapid light curve of <i>Nitzschia palea</i>	39
2.6	The impact of n-TiO ₂ on the <i>Fv/Fm</i> of <i>Nitzschia palea</i>	40
2.7	The impact of n-TiO ₂ on the (α) of <i>Nitzschia palea</i>	41
2.8	The impact of n-TiO ₂ on the rETR _m of <i>Nitzschia palea</i>	43
2.9	The impact of n-TiO ₂ on the E _k of <i>Nitzschia palea</i>	44
2.10	Light microscopy image showing aggregations of n-TiO ₂ on the cell surface of <i>Nitzschia palea</i>	45
3.1	Map of the River Frome and the surrounding catchment areas	60
3.2	Artificial mesocosm set-up for experiment	61
3.3	The impact of n-TiO ₂ on the total chlorophyll of riverine biofilm assemblages	69
3.4	The impact of n-TiO ₂ on the dry mass of riverine biofilm assemblages	71
3.5	Axis 1 and Axis 2 of NMDS, based on relative abundances of diatoms grown in riverine biofilm assemblages	74
3.6	Rapid light curves produced from riverine biofilm assemblages at 24 and 72 hours	75
3.7	The impact of n-TiO ₂ on the <i>Fv/Fm</i> of riverine biofilm assemblages	76

3.8	The impact of n-TiO ₂ on the (α) of riverine biofilm assemblages	77
3.9	The impact of n-TiO ₂ on the rETR _m of riverine biofilm assemblages	78
3.10	The impact of n-TiO ₂ on the E _k of riverine biofilm assemblages	80

List of Tables

1.1	Summary of studies investigating n-TiO ₂ impacts on freshwater algae	14
2.1	Elemental composition of OECD media.	27
2.2	Definitions of photosynthetic parameters	32
2.3	Weight ratios of chemical elements found in the n-TiO ₂ power sample	34
2.4	Daily growth rates of <i>Nitzschia palea</i>	36
3.1	Environmental parameters in stream mesocosm river water	68
3.2	The amount and ratios of chlorophyll pigments in riverine biofilm assemblages at each treatment	70
3.3	Species composition, relative abundance and Spearman's Rank Correlation coefficient for riverine biofilm assemblages in each treatment	73

List of Equations

2.1 Growth Rate Equation	30
2.2 Growth Inhibition Equation	30
2.3 Fv/Fm Equation	32
3.1 Total Chlorophyll Equation	64
3.2 Chlorophyll a Equation	64
3.3 Chlorophyll b Equation	64
3.4 Chlorophyll c Equation	64

CHAPTER 1

An Introduction To Engineered Nanoparticles (ENPs) with specific focus on titanium dioxide (TiO₂)

1.1 Types of engineered nanoparticles (ENPs)

An object that is defined as "nanoscale" denotes one that has a size range spanning 1-100 nm. The International Organization for Standardization (ISO) classifies nanoobjects into three categories depending on the number of dimensions at the nanoscale (**Figure 1.1**). The focus of this research is on nanoparticles (NPs), which are defined as particles with a size range of 1-100 nm, possessing three outer dimensions at the nanoscale.

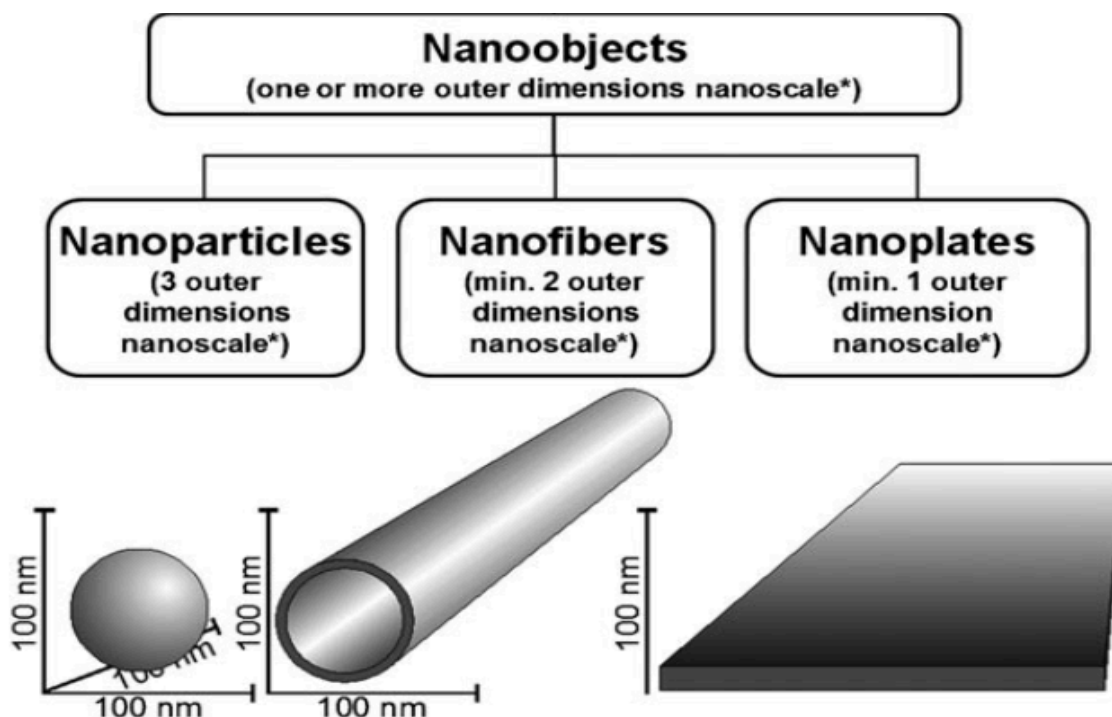


Figure 1.1: The classification of nanoobjects into three separate categories depending on the number of dimensions at the nanoscale. Nanoobjects can include nanoparticles (3 outer dimensions), nanofibers (2 outer dimensions) and nanoplates (1 outer dimension). Diagram taken and adapted from Krug & Wick (2011).

In the natural environment, NPs are present in clays, organic matter and iron oxides, and play important roles in biogeochemical processes (Maurer-Jones *et al.*, 2013; Bakshi *et al.*, 2015). Artificial manufacture of NPs is also common, and industrial output greatly outweighs the volume of naturally-occurring NPs (Klaine *et al.*, 2008). Man-made NPs are termed "engineered nanoparticles" (ENPs) and they can be classified based on their

morphological, physical and chemical properties (Khan *et al.*, 2017). Some common classes of ENPs include: carbon-based, metal, ceramic, semi-conductor, polymeric and lipid ENPs (Khan *et al.*, 2017). One of the most prevalent groups of ENPs are the metal oxides (e.g. TiO_2 , Ag_2O , ZnO); their physico-chemical properties such as size, surface area, shape and chemical composition differ greatly from their bulk counterparts (Gatoo *et al.*, 2014). These physico-chemical transformations at the nano-scale offer a range of desirable properties, such as a high surface area:volume ratio (SA:V), which may enhance their photocatalytic activity, and therefore artificially derived ENPs are increasingly being used in a broad range of consumer products, including cosmetics and medicines (De Jong & Borm, 2008; Raj *et al.*, 2012; Zhang *et al.*, 2015).

1.2 Titanium dioxide nanoparticles (n-TiO₂s)

1.2.1 Particle Size

This thesis focuses on the potential toxic effects of n-TiO₂; this particular ENP was selected because they are one of the most frequently manufactured ENPs worldwide, with 10,000 tonnes produced per year (Piccino *et al.*, 2012; Vance *et al.*, 2015). The production of n-TiO₂ is expected to increase to 2.5 million tonnes by 2025 (Mezni *et al.*, 2018), so it is likely that the release of n-TiO₂s into surrounding environments, including freshwater bodies, will increase. It is also important to question the potential toxic effects of n-TiO₂s because the fine particles (particles with a size of 100 nm-3000 nm) of TiO₂ are often reported to possess low toxicity (Shi *et al.*, 2013; Warheit & Brown, 2019), and therefore they are regularly used in biomedical applications. They have even been used as negative controls in toxicological studies (Shi *et al.*, 2013). However, when these particles become 'nano-scale', the toxic profile of the particles is likely to change. The smaller size of ENPs compared to fine particles, leads to an increased SA:V ratio, meaning there are more atoms on the particle surface (Fu *et al.*, 2015). When irradiated with ultra-violet (UV) light, electron hole pairs are produced which gives the n-TiO₂ photocatalytic properties (Fu *et al.*, 2015). This photocatalytic ability renders them highly reactive, causing increased aggregation with other ENPs (homoaggregation) and biological cells (heteroaggregation) (Ju-Nam & Lead,

2008).

1.2.2 Crystalline Structure

The three dominant crystalline phases of n-TiO₂ are anatase, rutile and brookite. A mixture of both anatase and rutile typically make up the n-TiO₂s that are used in industry (Shah *et al.*, 2017), each phase providing desirable commercial characteristics. Higher proportions of anatase in ENPs for example, provides high photocatalytic ability (Mahmoud *et al.*, 2017) and the rutile crystalline phase is used in paint as a white pigment (Cassaignon *et al.*, 2007). These characteristics give them a myriad of desirable traits that are exploited by cosmetic, medical and textile industries. Cosmetic brands are responsible for 50-80% of n-TiO₂ production (Piccino *et al.*, 2012); they are used in commercial sunscreens, taking advantage of the practical property of blocking damaging UV radiation along with the cosmetic benefit of staying transparent when applied to human skin (Kessler, 2011). They are also valuable in medicine, possessing useful bacteriacidal properties (Jesline *et al.*, 2014). In the textile industry, they have been used as a paint additive due to their self-cleaning features (Smulders *et al.*, 2014). Also, n-TiO₂s have environmental benefits, as they have been found useful in environmental bioremediation techniques, such as the sequestration of nutrients (Bessa da Silva *et al.*, 2016).

1.3 Fate of ENPs in the environment

1.3.1 The entry of ENPs into the aquatic environment

As consumer demand continues to grow, the production of consumer items containing ENPs is escalating. Accordingly, increasing amounts of ENPs are being released into the environment, including freshwater ecosystems. Freshwater environments are predominantly exposed to ENPs through leaching of degraded consumer products from agricultural run-off, sewage treatment plants and industrial sources (Shevlin *et al.*, 2018). In particular, n-TiO₂s are indirectly released into water bodies by spraying sunscreens and aerosols, and through drainage of rainwater containing ENPs found in commercial paints (Zhang *et al.*, 2015).

ENPs can also be deliberately introduced into an aquatic system through environmental remediation techniques (Bessa da Silva *et al.*, 2016).

Measuring and characterizing ENPs in the aquatic environment is challenging (Luo *et al.*, 2014), as straightforward analytical methods are unavailable. One approach to overcome this has been the application of computer models to predict environmental concentrations (Bundschuh *et al.*, 2018). It is notoriously difficult to predict actual concentrations, because the distribution of ENPs in water systems is uneven, with the highest concentrations found in areas of highest human activity, such as near-shore waters and sampling effort has been very patchy and not wide-spread (Gottschalk & Nowack, 2011). Modeled environmental concentrations of ENPs show that n-TiO₂ had the highest concentration relative to other ENPs in the soil, sediment and sewage treatment plants in Europe and the US (Gottschalk *et al.*, 2009). Mueller & Nowack (2008) estimated predicted environmental concentration (PEC) values for n-TiO₂ in water in Switzerland and suggested that concentrations could be up to 16 µg/l.

1.3.2 Fate and behaviour of ENPs in the aquatic environment

The fate of ENPs in aquatic systems (i.e. in which zone of the water body the ENPs will end up) is dependent on, predominantly, the degree of ENP aggregation. Understanding the aggregation status of ENPs requires knowledge on physico-chemical properties of both the ENPs and the media in which they are immersed. Properties of ENPs such as size and surface charge can change when presented with changes in ionic strength (IS), natural organic matter (NOM) and pH (Dunphy-Guzman *et al.*, 2006; French *et al.*, 2009; Zhu *et al.*, 2014; Xu, 2018).

1.3.3 The influence of pH on the properties and behaviour of titanium dioxide nanoparticles in aqueous media

The effect of pH on the behaviour of n-TiO₂s in aqueous media has been frequently studied (Dunphy-Guzman *et al.*, 2006; French *et al.*, 2009; Hu *et al.*, 2018; Tang & Cheng,

2018). The degree of homoaggregation is determined by the difference between the pH of the media and the pH_{pzc} of the ENPs (pzc = point zero charge). As the medium pH approaches the pH_{pzc} of n-TiO₂ (pzc of n-TiO₂ = 6) (Zhu *et al.*, 2014) the particles tend to aggregate more easily.

1.3.4 The influence of ionic strength (IS) on the properties and behaviour of titanium dioxide nanoparticles in aqueous media

An increase in ionic strength (IS) has been found to increase homoaggregation through compression of the double electric layer (**Figure 1.2**), meaning the Van Der Waals attractive forces will increase (Danielsson *et al.*, 2017), overcoming the electrostatic repulsion between objects that are similar in charge (Navarro *et al.*, 2008). Evidence of enhanced homoaggregation under high IS levels has been recorded multiple times (Doyle *et al.*, 2014; Lin *et al.*, 2017; Wang *et al.*, 2018). He *et al.* (2015) showed that under 0.01 mM KCl, the sedimentation efficiency of n-TiO₂ was 20% after 4 hours, increasing to 70% under 100 mM KCl. This effect of enhanced homoaggregation under high IS conditions has also been observed in the field, where comparisons of four lakes showed n-TiO₂ homoaggregation to be highest in brackish waters (high IS) (Li *et al.*, 2016).

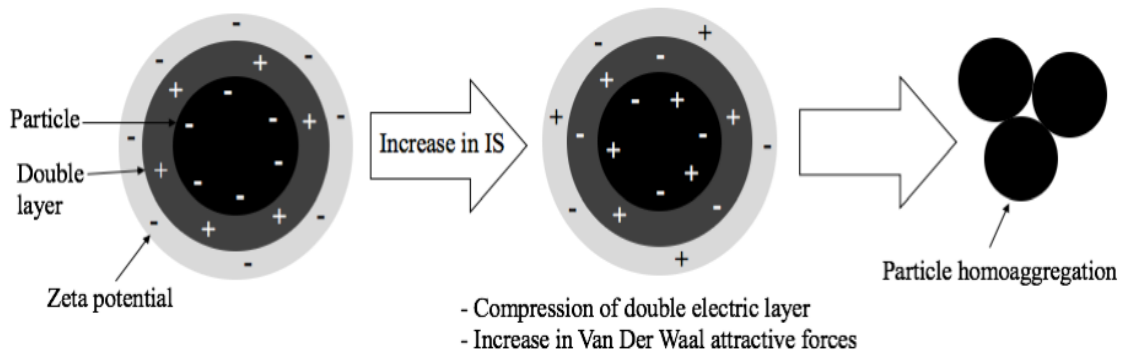


Figure 1.2: Schematic diagram of the effects of increased ionic strength (IS) on a n-TiO₂ particle. The zeta potential is used as a measure of surface charge. An increase in IS causes compression of the double electric layer and increases the Van Der Waals attractive forces. This changes the zeta potential of the particle and increases attractive forces which reduces electrostatic repulsion between other particles, and particle homoaggregation occurs.

1.3.5 The influence of natural organic matter (NOM) on the properties and behaviour of titanium dioxide nanoparticles in aqueous media

Natural organic matter (NOM) is a general term used to describe a mixture of organic compounds found in water. In the literature, some studies use the term dissolved organic matter (DOM) which is a subdivision of NOM, whereby the particles pass through a 0.45 μm filter (Perdue & Ritchie, 2003). Metal oxide ENPs may interact with NOM in the surrounding environment. The adsorption of NOM onto the ENP surface may lead to surface modifications, including a change in ENP surface charge (Mensch *et al.*, 2017). Humic acids (HA) are a common and important group of NOM found in the environment, as are fulvic acids (FA). Studies have shown that NOM has varying roles in aquatic systems; it can enhance or reduce ENP aggregation depending on localized pH and IS conditions (Zhu *et al.*, 2014; Danielsson *et al.*, 2017; Luo *et al.*, 2018). For example, when $\text{pH} > \text{pH}_{\text{pzc}}$ n-TiO₂ (pzc of n-TiO₂ = 6), (Zhu *et al.*, 2014), as is common in UK freshwater systems, typically ranging from pH 6-9, (Water Framework Directive, 2014), the presence of HA does not alter the zeta potential of n-TiO₂s, meaning there is no change in aggregation. When $\text{pH} < \text{pH}_{\text{pzc}}$ n-TiO₂ ($\text{pH} = 4$), which is a pH likely in acidic wastewater effluent (Al-Harashseh *et al.*, 2014), HA presence can either promote homoaggregation, or, if in excess ($> 94.5 \mu\text{g/l}$), reverse the charge, thereby stabilizing the ENPs (Zhu *et al.*, 2014).

1.3.6 The influence of extracellular polymeric substances (EPS) on the properties and behaviour of titanium dioxide nanoparticles in aqueous media

Many algae produce extracellular polymeric substances (EPS), which contain a range of polymeric organic compounds. The EPS secreted from algal cells plays an important role in motility, adhesion and nutrient adsorption in algae (Goto *et al.*, 1999). Benthic algae produce EPS to allow adhesion with other cells when forming a biofilm. EPS can also be

released as a defense mechanism when exposed to an arbitrary toxicant, as the EPS can help to mop up toxic compounds, including heavy metals (Gutierrez *et al.*, 2012; Deccho & Gutierrez, 2017). EPS can be divided into two groups: cell surface bound EPS (B-EPS) and soluble EPS (S-EPS). Cell surface bound EPS (B-EPS) is not attached to the algal cell surface and can be dissociated in culture medium (Gao *et al.*, 2018). EPS has been shown to have a high adsorption capacity for n-TiO₂s, especially particles which possess the anatase crystalline form. The adsorption of n-TiO₂s by EPS could contribute to greater heteroaggregation between the algae and the n-TiO₂s (Xu *et al.*, 2016; Gao *et al.*, 2018). Soluble EPS (S-EPS) has been shown to have a higher adsorption capacity compared to cell surface bound EPS (B-EPS) (Gao *et al.*, 2018), which could lead to increased homoaggregation between particles, and ultimately the sedimentation of n-TiO₂s which could alter exposure conditions throughout a toxicity experiment. Benthic diatoms are known to produce large amounts of EPS for movement (Verneuil *et al.*, 2015) (though not all are motile), so it may be that benthic diatoms with sticky cell walls have higher levels of n-TiO₂ adsorption due to increased amounts of EPS.

These external factors do not work in isolation and can either enhance aggregation via charge neutralization or reduce aggregation via electrostatic repulsion/steric hindrance (Xu, 2018). The zeta potential is an index used to measure this level of aggregation and colloidal stability (Berg *et al.*, 2009). It is important to consider all these factors for toxicity testing, because aggregation may determine ENP settling rates (Zhang *et al.*, 2017), meaning we can infer whether pelagic or benthic aquatic organisms are more at risk of n-TiO₂ exposure.

1.4 Regulations for the production, toxicity testing and evaluation of ENPs

At present, there are no internationally agreed regulations for the production, toxicity testing and evaluation of ENPs (Jeevanandam *et al.*, 2018). In Europe and the USA, ENP production is regulated by the Environmental Protection Agency (EPA) under the toxic substances control act (TSCA). Governing bodies such as the Food and Drug Administration

(FDA) regulate the amount of ENPs entering readily available consumer products (Hedge *et al.*, 2016). Regulating the production of ENPs can be challenging because each particle varies in chemical element composition, size, and sometimes possess different coatings on the surface. Failure to consider size estimation of ENPs often prevents comparison of their toxicity to their bulk counterpart (Laux *et al.*, 2018). Rising concerns on the safety of ENPs led to the subsequent formation of the "Working Party of Manufactured Nanomaterials (WPMN)" founded by the Organisation for Economic Cooperation and Development (OECD) in 2006. Regarding the field of Environmental Ecotoxicology, the primary objective of the framework was to analyse current OECD toxicity testing guidelines and adapt these to testing 13 different ENPs. Eight OECD testing guidelines were modified based on the testing of ENPs considered to be ion-releasing and those considered to be inert ENPs (Hund-Rinke *et al.*, 2016). For ENP toxicity testing using microalgae, the authors recommended that iron should be supplied as FeSO_4 rather than FeCl_3 to ensure good growth of the algae. It was also suggested that the amount of phosphorus in the media should be increased by 5 times (Hund-Rinke *et al.*, 2016). These recommendations come from just one study, however, and they have not been backed up by any further references. More recently, the OECD has released specific guidelines for testing the toxicity of ENPs. The guidelines consider the effects of undissolved particles and consider changes in exposure conditions throughout the duration of the experiment, which are inherent issues requiring consideration to improve the consistency and reproducibility of data (OECD, 2018).

1.5 Variation in toxicity testing protocols for microalgae

Microalgae are useful organisms to evaluate the toxicity of a particular substance. A guideline for testing the toxicity of chemicals to freshwater microalgae is The Freshwater Alga and Cyanobacteria Growth Inhibition Test (OECD TG 201, 2011). There is a similar guideline in the U.S. developed by the Environmental Protection Agency for investigating toxicity of substances to freshwater algae (EPA, 1994), but the focus of this thesis will be on the OECD guideline as this method has been more widely applied to date. Toxicity testing of ENPs can be categorized by the length of the test; acute toxicity tests are typically 72

hours long and are the most frequently used method (OECD TG 201, 2011). During these tests, multiple parameters can be recorded to further understand the effect and mechanisms of toxicants, such as ENPs, on algal health. The most common endpoint that has been applied in ENP toxicity testing is growth inhibition, which is then expressed as an inhibitory concentration (IC(x)) value. Many researchers call this value the effective concentration (EC₅₀), which refers to the concentration of a toxicant which induces a response halfway between the baseline and maximum after a specified exposure time. The IC₅₀, however, refers to the concentration of a toxicant that brings about a 50% inhibition of growth, therefore, this is the most appropriate definition when evaluating the toxicity of a substance on the growth of algae (Tang *et al.*, 2018a). Other common toxicity test endpoints involve biomass determination, either through algal cell counts with a haemocytometer (Chen *et al.*, 2012; Metzler *et al.*, 2012; Hartmann *et al.*, 2013; Ivask *et al.*, 2014), flow cytometry (Manier *et al.*, 2015; Suman *et al.*, 2015; Sendra *et al.*, 2017), or through chlorophyll *a* measurements *in-vitro* (Aruoja *et al.*, 2009; Lee & An, 2013; Nam *et al.*, 2018). Other methods have been applied to measure overall algal photosynthetic health including growth rate analysis and *in-vivo* chlorophyll fluorescence measurements using a pulse amplitude modulated fluorometer (PAM) (Deng *et al.*, 2017; Middepogu *et al.*, 2018). Another useful endpoint includes algal cell reactive oxygen species (ROS) analysis (Fu *et al.*, 2015; Deng *et al.*, 2017).

The Freshwater Alga and Cyanobacteria Growth Inhibition Test (OECD TG 201, 2011) recommends the use of several model species for the toxicity testing of hazardous substances. They consist of two green alga species (*Raphidocelis subcapitata* (formerly *Pseudokirchneriella subcapitata*)), *Desmodesmus subspicatus*), two cyanobacterial species (*Anabaena flos-aquae*, *Synechococcus leopoliensis*) and one diatom species (*Fistulifera pelliculosa* (formerly *Navicula pelliculosa*)). The green algae have been the most frequently used in toxicity tests, including nanotoxicological assessments, with *R. subcapitata* being the most commonly used species (Tang *et al.*, 2018a). Published research on the toxicity effects of ENPs to freshwater diatoms to date, however, is minimal with most of the studies focusing on the impacts of ENPs to marine diatoms (Miller *et al.*, 2010; Miller *et al.*, 2012; Xia *et al.*, 2015; Deng *et al.*, 2017). Relatively fewer studies have investigated the impact of ENPs on freshwater

diatoms (e.g. Kulacki & Cardinale, 2012; Joonas *et al.*, 2019; Jia *et al.*, 2019). Although the OECD already recommends a model diatom species, it is thought amongst researchers that *F. pelliculosa* is a very difficult species to work with, as the cells tend to clump, and form aggregates easily (OECD TG 201, 2011), and their extremely small size makes them difficult to count under the standard light microscopes (Schoeman *et al.*, 1976), typically available to many researchers. In preliminary trials undertaken at Bristol University, this species proved to be particularly problematic as it was difficult to separate clumps of cells for counting, which made it difficult to differentiate between cells and nanoparticulates (Hana Masani, personal communication). Research has shown that n-TiO₂ (concentration = 100 mg l⁻¹) did not inhibit the biomass or photosynthesis of *F. pelliculosa* (Joonas *et al.*, 2019), leading them to suggest that this species may be relatively tolerant, and therefore may not be a suitable indicator diatom species for ENP toxicity testing.

1.6 Evidence of toxicity of n-TiO₂s to freshwater microalgae

Recent published evidence suggests that n-TiO₂ is toxic to aquatic life, including microalgae (Aruoja *et al.*, 2009; Sadiq *et al.*, 2011; Chen *et al.*, 2012; Lee & An, 2013; Sendra *et al.*, 2017; Middepogu *et al.*, 2018; Jia *et al.*, 2019). Discrepancies exist throughout the literature, however, with other research concluding n-TiO₂ may have no negative impacts (Metzler *et al.*, 2011; Joonas *et al.*, 2019). To facilitate comparisons, a detailed summary of the results from published studies investigating n-TiO₂ impacts on single species of freshwater algae, both green and diatoms, has been compiled (**Table 1**). It is apparent that n-TiO₂ exposure has caused growth inhibition and photosynthetic impairment in several green algal species and one diatom species. It was evident from this comparison that researchers had adopted a range of test methods including differences in test media, differences in ENP size and crystalline form and difference in algal species used. In addition to this, researchers use different light regimes, different volumes of experimental chambers, and different shaking regimes, hence it is not possible to draw any firm conclusions given the range of protocols applied.

1.6.1 Particle Composition and Size

The ratio of the two dominant crystalline phases (anatase and rutile) of n-TiO₂s may determine degree of toxicity. It is documented that anatase is a more toxic phase than rutile (Shah *et al.*, 2017), which can be attributed to its higher adsorption capacity for the extracellular polymeric substances (EPS) surrounding algal cells (Gao *et al.*, 2018), thus leading to greater heteroaggregation with algal cells, which therefore increases reactive oxygen species (ROS) generation (Gao *et al.*, 2018). The question of differential toxicity, due to particle phase, was addressed by two research groups, focusing on the crystalline phase; both groups finding that particles with higher rutile composition exhibited a lower toxicity to two species of green algae, *Chlorella sp.* (Iswarya *et al.*, 2015) and *Raphidocelis subcapitata* (Manier *et al.*, 2016).

The impact of particle size on n-TiO₂ toxicity towards algae has also been considered. Experimenters have used n-TiO₂s with a size range spanning 1-100 nm (**Table 1**). Experimenters that used a primary particle size of < 25 nm typically reported greater toxicity impacts (Lee & Ann, 2013; Iswarya *et al.*, 2015; Manier *et al.*, 2016). A study evaluating the effects of three different particle sizes of n-TiO₂ (10, 30, 100 nm) found that the 10 nm particles caused greatest growth inhibition in *R. subcapitata* (Hartmann *et al.*, 2010). Smaller sized particles may have an increased chance of passing through pores in the algal cell wall, which have a diameter of typically 5-20 nm (Navarro *et al.*, 2008). Evidence of n-TiO₂ internalization (particle size: 25 nm) in algal cells has been shown in the marine diatom *Nitzschia closterium* (Xia *et al.*, 2015), and *Chlorella pyrenoidosa* (Gao *et al.*, 2018) and in a cyanobacterium *Anabaena variabilis* (Cherchi *et al.*, 2011).

1.6.2 Growth Medium

It is evident from reviewing publications where impacts of n-TiO₂ have been tested, that a number of researchers have not used the standard toxicity testing media, recommended by OECD. Several types of media are used in ecotoxicological experiments with algae. Chem-

ical differences amongst the media may cause differences in n-TiO₂ toxicity (Wang *et al.*, 2018). As displayed in Table 1, studies that have used OECD media reported high n-TiO₂ toxicity (Aruoja *et al.*, 2009; Lee & Ann, 2013; Iswarya *et al.*, 2015; Manier *et al.*, 2016). In contrast, studies that used soil extract (SE) medium (Ji *et al.*, 2011) showed lower toxicities.

It is also likely that these factors may not be acting in isolation, and that multiple factors affect n-TiO₂ toxicity. Differences in pH, IS and NOM between media used in experiments may determine the aggregation status of ENPs, and thus the overall toxicity. Additionally, the impact of test species used in toxicity experiments must be considered, as there may be species-specific tolerance to n-TiO₂s.

Table 1.1: A summary of studies investigating the impacts of n-TiO₂s on different species of freshwater autotrophs. Studies in alphabetical species order, with green algae (g) shown first, then diatoms (d). Under the particle composition section, A = anastase and R = rutile. Under the endpoint measured section, PA = photosynthetic activity, GI = growth inhibition.

Test Species	Particle Size (nm)	Particle Composition (%)	Growth Medium	Endpoint Measured	Characterization for Toxicology (mg l ⁻¹)	Reference
<i>Chlamydomonas reinhardtii</i> (g)	21	Mix of A and R	SE	PA	Decreased at > 1	Chen <i>et al.</i> , 2012
<i>C. reinhardtii</i> (g)	38	A = 79 R = 21	N/A	GI	72 hr EC ₅₀ : >50	Sendra <i>et al.</i> , 2017
<i>Chlorella</i> sp. (g)	(5-10)	A = 99	SE	GI	144 hr EC ₃₀ : 30	Ji <i>et al.</i> , 2011
<i>Chlorella</i> sp. (g)	<25	A = 99.7	OECD	GI	72 hr EC ₅₀ : 3.36	Iswarya <i>et al.</i> , 2015
	100	R = 99.5			72 hr EC ₅₀ : 6.26	
<i>Chlorella pyrenoidosa</i> (g)	12	Mainly A	OECD	GI	96 hr IC ₅₀ : 9.1	Middepogu <i>et al.</i> , 2018
<i>Desmodesmus subspicatus</i> (g)	25	A = 100	OECD	GI	72 hr EC ₅₀ : 44	Hund-Rinke & Simon, 2006
	100	Mainly A			72 hr EC ₅₀ : >50	
<i>Raphidocelis subcapitata</i> (g)	25-70	N/A	OECD	GI	72 hr EC ₅₀ : 5.83	Aruoja <i>et al.</i> , 2009
<i>R. subcapitata</i> (g)	10	A = 99	USEPA	GI	96 hr IC ₂₅ : 1-2	Hall <i>et al.</i> , 2009
<i>R. subcapitata</i> (g)	30	A = 72.6; R = 18.4	OECD	GI	72 hr EC ₅₀ : 71.1	Hartmann <i>et al.</i> , 2010
<i>R. subcapitata</i> (g)	35.1	A = 80-90	N/A	GI	72 hr EC ₅₀ : 113	Metzler <i>et al.</i> , 2011
<i>R. subcapitata</i> (g)	21	A = 72.6; R = 18.4	OECD	GI	72 hr EC ₅₀ : 2.53	Lee & An, 2013
<i>R. subcapitata</i> (g)	16.2	A = 99	EC	GI	96 hr EC ₅₀ : 6.3	Fu <i>et al.</i> , 2015
<i>R. subcapitata</i> (g)	10	A = 98.5	OECD	GI	72 hr EC ₅₀ : 8.5	Manier <i>et al.</i> , 2016
	20	R = 89			72 hr EC ₅₀ : >50	
<i>Fistulifera pelliculosa</i> (d)	22-25	Mix of A & R	OECD	GI	72 hr EC ₅₀ : >100	Joonas <i>et al.</i> , 2019
<i>Nitzschia frustulum</i> (d)	20	N/A	CSI	GI	72 hr EC ₅₀ : 28.98	Jia <i>et al.</i> , 2019

1.7 Freshwater benthic biofilms and their uses as bio-indicators of water quality

Freshwater benthic biofilms, also termed periphyton, consist of a diverse community of phototrophic and heterotrophic microorganisms. Microbial life in a freshwater biofilm spans the whole tree of life; including bacteria, fungi, heterotrophic protists, microinvertebrates, and algae. Within these complex assemblages, microorganisms are tightly bound in a matrix-like structure, which is held together by their own secretions of EPS (Biggs *et al.*, 1998; Sekar *et al.*, 2002; Yallop & Kelly, 2006). The surrounding EPS on the surface of the biofilm may sequester nutrients or toxins e.g. heavy metals in surrounding water, and protects the biofilm from disturbance, predation and potentially anthropogenic pollutants (Sutherland *et al.*, 2001; Sabater *et al.*, 2016). Biofilms vary in structure and composition depending on the surface on which they develop. In benthic freshwater environments, biofilms tend to grow on inert substrata such as rocks, cobbles and hard sediment (such as clay or silt) (Romani & Sabater, 2001). Biofilms are extremely valuable to the structure and functioning of freshwater ecosystems. They provide many ecosystem services, such as contributing to oxygen production, serving as a vital habitat for aquatic invertebrates, and playing a critical role in nutrient cycling (Li *et al.*, 2016).

1.7.1 The importance of biofilms and benthic diatoms in water quality assessment

Benthic biofilms have been found to be extremely useful in the field of ecotoxicology; they have an excellent ability to degrade anthropogenic pollutants (Mitra & Mukhopadhyay, 2016) and play an important role as bioindicators in freshwater ecosystems (Battin *et al.*, 2009; Ferry *et al.*, 2009). Biofilms are relatively easy to sample, and pollution of water systems can have profound effects on the biofilm community. For example, high levels of an arbitrary pollutant can trigger a shift in favour of pollution-tolerant species (Lavoie *et al.*, 2018). Freshwater biofilms have been used as bioindicators to test the impacts of anthropogenic stressors, including heavy metals (e.g. Hill *et al.*, 1997; Morin *et al.*, 2008; Leguay *et al.*, 2015) and pesticides (e.g. Guasch *et al.*, 2003; Villeneuve *et al.*, 2016). In

the aquatic environment, certain abiotic factors such as high light and differences in flow regime can influence biofilms' response to certain stressors. Guasch & Sabater (2002) found that biofilms were more sensitive to the herbicide atrazine under high light intensities. Flow regime has also shown to impact biofilm tolerance; Villeneuve *et al* (2011) observed that biofilms were more sensitive to pesticides when grown under a turbulent flow regime, compared to a laminar flow regime.

Benthic diatoms are a dominant phototrophic component in these biofilm assemblages (Rimet *et al.*, 2009). Diatoms are a major group of algae in the class Bacillariophyceae (Phylum: Bacillariophyta) characterized by their outer silica cell wall (Lewin, 1962); differences in cell wall morphology are an essential tool for taxonomic identification. For decades, scientists have investigated the use of benthic diatoms as a useful biological monitoring tool for assessing the ecological status of water bodies (Kolkwitz & Marsson, 1908; Sládeček, 1986; Kelly & Whitton, 1995; Bennion *et al.*, 2014). Many protocols have been developed to measure levels of eutrophication in water bodies using diatoms. Research by Kelly & Whitton (1995) resulted in the formulation of the 'Trophic Diatom Index' (TDI). This measure is based upon the fact that the inorganic pollution state of a water body is strongly associated with the diatom species array present. Diatoms are given a sensitivity value directly relating to their sensitivity to inorganic nutrient pollution. Species such as *Nitzschia palea* tend to be associated with high pollution areas and thus, are a high scoring species (Kelly *et al.*, 2008). Since the development of the TDI, newer revised protocols have been developed, including "DARLEQ" (Diatoms for assessing river and lake ecological quality); this system allows comparisons between the actual state of a water body and that expected as a result of human activity (Kelly *et al.*, 2008; Bennion *et al.*, 2014). Diatoms have also been used to measure other variables in water bodies including changes in pH (Juggins *et al.*, 2016) and heavy metal pollution (Medley & Clements, 1998) in freshwater environments.

1.7.2 Freshwater biofilms for measuring the impacts of ENPs

Freshwater benthic biofilms may be useful indicators for assessing the environmental risk of ENPs, as they are thought to be the ultimate repository for ENPs (Battin *et al.*, 2009;

Ferry *et al.*, 2009; Kroll *et al.*, 2014). Researchers have evaluated the effects of gold and titanium nanoparticles on freshwater biofilm communities (Battin *et al.*, 2009; Ferry *et al.*, 2009; Wright *et al.*, 2018). Exposure to n-TiO₂ in freshwater biofilms has been shown to cause severe cell membrane damage, but this effect was greater in free-living cells (cells not attached to the biofilm) compared to cells in the biofilm, demonstrating the protective role of cell encapsulation against n-TiO₂s (Battin *et al.*, 2009). Exposure to n-TiO₂ has also shown to have profound effects on species composition in biofilms, where exposure to high concentrations (5 mg l⁻¹) of n-TiO₂ caused a shift in the species, where pollution-sensitive taxa dominated by biofilms after 28 days of exposure (Wright *et al.*, 2018).

1.8 Knowledge gaps and aims of thesis

1.8.1 Knowledge gaps

There were two main knowledge gaps identified from this review of the published literature. Firstly, a lack of information on the toxicity of n-TiO₂s to benthic freshwater diatom species, and as the sedimentation rate of n-TiO₂ in freshwater is high (Sharma *et al.*, 2009), diatoms in the benthic sediment may be more exposed than planktonic algae. Secondly, there is a lack of a suitable benthic diatom species for routine toxicity testing of ENPs. Almost nobody has tested the impacts of n-TiO₂ exposure on the OECD recommended diatom, *F. pelliculosa*, and this species is known to be problematic in toxicity testing due to its small size and cell clumping. Therefore, there is a need to find a more suitable indicator species for toxicity of ENPs to benthic diatoms in freshwater.

There is also a need to assess the impacts of n-TiO₂ exposure to benthic diatoms in field conditions. From the review of the literature, it was also apparent that, protocol differences aside, there were marked species-specific differences in the toxicity of n-TiO₂. Therefore, trying to assess the responses in the field is problematic, due to the mixed community of algal species having differential tolerances to n-TiO₂. Moreover, in the field, there is a plethora of changing variables, such as light, pH, temperature, flow rate and the presence of UV irradiation. These changing variables may directly alter the toxicity of n-TiO₂s by in-

creasing/decreasing the toxicity to algae, or indirectly, by making the algae more susceptible to toxicity due to presence of high light, and high UV irradiation.

1.8.2 Aims of thesis

The main aim of this project is to explore the toxic effects of n-TiO₂s on benthic freshwater algal communities, through single-species testing and whole biofilm communities testing. In laboratory experiments, I will use a benthic diatom species (*N. palea*) to test its suitability as a test species and examine single species effects of n-TiO₂s finding out if they are more sensitive than green planktonic species. In field experiments, I will examine the whole benthic community effects of n-TiO₂s. In my synthesis, I will aim to compare field and laboratory results to determine whether *N. palea* is a good indicator species for determining n-TiO₂ pollution, explore the methodological variations of nanoparticle toxicity testing, and explore the global impacts of nanoparticle pollution.

1.9 Thesis Outline

Chapters 2 and 3 are the data chapters of this thesis, both exploring the impact of n-TiO₂s on freshwater benthic algae. They both follow the structure of Introduction, Methods, Results, Discussion, then Conclusion.

The research presented in **Chapter 2** focuses on testing the toxicity of n-TiO₂ to a single species freshwater benthic diatom, *Nitzschia palea* under laboratory conditions. A discussion on the application of the OECD guidelines for toxicity testing is discussed, and the impacts of n-TiO₂ on freshwater algae are reviewed. A revised protocol was then devised to quantify the impact of n-TiO₂ on the growth and photophysiology of *N. palea*. The impacts of n-TiO₂ to *N. palea* are illustrated and discussed, and comparisons are made between other studies investigating the impacts of n-TiO₂ on other species of freshwater algae.

The research presented in **Chapter 3** focuses on testing the toxicity of n-TiO₂ to benthic freshwater biofilm communities, under field conditions using river water from a Mill

Stream which is a tributary of the River Frome (Dorset, UK). The literature on the impacts of n-TiO₂ on freshwater biofilms is reviewed. Using outdoor artificial mesocosms, the biomass, photophysiology and diatom species composition was investigated following n-TiO₂ exposure. The impacts of biomass, photophysiology and diatom species composition are illustrated and then discussed with relevant literature.

Chapter 4 is a synthesis of the research. This chapter draws conclusions from the findings of this study, exploring the parallels that can be drawn between laboratory and field studies. This chapter also states the limitations of testing the toxicity of nanoparticles to algae, and details recommendation for the future of titanium nanoparticle testing. The synthesis also explores the wider implications of wide-scale application of n-TiO₂ globally.

CHAPTER 2

The effects of titanium dioxide nanoparticles (n-TiO₂) on the freshwater benthic diatom species, *Nitzschia palea*, (Kützing) W. Smith.



Watercolour of diatoms by Amy Ockenden

2.1 Introduction

2.1.1 The importance of testing the impacts of ENPs on benthic diatoms

MOST studies evaluating the toxicity of ENPs to microalgae have been conducted on green, planktonic algal species (e.g. Hund-Rinke & Simon, 2006; Aruoja *et al.*, 2009; Ji *et al.*, 2011; Lee & An, 2013; Fu *et al.*, 2015; Sendra *et al.*, 2017; Marchello *et al.*, 2018; Middepogu *et al.*, 2018). Few studies, however, have investigated the impacts of ENPs on freshwater benthic diatoms (see section 2.1.2) (Kulacki *et al.*, 2012; Bour *et al.*, 2015; Gonzalez *et al.*, 2016; Verneuil *et al.*, 2015; Wright *et al.*, 2018; Jia *et al.*, 2019; Joonas *et al.*, 2019), and only a few of these studies have tested the impacts of n-TiO₂ to freshwater benthic diatoms (Kulacki *et al.*, 2012; Wright *et al.*, 2018; Jia *et al.*, 2019; Joonas *et al.*, 2019). Studies have shown that the sedimentation rate of n-TiO₂ in water is high (Sharma, 2009; Keller *et al.*, 2010; Doyle *et al.*, 2014). Mueller & Nowack estimated n-TiO₂ concentration values to be 16 µg/l in water bodies in Switzerland, and reports from Europe and the US state that the highest concentrations of n-TiO₂s in were found in the sediment; there being 0.2-0.6 mg/kg (Gottschalk *et al.*, 2009). This information indicates that the benthic sediment may be, at least, a temporary repository for these ENPs (Li *et al.*, 2014; Moreno-Garrido *et al.*, 2015). Benthic diatoms may therefore have a higher chance of increased ENP exposure, compared to planktonic algal species, therefore it is essential that more effort should be focused on toxicity testing of the effects of ENPs on biota in the benthos. Comparisons between the two sets of outputs would help us to better understand whether ENP exposure affects benthic and planktonic algae differently. Furthermore, the OECD states that the recommended diatom species for toxicity testing, *Fistulifera pelliculosa*, "may form aggregates under certain growth conditions" and that "special measures have to be taken for biomass determination in order to obtain representative samples", including vigorous shaking (OECD TG 201, 2011). Given the concerns raised about difficulties associated with biomass determination for *F. pelliculosa*, it is important to find a suitable model species for testing the toxicity of ENPs to benthic diatoms i.e. to find a benthic equivalent of *Raphidocelis subcapitata*.

2.1.2 The impacts of ENPs on benthic diatoms

The effects of ENPs (including TiO₂, CeO₂, and multi-walled carbon nanotubes (MWCNT)) on benthic diatom species from freshwater and marine environments have been studied in just a few cases (Verneuil *et al.*, 2015; Bour *et al.*, 2015; Xia *et al.*, 2015; Jia *et al.*, 2019; Joonas *et al.*, 2019). Studies investigating the effects of n-TiO₂ on the diatoms *Nitzschia closterium* (synonym *Cylindrotheca closterium*) and *Nitzschia frustulum* have shown growth inhibition, production of ROS and internalization of n-TiO₂s in algal cells (Xia *et al.*, 2015; Jia *et al.*, 2019). However, one study on the freshwater diatom *F. pelliculosa* reported no adverse effects on algal health when cells were exposed to n-TiO₂ (Joonas *et al.*, 2019). Nonetheless, there is a lack of standardization of methods in the literature for carrying out toxicity testing, and variations in response may be related to different methodological approaches.

2.1.3 The OECD Freshwater Alga and Cyanobacteria Growth Inhibition Test: A guide for ENP toxicity testing

Most ecotoxicological studies using microalgae are performed using The Freshwater Alga and Cyanobacteria Growth Inhibition Test (OECD TG 201, 2011), and some researchers who have carried out toxicity testing using ENPs have used this protocol as a guide for running experiments (Aruoja *et al.*, 2009; Manier *et al.*, 2015; Metzler *et al.*, 2018; Ozkaleli & Erdem, 2018), though invariably, modifications have been adopted. The tests were originally applied for testing soluble toxicants and the methods may not always be suitable when testing for particular ENPs. On closer inspection, there are a number of methodological variations between studies testing ENP toxicity to benthic diatoms (including variations in ENP preparation, shaking regimes, lighting conditions, endpoints and the presence of EPS). There is a need for a standardized approach to testing impacts of ENPs on benthic algae.

2.1.3.1 The preparation of ENPs

Dispersion of ENPs into aquatic media is important to achieve an initial uniform stock solution (Crane *et al.*, 2008). Researchers tend to use two approaches to achieve effective

dispersion of ENPs, sonication or prolonged stirring (Handy *et al.*, 2008). Both stirring and sonication help to break up any ENP aggregates and ensure initial dispersion. Published research has speculated that differences in dispersion preparation methods may be a reason for observed variation in toxicity throughout the literature (Hartmann *et al.*, 2015). For example, Hund-Rinke & Wenzel (2010) showed that n-TiO₂ samples that had been stirred for 7 days were not toxic, but EC₂₀ values were produced for shorter stirring and sonication times.

2.1.3.2 Shaking of algae during toxicity testing

The OECD test recommends that algae are continuously shaken or stirred throughout the test to facilitate the transfer of CO₂ (OECD TG 201, 2011). However, this may not be beneficial for benthic algae that grow naturally in a biofilm. Some researchers carrying out toxicity tests on benthic algae have stated that they chose not to shake cultures to allow sedimentation and adhesion of algae (Moreno-Garrido *et al.*, 2003; Verneuil *et al.*, 2015; Bour *et al.*, 2015; Xia *et al.*, 2015). Various regimes have been reported in benthic diatom research, including continuous shaking of cultures (Joonas *et al.*, 2019), shaking three times a day at eight-hour intervals (Jia *et al.*, 2019) and no shaking at all (Verneuil *et al.*, 2015).

2.1.3.3 Extracellular polymeric substances as a confounding issue with toxicity testing for ENPs

Many algae produce extracellular polymeric substances (EPS), and benthic diatoms produce a lot of EPS which may facilitate biofilm adhesion in culture vessels (Moreno-Garrido *et al.*, 2015). The presence of EPS in the culture sample may affect the aggregation state of ENPs (Lin *et al.*, 2016; Xu *et al.*, 2016). Verneuil *et al.* (2015) recommended that when working with benthic algae, the old inoculum should be removed prior to experimental start and resuspend the alga in fresh media, to remove the EPS and reduce ENP aggregation. Whilst this should be standard practice, this washing step has not always been stated in the literature, which may account for the inconsistencies when reporting the level of toxicological impacts of ENPs in benthic diatoms. Also, when sampling the algae for cell counts, it is essential that the sides and bottom of the well/petri dish are vigorously scraped with a

cell scraper, as benthic algae are likely to be tightly stuck to the walls. This ensures all the cells are lifted from the bottom.

2.1.3.4 Lighting conditions for toxicity testing of ENPs

The OECD guidelines state that algal cultures should receive continuous, uniform fluorescent illumination for the duration of the experiment at a light intensity of 60-120 μmol (photons) $\text{m}^{-2} \text{s}^{-1}$ (OECD TG 201, 2011). One study testing n-TiO₂ toxicity to *F. pelliculosa* was compliant with these guidelines (Joonas *et al.*, 2019), but others have used varying photoperiods, such as 16h:8h light dark cycles (Verneuil *et al.*, 2015) and 12h:12h light dark cycles (Xia *et al.*, 2015; Jia *et al.*, 2019).

2.1.3.5 Variations in endpoint determination in toxicity testing

The choice of end point is also something that varies across published studies evaluating ENP toxicity on benthic diatoms. The OECD recommended test end point is the inhibition of growth (OECD TG 201, 2011), which has been used in several studies evaluating ENP toxicity to benthic diatoms (Verneuil *et al.*, 2015; Xia *et al.*, 2015; Jia *et al.*, 2019; Joonas *et al.*, 2019). The inhibition of growth is expressed as a logarithmic increase in biomass (average growth rate) during a set time period. The growth rate value is then used to work out the x% inhibition of growth which is expressed as an IC(x) value (e.g. IC₅₀). The guideline also states that yield can be used as an end point, which is defined as "the biomass at the end of the exposure period minus the biomass at the start of the exposure period" (OECD TG 201, 2011). Percentage inhibition of yield is then calculated and expressed as an IC(x) value. The x% yield, however, is rarely used throughout the literature, as it is not scientifically preferred, and included in this guideline to satisfy current regulatory requirements in some countries. To gain a better understanding of impacts of ENPs on cell functioning, pulse-amplitude modulated fluorometry (PAM) techniques have been used by some researchers to evaluate the impact of ENPs on green algae (Deng *et al.*, 2017; Middepogu *et al.*, 2018) and on benthic diatoms (Joonas *et al.*, 2019). This technique can be made rapidly and non-intrusively (Consalvey *et al.*, 2005). One particular measure (Fv/Fm), has been widely used as an indicator of photosynthetic health (Dijkman & Kromkamp, 2006; Murchie &

Lawson, 2013). A rapid light curve (RLC) can be generated, and from these curves multiple photosynthetic parameters can be obtained and analyzed, including the maximum quantum yield of photosystem II (PSII) in the dark-adapted state (F_v/F_m), the maximum electron transport rate (ETR_m), the theoretical maximum light utilization coefficient (Alpha (α)), and the light saturation coefficient (E_k).

2.1.4 The rationale for selecting *Nitzschia palea* as a possible test species for evaluating n-TiO₂ toxicity on benthic diatoms

The chosen species for this experiment was the pennate, benthic diatom, *Nitzschia palea*. This species was chosen because it has a wide distribution (Kim-Tiam *et al.*, 2018) and is frequently dominant in freshwater biofilms (Gonzalez *et al.*, 2016). This species is also useful in toxicity testing as it grows well in cultures in the laboratory with a fast generation time, it is relatively large (length: 12-42 μ m) and thus easy to enumerate. In recent years, *N. palea* has been used to test the toxicity of potentially hazardous substances, including heavy metals (Chen *et al.*, 2013; Kim-Tiam *et al.*, 2018). This species has also been used to test impacts of certain ENPs, including silver (Ag₂O), cerium dioxide (CeO₂) and carbon nanotubes (Verneuil *et al.*, 2015; Bour *et al.*, 2015; Gonzalez *et al.*, 2016). However, to my knowledge, the toxicity effects of n-TiO₂ to *N. palea* have not been reported in the literature to date. Given the long history of testing the impacts of other potential hazardous substances on *N. palea*, it was decided to trial this species for testing the impacts of n-TiO₂s on freshwater benthic diatoms.

2.2 Aims of study

This laboratory study was carried out to investigate the species-specific effects of increasing n-TiO₂ exposure on the growth of a single benthic diatom, *N. palea* and to evaluate whether this diatom was more susceptible to n-TiO₂ exposure by comparison with the published findings for the planktonic, green algae. Specific aims were: (i) to assess whether increasing n-TiO₂ exposure concentration caused changes in the growth rate and growth rate inhibition of the diatom and (ii) to assess whether increasing n-TiO₂ exposure concen-

tration caused changes in diatom photophysiology. The results of this study will contribute to ongoing evaluations of the possible impacts of n-TiO₂. To date, most studies have focused on measuring impacts to planktonic green algae. It was hypothesised that, the impacts of n-TiO₂ may be greater for benthic diatom species, as these ENPs are thought to aggregate rapidly on reaching the water column and settle in the benthic sediment (Sharma *et al.*, 2009; Keller *et al.*, 2010; Doyle *et al.*, 2014). The following specific hypotheses were posed:

(i) It was hypothesised that an increasing n-TiO₂ concentration would negatively impact the growth rate and growth rate inhibition of *N. palea*, and negative impacts would increase over time.

(ii) It was hypothesised that an increasing n-TiO₂ concentration would negatively impact the photophysiology of *N. palea*, causing reductions in all measured photosynthetic parameters.

2.3 Methods

2.3.1 Specimen collection and maintenance

The freshwater benthic diatom used in this experiment (*Nitzschia sp.*) was sourced from Sciento (Manchester, UK). Diatom cleaning methods (see methods section 3.3.9 in chapter 3 for instructions on diatom cleaning) confirmed the species was *Nitzschia palea* (identified by Professor Marian Yallop). Diatoms were cultured in modified OECD media (OECD TG 201, 2011) (see Table 2.1 for elemental composition). Based on a review of previous published literature, various modifications were applied to the standard OECD guidelines (OECD TG 201, 2011) including:

1) The addition of a higher concentration of silica (matching the concentration used in the preparation of Diatom Medium (Culture Collection of Algae and Protozoa (CCAP), Argyll, Scotland)). Higher concentrations of silica were added to allow diatom frustule for-

mation.

2) MOPS (3-(*N*-morpholino)propanesulfonic acid) buffer was added, and the pH adjusted to 7.2, as this has been demonstrated to better maintain pH over the growth cycle, compared to the OECD buffer sodium bicarbonate (De Schamphelaere & Janssen, 2004). The addition of MOPS controlled for any pH changes that may occur during the addition of n-TiO₂ and to give better control of pH for compliance with OECD tests during experiments (OECD TG 201, 2011).

Prior to experimental start point, diatoms were grown in vented petri dishes in Diatom Media under a 14h:10h light:dark cycle, under static conditions, for four days and then placed in new OECD media prior to experimental start point to standardize the stage in exponential phase. The cultures were not shaken during the experiment to allow biofilm formation. During the experiment, cultures were maintained under experimental conditions in a Ref Tech growth room at 18 °C under a 24-hour continuous light cycle, illuminated from below ($120 \mu\text{mol. photons m}^{-2} \text{ s}^{-1} \equiv 6480 \text{ lux}$) using cool white fluorescent lights (Luxline Plus F58W/830, Sylvania, Erlangen, Germany). Light irradiance was measured using a QRT1/PAR light sensor (Hansatech Instruments Ltd, Norfolk, UK).

Table 2.1: Elemental composition of OECD media.

Element	mg/L
Carbon	7.148
Nitrogen	3.927
Phosphorus	0.285
Potassium	0.459
Sodium	13.704
Calcium	4.905
Magnesium	2.913
Iron	0.017
Manganese	0.115

2.3.2 Titanium dioxide nanoparticle (n-TiO₂) characterization

The titanium dioxide nanoparticles (n-TiO₂s) in a dry powder form, with a primary particle size of 50 nm were purchased from US Research Nanomaterials Inc. (Stock number: US3530, Houston, USA). Raman spectroscopy, using an inViaTM confocal Raman microscope (Renishaw, Gloucestershire, UK) was used to determine the crystalline phase composition (anatase and/or rutile) of the n-TiO₂s. Energy dispersive X-ray spectroscopy (EDS) was used to analyze the chemical elements present in the n-TiO₂ sample. Phase maps showing elemental distribution of the n-TiO₂s were provided by the TEAMTM EDS analysis software (EDAX Inc., New Jersey, USA). The size of the n-TiO₂s was verified by observing the n-TiO₂ nano powder under the SEM (Zeiss EVO15, Cambridge, UK). The n-TiO₂ characterization results were obtained with the assistance of Dr. Adel El-Turke (School of Physics, University of Bristol).

2.3.3 Preparation of the titanium dioxide nanoparticles (n-TiO₂s)

A primary stock suspension was prepared by directly adding the n-TiO₂ nano powder to MilliQ water to obtain an initial n-TiO₂ concentration of 2000 mg l⁻¹. The suspension was then sonicated (Branson 3800, Branson Ultrasonics, Danbury, USA) for 30 minutes to disperse the n-TiO₂s. Five treatment concentrations plus one control (Control, 0.05, 0.5, 5, 10, 50 mg l⁻¹) were made up in the modified OECD media (pH = 7.2) and MilliQ water in 50 ml falcon tubes and these were left for 24 hours to age under experimental conditions (see section 2.3.1 for experimental conditions). The lowest concentration of n-TiO₂ (0.05 mg l⁻¹) was selected to be more indicative of environmentally relevant values recorded between 0.0007-0.016 mg l⁻¹ (Mueller & Nowack, 2008). The 5 mg l⁻¹ treatment was selected to represent a high environmental concentration scenario, such as in raw sewage (Westerhoff *et al.*, 2011). The 10 and 50 mg l⁻¹ n-TiO₂ are very high concentrations, and not environmentally relevant. However, with increased production of n-TiO₂, environmental concentrations could massively increase.

The ageing of the n-TiO₂s in OECD media was carried out in falcon tubes due to

changes that take place when the n-TiO₂ is added to the media, changes that are not observed in MilliQ water (Doyle *et al.*, 2014). The n-TiO₂s have been shown to aggregate more in OECD media than in MilliQ water, which is likely due to the media containing a lot of salts e.g. CaCl₂ and MgSO₄, giving a relatively high ionic salt (IS) content (Lin *et al.*, 2017) (see diagram in section 1.3 of literature review). The n-TiO₂s were aged under experimental conditions (see section 2.3.1) and not aged under UV irradiation because the n-TiO₂ crystalline phase was 100% rutile, which according to published literature, is not considered to produce ROS when photoactivated by UV light (Sayes *et al.*, 2006).

2.3.4 Experimental set-up

The experiment was conducted at the University of Bristol Life Sciences Building over a period of four consecutive days. The algae, in exponential growth phase, were processed by gently centrifuging the culture using a centrifuge (Model: 5810 R, Eppendorf, Stevenage, UK) at 1000 RPM/201 RCF) for 10 minutes to remove the old diatom media and then resuspending the pelleted diatoms in fresh OECD media. Aliquots of well mixed algae were spiked into each of the 50 ml falcon tubes containing n-TiO₂ at differing concentrations (5 treatments + 1 control) to obtain a starting inoculum of 10,000 cells/ml (counted using a haemocytometer), matching the recommended starting concentration for the OECD recommended diatom, *F. pelliculosa* (OECD TG 201, 2011). The algal-nano suspensions (10 ml) were then plated out into 55 mm triple vented petri dishes (Zoro, Leicester, UK) with four replicates per treatment and incubated for 72 hours.

2.3.5 Cell growth analysis

To measure the effects of increasing concentrations of n-TiO₂ on algal biomass at defined intervals over the experiment, the OECD TG 201 algal growth inhibition test guidelines (OECD TG 201, 2011) were followed. Cell enumeration was carried out on an optical microscope (Olympus, CHA, Japan), at a magnification x 400, using a haemocytometer (Fuchs Rosenthal, cell depth = 0.2 mm, Hausser Scientific, Germany) at a standardized time point over a period of 72 hours, with 24-hour intervals (24, 48, 72 hour). Using aseptic techniques, the bottom of the petri-dishes were firstly scraped with a cell-scraper (10 vertical

and 10 horizontal scrapes for standardization) (Corning, 1.8 cm sterile blade) to dislodge the cells; a 1 ml sub-sample was homogenized for 20 seconds using a vortex and was preserved for cell enumeration using Lugols Iodine (1% final volume), kept in the dark, and counted within 1 month. Cells were counted and then average growth rates at 24, 48 and 72 hours were determined based upon the number of days the experiment had been running (**Equation 2.1**). Initial trial experiments indicated that the average control growth rate for the duration of the experiment was 0.98 d⁻¹ which is consistent with the recommended minimum average control growth rate of OECD guidelines (0.92 d⁻¹). The average growth rates were then used in **Equation 2.2** to calculate the average growth rate inhibition (GI) of each sample.

$$\mu_{i-j} = \frac{\ln(X_j) - \ln(X_i)}{t_j - t_i} \text{day}^{-1} \quad (2.1)$$

Where:

μ_{i-j} = average specific growth rate from time i - j

X_i = biomass at time i

X_j = biomass at time j

t_j = time j

t_i = time i

$$GI(\%) = \frac{\mu_c - \mu_t}{\mu_c} \times 100 \quad (2.2)$$

Where:

$GI(\%)$ = percent inhibition of the sample growth rate

μ_c = mean value for average specific growth rate (μ) in the control group

μ_t = average specific growth rate for the treatment replicate

Dose response curves were then produced by plotting the %GI against the logarithmic

of the concentration of n-TiO₂s. These curves were then used to estimate the IC₂₀ and IC₅₀ (the concentration at which 20% and 50% of the cell growth is inhibited) of n-TiO₂ at 24, 48 and 72 hours independently.

2.3.6 Pulse amplitude modulated (PAM) fluorometry

The photophysiology of *N. palea* was evaluated using pulse amplitude modulated fluorometry (PAM). Measurements were taken at 24-hour intervals over a 72-hour period using a WATER-PAM fluorometer (Walz, Effeltrich, Germany) without stirring, to avoid a biased fluorescence signal due to movement of cells from between areas, which vary in light intensity, in the cuvette (Cosgrove & Borowitzka, 2006; Herlory *et al.*, 2013). All treatments were harvested and analysed separately to ensure a standardised dark adaption time of 20 minutes (Consalvey *et al.*, 2005). The purpose of dark adaption time is to determine the maximum quantum yield of PSII in the dark-adapted state (Fv/Fm). During dark adaption, all PSII reaction centres are open, allowing measurement of the minimum fluorescence (Fo). When a saturating pulse is delivered to dark-adapted diatoms, all reaction centres are stimulated to close, giving a maximum fluorescence value (Fm). The difference between Fo and Fm represents the variable fluorescence (Fv), (Barbagallo *et al.*, 2003; Murchie & Lawson, 2013). Thus, the Fv/Fm parameter was calculated using these values in **Equation 2.3**. Following dark adaption, 3 ml of OECD media was added to a cuvette to auto-zero the WATER-PAM. Rapid light curves (RLCs) were performed for each treatment and each of the four replicates. RLCs were carried out with a 4000 mol (photons) m⁻² s⁻¹ saturating pulse, with 9 x 20 second actinic light increments ranging from 28 to 1406 mol (photons) m⁻² s⁻¹. Irradiance levels were set up using the Win-Control calibration routine using a spherical micro quantum sensor (US-SQS/WB) which is required for quantitative assessment of the photosynthetic active radiation (PAR). The RLC is fitted based on the model of Eilers and Peeters (1988). Analysis of RLCs using WINCONTROL software (WinControl-3, Walz, Effeltrich, Germany) allowed calculation of the following photosynthetic parameters: rETR_m, alpha (α), E_k and the Fv/Fm (definitions are provided in **Table 2.2**).

$$\frac{Fv}{Fm} = \frac{Fm - Fo}{Fm} \quad (2.3)$$

Where:

Fv/Fm = maximum light utilisation efficiency of PSII

Fo = dark-adapted minimum fluorescence yield

Fm = dark-adapted maximum fluorescence yield during the saturating flash

Table 2.2: Definitions of photosynthetic parameters: alpha (α), Fv/Fm , rETRm, and E_k . Definitions taken from Consalvey *et al* (2005).

Photosynthetic Parameter	Definition
Fv/Fm	The maximum quantum yield of photosystem II (PSII) in the dark-adapted state
Alpha (α)	The theoretical maximum light utilisation coefficient
ETRm	The maximum electron transport rate
E_k	The light saturation coefficient

2.3.7 Imaging Diatom Cells

At 72 hours, the algal cells in the control and 50 mg l⁻¹ n-TiO₂ treatment were observed using light fluorescence microscopy at a magnification x 1000 (Microscope: Leica DM3000 B; Camera: Olympus DP70, CHA, Japan).

2.3.8 Statistical analysis

All statistical analysis was carried out using IBM SPSS Statistics 23 (IBM Corp., New York, USA). Homogeneity of variance was tested using Levene's test; normality of residuals was tested using a Kolmogorov-Smirnov test. Where data were non-normally distributed, it was logarithmically transformed. One-way ANOVA's were performed to examine differences between n-TiO₂ treatments at independent time points. Where data were significant, *post-*

hoc Bonferroni tests were applied to identify significant differences between treatments. The n-TiO₂ concentration at which 20% and 50% of algal growth was inhibited (IC₂₀ and IC₅₀) was estimated by plotting the logarithmic test concentration against percentage growth inhibition (relative to the control). At 24, 48 and 72 hours, the IC₂₀ and IC₅₀ values were determined. The Excel add-in ed50v10 was used to estimate the IC₅₀ and IC₂₀ values. Statistical significances were accepted when the probability of the observed results (p) is equal to or less than 0.05, assuming the null hypothesis is true.

2.4 Results

2.4.1 Titanium dioxide nanoparticle (n-TiO₂) characteristics

Raman Spectroscopy confirmed the n-TiO₂ composition to be a crystalline phase of 100% rutile, indicated by three spectral peaks characteristic of the rutile phase (236, 446, 612 cm⁻¹) (**Figure 2.1**).

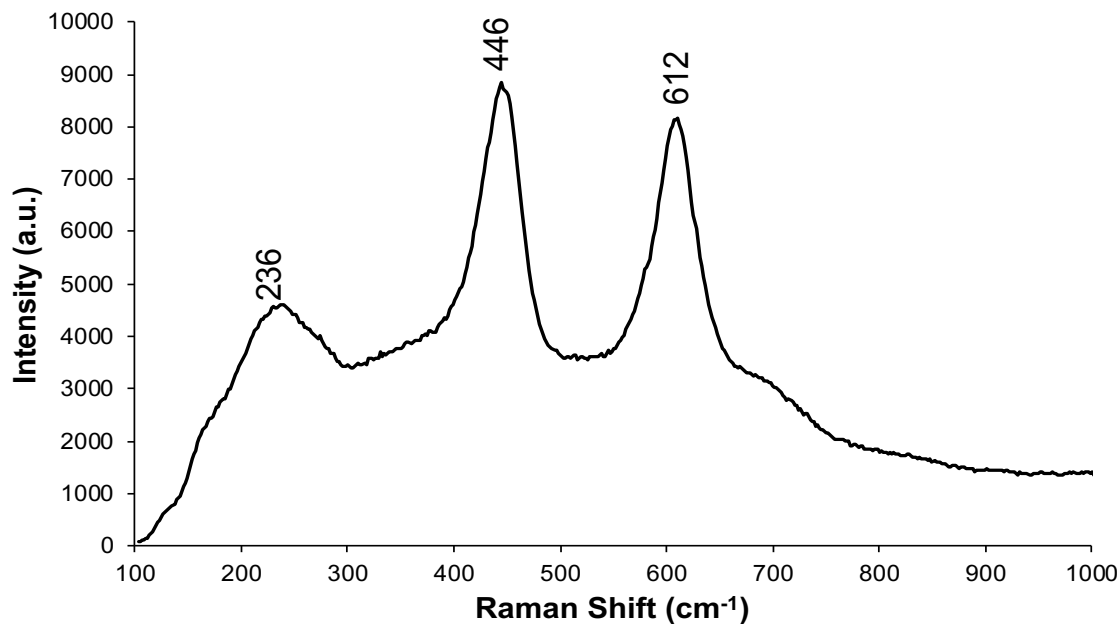


Figure 2.1: Raman spectra typical of the n-TiO₂ powder used in this experiment. In this spectra, three peaks at 236, 446, and 612 cm⁻¹ are well observed, which are typical of the rutile crystalline phase (Kernazhitsky *et al.*, 2014).

The EDS spectrum confirms the presence of titanium (Ti) in the sample, shown by the characteristic K_a and K_B peaks of Ti (K_a = 4.51 keV; K_B = 4.93 keV) (**Figure 2.2**). The weight of each chemical element, (mean of three independent surface areas of the sample \pm SE), identified in the sample are shown in **Table 2.3**.

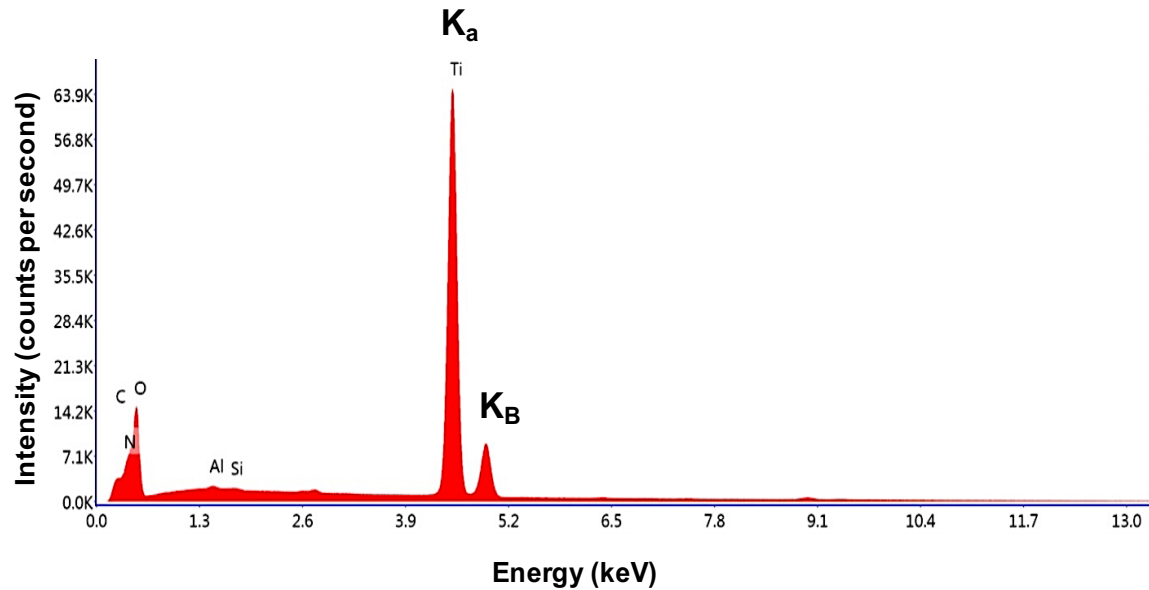


Figure 2.2: EDS element phase map showing the distribution of chemical elements in the n-TiO₂ powder sample. Two characteristics peaks of Ti (K_a and K_B) are shown on the phase map.

Table 2.3: The weight ratios of independent chemical elements found in the n-TiO₂ powder sample. Weight is shown as a mean of three independent areas of the sample and standard error is displayed.

Element	Weight (%)	Standard Error (SE)
Carbon (C)	7.62	0.39
Oxygen (O)	37.79	2.54
Aluminium (Al)	0.37	0.12
Silicon (Si)	0.09	0.02
Titanium (Ti)	52.97	3.91

2.4.2 The impact of an increasing n-TiO₂ exposure concentration on the growth of *Nitzschia palea*

2.4.2.1 The growth curves of *Nitzschia palea* exposed to n-TiO₂

The cell density of *N. palea* was measured at 0, 24, 48 and 72 hours using a haemocytometer for the control and all five treatments, these measurements were then used to plot a growth curve (**Figure 2.3**).

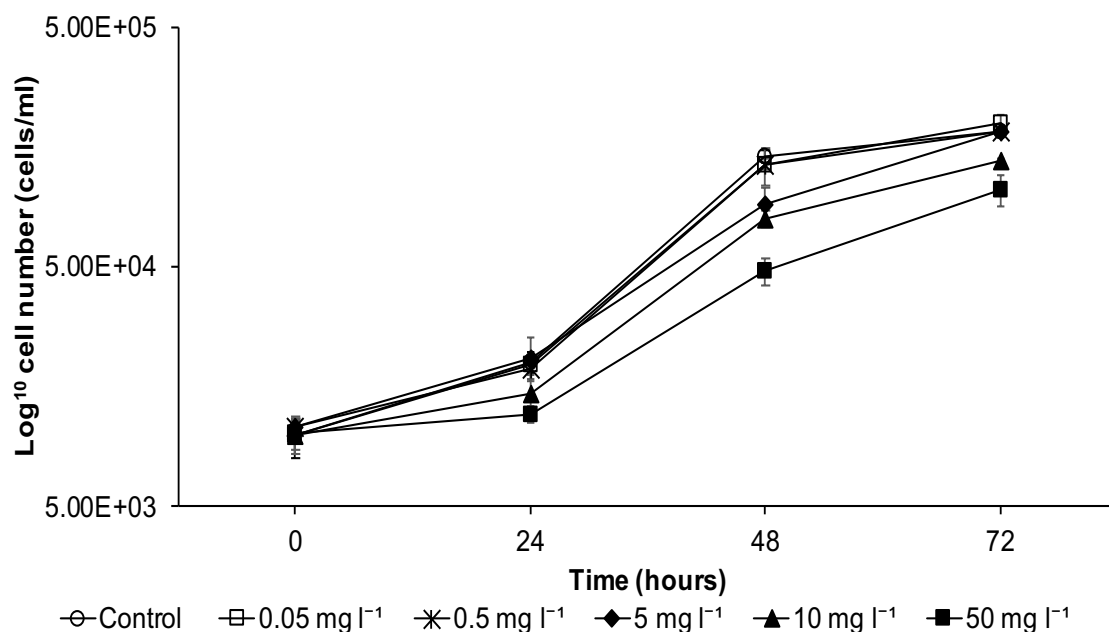


Figure 2.3: Growth curve of *N. palea* exposed to increasing concentrations of n-TiO₂ over a period of 72 hours. Error bars shown mean \pm SE of four independent replicates.

Cells of *N. palea* grown under relatively low concentrations of n-TiO₂ (0.05, 0.5 and 5 mg l⁻¹) showed similar growth profiles to the untreated cells. The final cell yield (cells/ml) at 72 hours were 1.74E+05 (\pm 1270 SE) (control), 1.86E+05 (\pm 7943 SE) (0.05 mg l⁻¹), 1.71E+05 (\pm 3937 SE) (0.5 mg l⁻¹), 1.73E+05 (\pm 4066 SE) (5 mg l⁻¹), 1.27E+05 (\pm 1735 SE) (10 mg l⁻¹), 9.43E+04 (\pm 7495 SE) (50 mg l⁻¹). Cell counts were then used to determine the growth rate and growth rate inhibition of all the samples (see equations 2.1 and 2.2).

2.4.2.2 Growth rates (K')

The growth rates of *N. palea* were calculated every 24 hours. The daily growth rates were calculated to determine any temporal changes in growth rates for all of the samples (Table 2.4).

Table 2.4: The mean daily growth rates (K') (\pm SE of four independent replicates) of *N. palea* for the control and all the n-TiO₂ treatments.

n-TiO ₂ concentration (mg l ⁻¹)	Daily growth rate (K')		
	(0-24 hours)	(24-48 hours)	(48-72 hours)
0 (control)	0.70 \pm 0.05	1.96 \pm 0.03	0.25 \pm 0.07
0.05	0.66 \pm 0.01	1.91 \pm 0.09	0.39 \pm 0.04
0.5	0.56 \pm 0.04	1.96 \pm 0.02	0.31 \pm 0.02
5	0.66 \pm 0.10	1.45 \pm 0.11	0.70 \pm 0.02
10	0.40 \pm 0.09	1.67 \pm 0.04	0.54 \pm 0.01
50	0.17 \pm 0.04	1.37 \pm 0.07	0.77 \pm 0.07

From day 1-2 (0-24 hours), the growth rate of the algae in the 50 mg l⁻¹ treatment (0.17 \pm 0.039) was much lower than that of the control (0.70 \pm 0.049). By day 3-4 (48-72 hours) the control algal sample growth rate (0.25 \pm 0.069) was much lower than the growth rate of the algae in the 50 mg l⁻¹ treatment (0.77 \pm 0.070).

2.4.2.3 Growth rate inhibition

Average growth rate inhibition (GI% as a percentage of the control) of *N. palea* in response to n-TiO₂ exposure was used as a measure to investigate the effect of n-TiO₂ over time, as recommended by OECD guidelines (OECD TG 201, 2011). The GI% of *N. palea*

when exposed to an increasing n-TiO₂ concentration is shown in **Figure 2.4**.

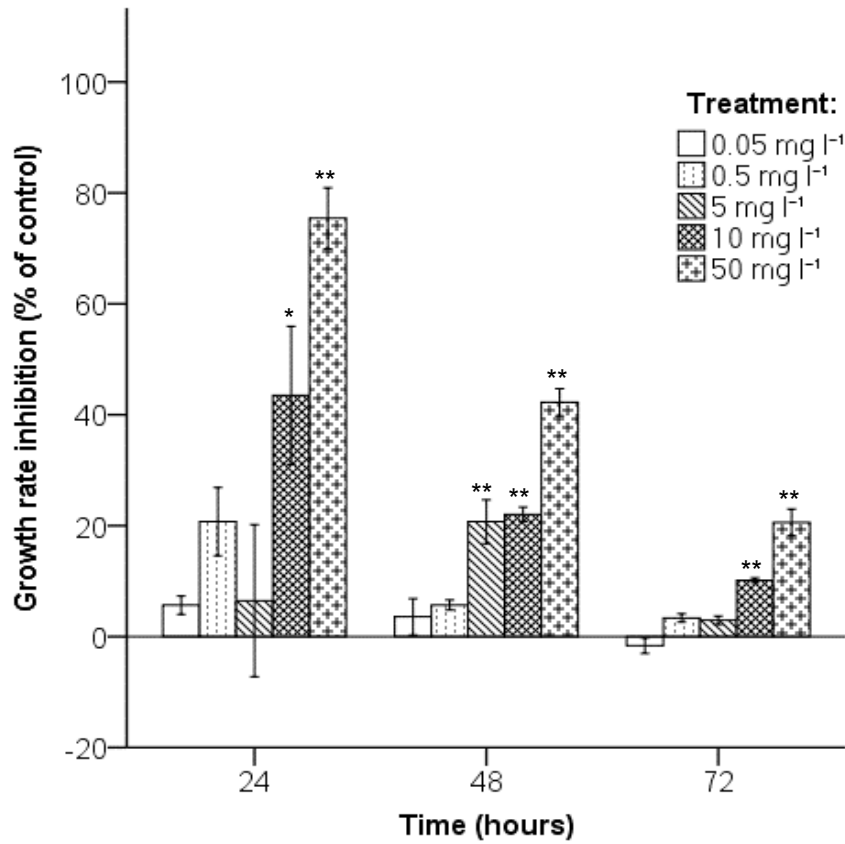


Figure 2.4: Average growth rate inhibition (GI%) of algae exposed to increasing concentrations of n-TiO₂, defined at three time intervals (24, 48 and 72 hours), and shown as a percentage of the control (0 mg l⁻¹ = 0% growth inhibition). Error bars shown mean \pm SE of four independent replicates. Significance, relative to the control, is shown at $p = < 0.05$ (*) and $p = < 0.01$ (**).

Temporal patterns

After 24 hours of n-TiO₂ exposure, the GI% was 6% (0.05 mg l⁻¹), 21% (0.5 mg l⁻¹), 7% (5 mg l⁻¹), 44% (10 mg l⁻¹) and 75% (50 mg l⁻¹). Cells exposed to the 10 and 50 mg l⁻¹ treatments showed significantly higher levels of GI% ($F_{(5, 18)} = 12.31$, $p = < 0.001$). The 24-hour IC₂₀ and IC₅₀ values were calculated to be 5.06 and 28.48 mg l⁻¹ n-TiO₂ respectively, based on the GI%.

After 48 hours of n-TiO₂ exposure, the GI% was 4% (0.05 mg l⁻¹), 6% (0.5 mg l⁻¹), 21% (5 mg l⁻¹), 22% (10 mg l⁻¹) and 42% (50 mg l⁻¹). All n-TiO₂ treatments had reduced GI% from 24 hours indicating less inhibition, except from the 5 mg l⁻¹ treatment which increased by 14%. Cells exposed to the 5, 10 and 50 mg l⁻¹ n-TiO₂ treatments showed significantly higher levels of GI% ($F_{(5, 18)} = 43.51$, $p = < 0.001$). The 48-hour IC₂₀ and IC₅₀ values were calculated to be 4.47 and 58.81 mg l⁻¹ n-TiO₂ respectively, based on the GI%.

After 72 hours of n-TiO₂ exposure, the GI% was -2% (0.05 mg l⁻¹), 3% (0.5 mg l⁻¹), 3% (5 mg l⁻¹), 10% (10 mg l⁻¹) and 21% (50 mg l⁻¹). The GI% of the algal cells in all treatments had reduced relative to 48 hours. Cells exposed to the 10 and 50 mg l⁻¹ treatments showed significantly higher levels of inhibition ($F_{(5, 18)} = 45.09$, $p = < 0.001$). The 72-hour IC₂₀ and IC₅₀ values were calculated to be 44.67 and 124.01 mg l⁻¹ n-TiO₂ respectively, based on the GI%.

2.4.3 The impact of an increasing n-TiO₂ exposure concentration on the photophysiology of *Nitzschia palea*

Using PAM fluorometry, Rapid Light Curves (RLCs) (see section 2.3.6 for methodology) were generated for each replicate of the control and the treatments. These curves were used to calculate the following photosynthetic parameters: Fv/Fm , rETR_m, alpha (α) and E_k. A light curve taken from a 0.05 mg l⁻¹ n-TiO₂ culture at 24 hours shows the relationship between alpha (α), rETR_m and E_k, which is demonstrated in the RLC below (**Figure 2.5**).

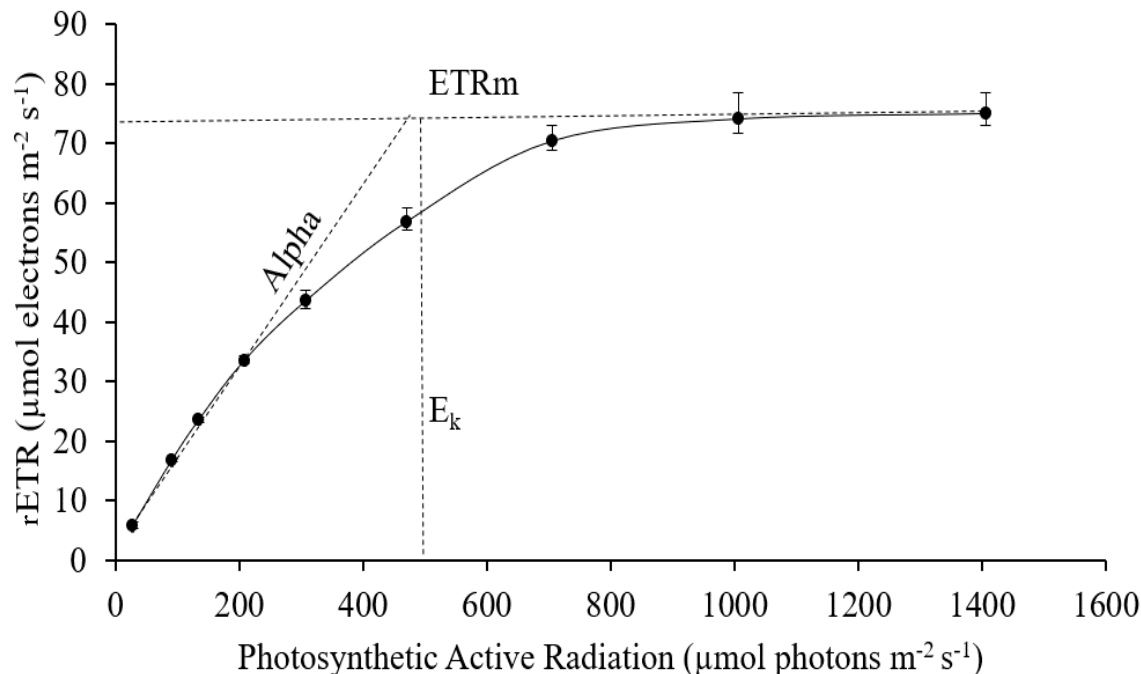


Figure 2.5: A rapid light curve (RLC) produced from a 0.05 mg l⁻¹ n-TiO₂ culture of *N. palea*. The curve shows an initial increase in the relative electron transport rate with increasing photosynthetic active radiation (PAR) before levelling off at the maximum electron transport rate (rETR_m). This levelling off the relative electron transport rate is characteristic of when the light begins to saturate which is shown on the graph by E_k (the light saturation coefficient). The initial slope of the graph is termed alpha (α), which denotes the maximum light utilization coefficient of PSII.

2.4.3.1 The effects of n-TiO₂ on the maximum quantum yield of PSII in the dark-adapted state (F_v/F_m)

The effect of an increasing n-TiO₂ concentration on the F_v/F_m of *N. palea* is presented in **Figure 2.6**. Measurements were taken at three time periods (24, 48 and 72 hours).

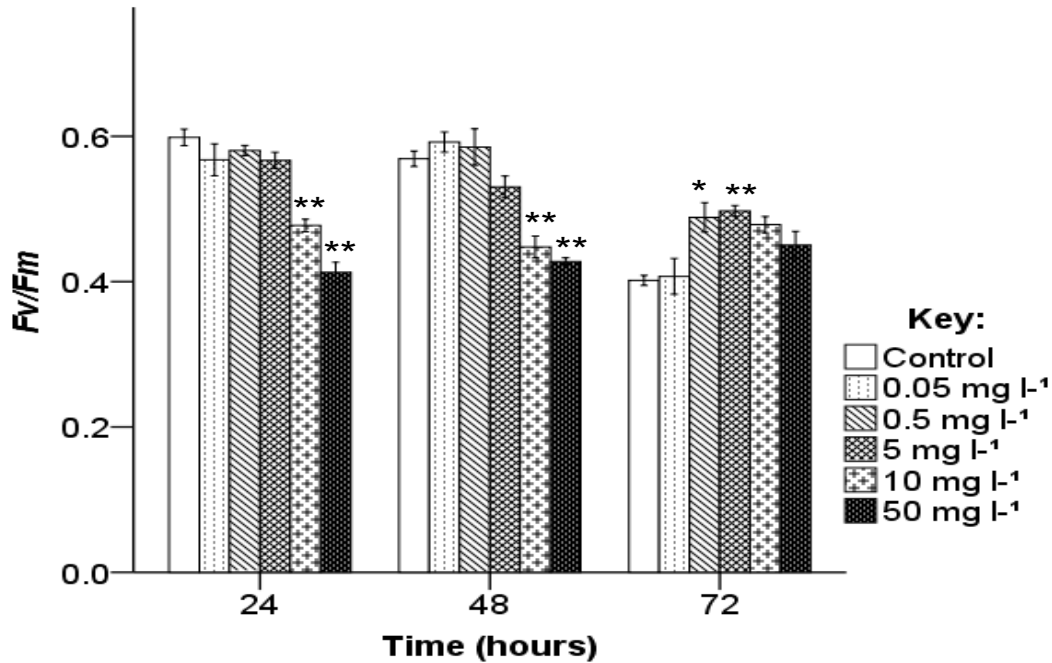


Figure 2.6: The effect of an increasing n-TiO₂ concentration on the maximum quantum yield of PSII in the dark-adapted state (F_v/F_m) for the diatom *N. palea* measured at 24 hours, 48 hours and 72 hours. Error bars show mean \pm SE of four independent replicates. Significance, relative to the control at each time point is shown at $p = < 0.05$ (*) and $p = < 0.01$ (**).

Temporal patterns

After 24 hours of n-TiO₂ exposure, the F_v/F_m was lower in all five n-TiO₂ treatments, relative to the control, though the F_v/F_m was only significantly lower in algae that were exposed to the highest n-TiO₂ treatments (10 and 50 mg l⁻¹), with values decreasing by 20% and 31% respectively, relative to the control ($F_{(5, 18)} = 30.29$, $p = < 0.001$).

After 48 hours of n-TiO₂ exposure, a similar pattern to that of 24 hours, was observed. A slight increase, though non-significant, was observed in the F_v/F_m for algae exposed to the 0.05 and 0.5 mg l⁻¹ treatments. Algae that were exposed to the highest treatments (10 and 50 mg l⁻¹) showed significantly lower F_v/F_m values and decreased by 21% and 25% respectively, relative to the control ($F_{(5,18)} = 21.75$, $p = < 0.001$).

At 72 hours, there was a reversal in the order of trend of Fv/Fm , based on concentration, for this species. All treatments showed higher Fv/Fm values compared to the control, and algae exposed to the 0.5 and 5 mg l⁻¹ treatments showed significantly higher Fv/Fm values, increasing by 22% and 24% respectively, relative to the control ($F_{(5, 18)} = 6.47$, $p = < 0.001$).

2.4.3.2 The effects of n-TiO₂ on the maximum light use coefficient for PSII (α/α) of *Nitzschia palea*

The effect of an increasing n-TiO₂ concentration on the (α) of *N. palea* is presented in Figure 2.7.

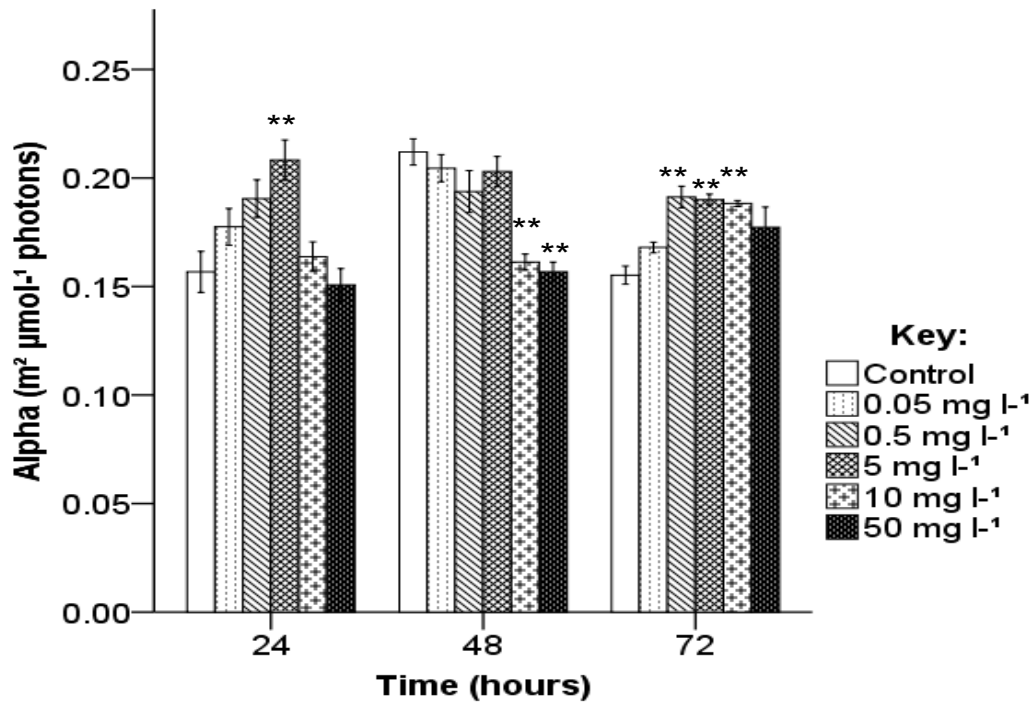


Figure 2.7: The effect of increasing n-TiO₂ concentrations on the maximum light use coefficient for PSII (α) of *N. palea* at 24 hours, 48 hours and 72 hours. Error bars show mean \pm SE of four independent replicates. Significance, relative to the control at each time point is shown at $p = < 0.05$ (*) and $p = < 0.01$ (**).

Temporal patterns

After 24 hours of n-TiO₂ exposure, the value of (α) was higher in algae exposed to the lower concentrations of n-TiO₂ (0.05, 0.5 and 5 mg l⁻¹) than in the controls. Algae exposed to the 5 mg l⁻¹ treatment significantly increased by 33% relative to the control at this time point ($F_{(5, 18)} = 6.78$, $p = < 0.001$).

After 48 hours, the value of (α) was lower in all treatments relative to the control; algae exposed to the 10 and 50 mg l⁻¹ decreased significantly by 25% and 26% respectively, relative to the control at this time point ($F_{(5, 18)} = 13.41$, $p = < 0.001$).

After 72 hours, the trend reversed and the value of (α) was higher in all treatments relative to the control; algae exposed to the 0.5, 5 and 10 mg l⁻¹ treatments significantly increased by 23%, 22% and 21% respectively ($F_{(5, 18)} = 8.65$, $p = < 0.001$).

2.4.3.3 The effect of n-TiO₂ on the maximum relative electron transport rate (rETR_m) of *Nitzschia palea*

The effect of an increased n-TiO₂ concentration on the rETR_m of *N. palea* is presented in **Figure 2.8**.

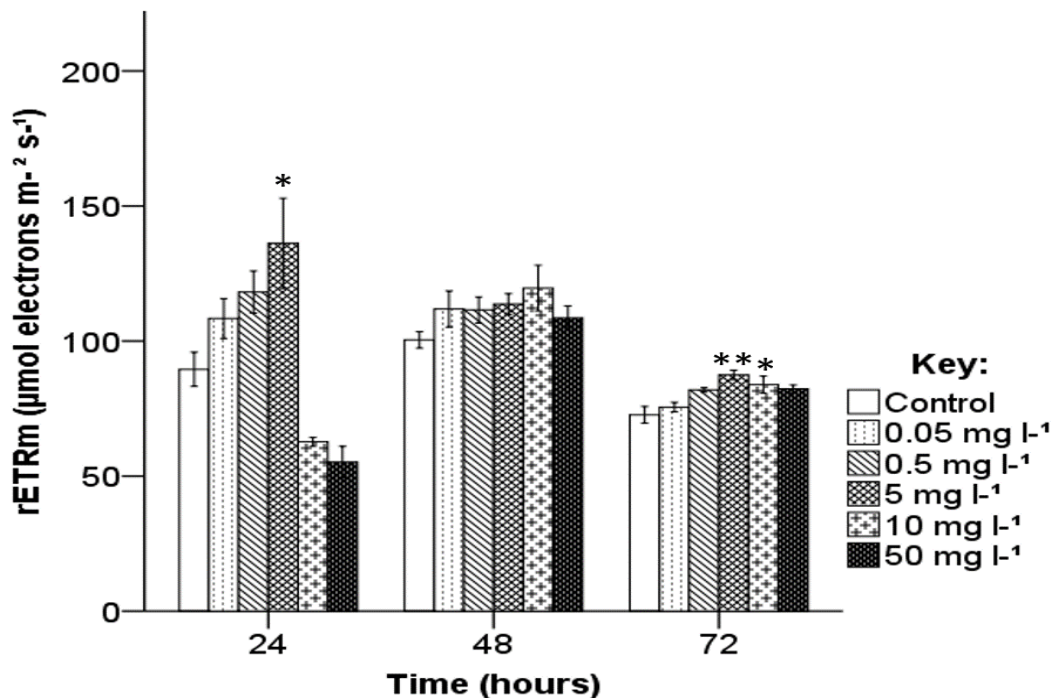


Figure 2.8: The effect of increasing n-TiO₂ concentrations on the maximum electron transport rate (rETRm) of *N. palea* at 24 hours, 48 hours and 72 hours. Error bars show mean \pm SE of four independent replicates. Significance, relative to the control at each time point is shown at $p = < 0.05$ (*) and $p = < 0.01$ (**).

Temporal patterns

After 24 hours of n-TiO₂ exposure, a slight increase was observed in algae exposed to the 0.05, 0.5 and 5 mg l⁻¹ treatments, as the rETRm increased by 21% and 32% in the 0.05 and 0.5 mg l⁻¹ treatments and significantly increased by 52% in the 5 mg l⁻¹ treatment ($F_{(5, 18)} = 3.16$, $p = 0.013$). The rETRm decreased by 30% and 38% in the 10 and 50 mg l⁻¹ treatments, but this decrease was not found to be significant relative to the control sample.

After 48 hours, the rETRm showed no significant differences between treatments at this time point ($F_{(5, 18)} = 1.32$, $p = 0.299$).

After 72 hours, the rETRm was higher in all treatments relative to the control. The rETRm significantly increased by 20% and 12% in algae exposed to the 5 and 10 mg l⁻¹

treatments ($F_{(5, 18)} = 6.51$, $p = < 0.001$).

2.4.3.4 The effect of n-TiO₂ on the light saturation coefficient (E_k) of *Nitzschia palea*

The effect of an increasing n-TiO₂ concentration on the E_k of *N. palea* is presented in Figure 2.9.

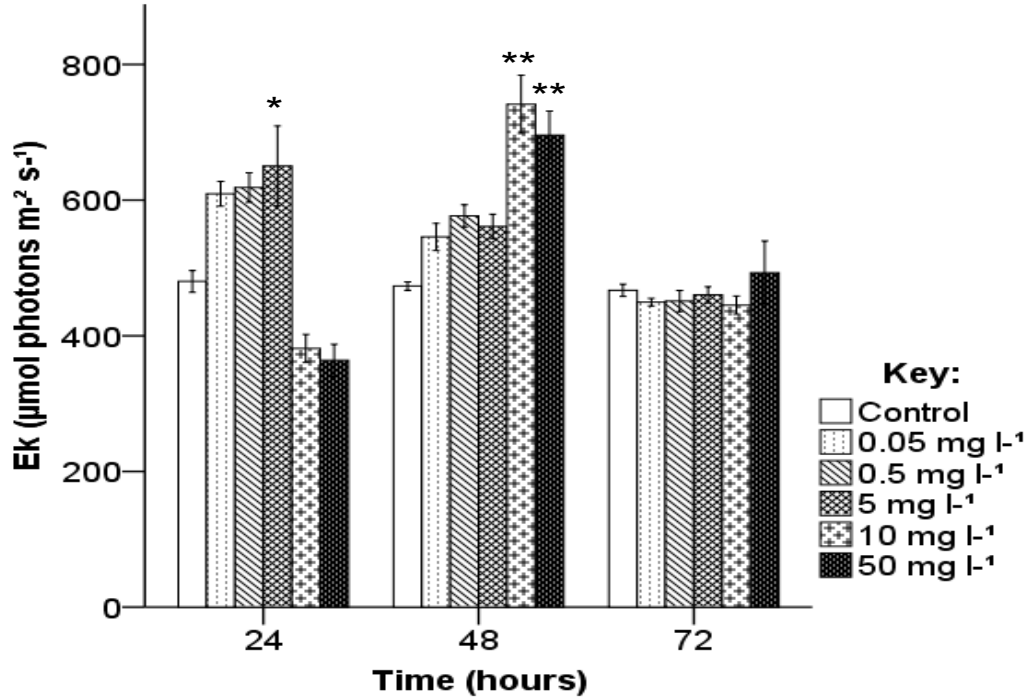


Figure 2.9: The effect of increasing n-TiO₂ concentrations on the light saturation coefficient (E_k) of *N. palea* at 24 hours, 48 hours and 72 hours. Error bars show mean \pm SE of four independent replicates. Significance, relative to the control at each time point is shown at $p = < 0.05$ (*) and $p = < 0.01$ (**).

Temporal patterns

After 24 hours of n-TiO₂ exposure, a slight increase in E_k was observed in algae exposed to the 0.05, 0.5 and 5 mg l⁻¹ treatments, as the E_k increased by 27% and 29% in the 0.05 and 0.5 mg l⁻¹ treatments and significantly increased by 35% in the 5 mg l⁻¹ treatment ($F_{(5, 18)} = 17.32$, $p = < 0.001$).

After 48 hours, an increase in E_k was observed in algae exposed to the 10 and 50 mg l⁻¹, as the E_k significantly increased by 57% and 47% respectively ($F_{(5, 18)} = 14.67$, $p = < 0.001$).

After 72 hours, no significant differences in E_k were found between treatments ($F_{(5, 18)} = 0.65$, $p = 0.668$).

2.4.4 Imaging diatom cells using light microscopy

Images of *N. palea* are shown for the control treatment (0 mg l⁻¹) (**Figure 2.10a**) and the 50 mg l⁻¹ treatment (**Figure 2.10b**). In the 50 mg l⁻¹ treatment, the formation of n-TiO₂ aggregates is evident, and is indicated in the figure by the red arrow. The n-TiO₂ aggregates can be seen adhered to the surface of an *N. palea* cell, showing evidence of heteroaggregation.

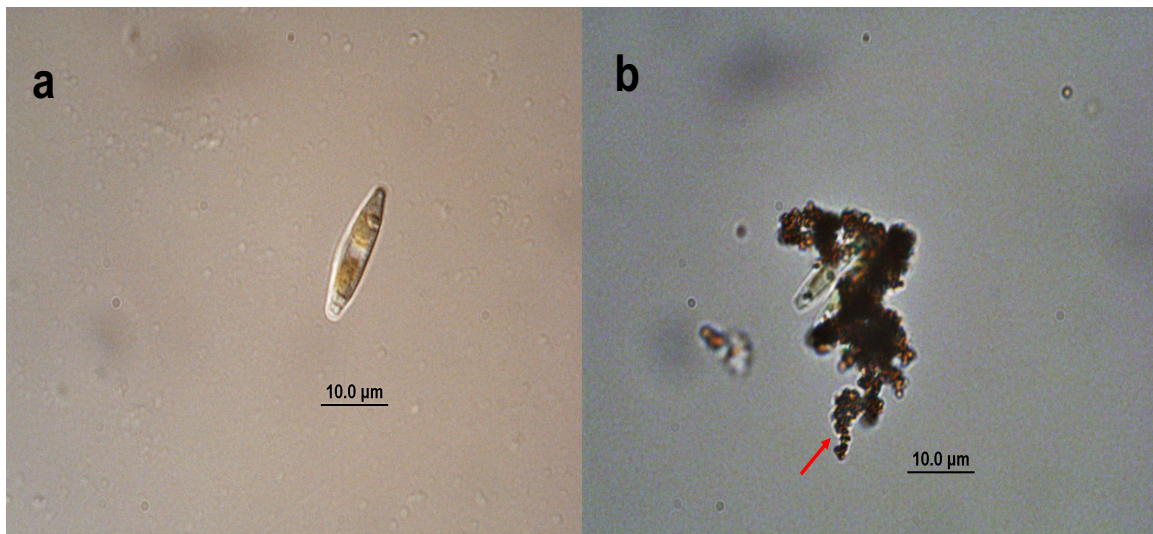


Figure 2.10: Images of *N. palea* using light microscopy for the control treatment (**a**) and the 50 mg l⁻¹ treatment (**b**). Red arrow shows aggregations of n-TiO₂.

2.4.5 Summary of results

- Algae exposed to n-TiO₂ at concentrations 10 and 50 mg l⁻¹ showed significantly higher GI at all time points
- The amount of GI reduced over time, with the highest GI found at 24 hours when algae were exposed to high concentrations of n-TiO₂ (50 mg l⁻¹)

- Algae exposed to n-TiO₂ concentrations 10 and 50 mg l⁻¹ showed significantly lower Fv/Fm at 24 and 48 hours, relative to the control at that time point. At 72 hours, there was a reversal in the order of trend for Fv/Fm and significant increases in Fv/Fm were observed in algae exposed to 0.5 and 5 mg l⁻¹ n-TiO₂, relative to the control at that time point.
- The rETR_m of the algae initially increased at relatively low n-TiO₂ concentrations and was lower at relatively high n-TiO₂ concentrations. As time passed, the treatments showed higher ETR_m values relative to the control.
- The alpha of the algae initially was higher at relatively low n-TiO₂ concentrations and lower at relatively high n-TiO₂ concentrations. As time passed, the treatments showed higher alpha values relative to the control.
- The E_k of the algae initially was higher at relatively low n-TiO₂ concentrations and lower at relatively high n-TiO₂ concentrations. At 48 hours, algae exposed to the 10 and 50 mg l⁻¹ treatments showed significantly higher E_k values. As time passed, the treatments showed higher E_k values relative to the control.

2.5 Discussion

The major aims of this chapter were to (i) establish whether an increasing n-TiO₂ exposure concentration impacted the growth rate and growth rate inhibition of *N. palea* and (ii) to establish whether an increasing exposure concentration impacted the photophysiology of *N. palea*. This study also aimed to compare whether *N. palea* was more or less impacted by n-TiO₂ exposure than green algae.

2.5.1 The effect of n-TiO₂ exposure on the growth of the freshwater diatom, *Nitzschia palea*

It was hypothesised that an increasing n-TiO₂ concentration would negatively impact the growth rate and growth rate inhibition of *N. palea*, and that negative impacts would increase over time. An increasing n-TiO₂ concentration did impact the growth rate and

growth rate inhibition, however, these negative impacts seemed to reduce over time. The IC₅₀ values obtained in this study indicate that n-TiO₂ exerts an acute toxicity effect on *N. palea*. This is confirmed by observed increases in the GI at 24 hours (24-hour IC₅₀: 28.48 mg l⁻¹), then GI rates are reversed at 48 hours (48-hour IC₅₀: 58.81 mg l⁻¹) and further reversed at 72 hours (72-hour IC₅₀: 124.01 mg l⁻¹). A similar finding was recorded in the marine diatom, *Phaeodactylum tricornutum*, where the GI in algal cells exposed to n-TiO₂ was highest at 24 hours (IC₅₀: 12.65 mg l⁻¹), before decreasing at 48 (IC₅₀: 72.70 mg l⁻¹) and 72 hours (IC₅₀: 167.79 mg l⁻¹) (Wang *et al.*, 2016). Reduction in GI has also been recorded in the green alga, *Chlamydomonas reinhardtii* (Wang *et al.*, 2008). Wang *et al.* (2008) showed that growth was completely inhibited after three days of n-TiO₂ exposure (>10 mg l⁻¹); by day five, algal cell concentration in the treatments had recovered and were similar to the control. Results from this study, however, do not concur with findings that have shown GI to increase with increasing exposure time to n-TiO₂ (Chen *et al.*, 2012; Li *et al.*, 2015; Deng *et al.*, 2017; Jia *et al.*, 2019). The growth of the diatom *Nitzschia frustulum* was inhibited at 24 hours (IC₅₀: 20.75 mg l⁻¹) and GI increased further at 48 hours (IC₅₀: 28.39 mg l⁻¹) and slightly more at 72 hours (IC₅₀: 28.98 mg l⁻¹) (Jia *et al.*, 2019).

One important question was to find out if *N. palea* was more or less susceptible to n-TiO₂ exposure compared to green algae. Published results of testing the impacts of n-TiO₂s on green microalgae show substantial variation which is likely due to methodological variations (including preparation of n-TiO₂s, incubation conditions, biomass quantification (see Table 1, Chapter 1). This makes it difficult to compare the sensitivity of *N. palea* and green algae to n-TiO₂s. Most studies on green algae have only determined 72-hour IC₅₀ values. The majority of studies on green algae, such as *R. subcapitata* and *Chlorella sp.*, report these algae are more susceptible to n-TiO₂ exposure after 72 hours, with IC₅₀s of 5.83 mg l⁻¹ (Aruoja *et al.*, 2009), 2.53 mg l⁻¹ (Lee & An, 2013), 6.26 mg l⁻¹ (Iswarya *et al.*, 2015) and 39 mg l⁻¹ (Manier *et al.*, 2015). However, some studies on *R. subcapitata* and *Desmodesmus subspicatus* show similar toxicity to n-TiO₂ at 72-hour values to this study, with recorded IC₅₀s of >50 mg l⁻¹ (Hund-Rinke & Simon, 2006), 160 mg l⁻¹ (Hartmann *et al.*, 2010) and 113 mg l⁻¹ (Metzler *et al.*, 2011). In this study, *N. palea* was most susceptible to n-TiO₂

exposure after 24 hours, suggesting that the species may be useful for rapid 24-hour toxicity tests using OECD guidelines. Importantly, this result indicates that they can recover from initial toxic shock; researchers that did not do 24 hour toxicity tests may have missed higher toxicity values at 24 hours. Many studies on green algae have not determined the IC₅₀ after 24 hours. However, due to changing characteristics of ENPs throughout the experiment (e.g. increased homoaggregation and heteroaggregation), doing so may be beneficial.

2.5.1.1 Temporal patterns: initial increase in growth inhibition from 0-24 hours

The increase in GI at 24 hours could be explained by heteroaggregation between the n-TiO₂s and the algal cells. Evidence of concentration-dependent heteroaggregation has been shown in a study investigating the effects of n-TiO₂ on green alga, *R. subcapitata*, where higher concentrations of n-TiO₂ caused greater heteroaggregation (Hartmann *et al.*, 2010). Heteroaggregation can be observed in this study in the light microscopy image of *N. palea* exposed to the 50 mg l⁻¹ n-TiO₂ treatment (**Figure 2.10b**), where n-TiO₂s are seen adhered to the algal cell surface, which traps the algae, despite *N. palea* being a motile species that could potentially move away from n-TiO₂ stress. Other studies have shown that the process of heteroaggregation can cause algal cells to become entrapped with n-TiO₂s (Aruoja *et al.*, 2009; Xia *et al.*, 2015). Adsorption of n-TiO₂s onto the algal cell surface can directly affect the algae by damaging the cell wall (Gao *et al.*, 2018) or indirectly through reducing the amount of photosynthetic light necessary for growth and affecting nutrient exchange (Xia *et al.*, 2015). There is evidence that indicates that n-TiO₂s can become internalized in algal cells, as shown in a study with *Nitzschia closterium* (Xia *et al.*, 2015), and once situated within the cell, the n-TiO₂s can bind to the chloroplast and induce ROS generation (Li *et al.*, 2015), which can cause severe oxidative damage to DNA, proteins and lipids (Sharma *et al.*, 2012). It was not possible within the timeframe of the project to look for evidence of internalisation of n-TiO₂ in *N. palea* cells. Algal cell wall pores have an average diameter of 5-20 nm, and n-TiO₂s with a size smaller than that have been found to pass directly through the cell wall (Xia *et al.*, 2015). Internalization of n-TiO₂s in this study, therefore, may be unlikely due to the large size of particles used (50 nm). However, because of their mitotic division, it may be that the diatoms are particularly vulnerable to n-TiO₂ internalisation

before the new cell wall is produced (Debenest *et al.*, 2008).

2.5.1.2 Temporal patterns: the reduction in growth inhibition from 24-72 hours

This temporal reduction in GI may result from algal adaptation to n-TiO₂ exposure and a subsequent recovery response. However, evidence produced from this experiment indicated that this reduction in GI could also mean the algal growth rate in control samples is slowing, whilst the growth rate of the high n-TiO₂ concentrations are not. As shown in **Table 2.3**, the algal growth rate for the control sample slowed from 1.96 day⁻¹ at 24-48 hours to 0.25 day⁻¹ at 48-72 hours. Slowing of the algal growth rate in the 50 mg l⁻¹ n-TiO₂ sample was less substantial, decreasing from 1.37 day⁻¹ (24-48h hours) to 0.70 day⁻¹ (48-72 hours). These results indicate the growth rate of the control is slowing down at 72 hours, potentially due to the cells reaching stationary phase and the high n-TiO₂ treatment cultures gradually "catching up" with the controls when nutrients become limiting (Nyholm, 1985). For toxicity testing, the OECD recommends starting biovolumes of 10⁴ and 5 x10³ cells/ml for *F. pelliculosa* and *R. subcapitata* respectively (OECD TG 201, 2011). In this experiment, the starting biovolume for *N. palea* was based on the recommendation for OECD recommended diatom, *F. pelliculosa*. However, *N. palea* is a fast growing and larger species (Licursi & Gomez, 2013) and a lower starting concentration may be necessary to avoid nutrient depletion after 72 hours. The initial cell density should be taken into consideration in future n-TiO₂ toxicity testing, as differences in initial cellular density may cause different toxicity outcomes (Moreno-Garrido *et al.*, 2000). Evidence has shown that as the number of initial cells increases, the negative impacts of n-TiO₂s are decreased (Metzler *et al.*, 2018). Moreover, the increasing cell density throughout the experiment could alter the toxicity of n-TiO₂s. As the algal cell density increases, the amount of EPS released from the algae also increases, which may interact with the n-TiO₂s and cause changes to particle behaviour (Sorensen & Baun, 2015). Research has shown EPS can adsorb n-TiO₂s, and that increased levels of EPS caused increased levels of homoaggregation (Gao *et al.*, 2018). Therefore, when the algae secrete EPS through motility, this may cause higher levels of homoaggregation.

The recovery in GI could be attributable to increased homoaggregation over time. Ho-

moaggregation between n-TiO₂s may occur due to the high ionic salt content of the media. The OECD media used in this experiment contains salts e.g. CaCl₂ and MgSO₄, which are required as nutrients to allow algal growth. The presence of these salts, however, may cause enhanced homoaggregation over time, as studies have shown that a high ionic strength media causes enhanced homoaggregation over typical 72-hour toxicity tests (Doyle *et al.*, 2014; He *et al.*, 2015; Danielsson *et al.*, 2017). The effect of homoaggregation means that the diameter of the n-TiO₂s will increase throughout the experiment, increasing the mean n-TiO₂ aggregate size. Increased homoaggregation is thought to reduce the number of active sites available on the n-TiO₂s, and therefore reducing the chances of heteroaggregation between the n-TiO₂s and the algal cells (Wang *et al.*, 2016). This indicates that 72-hour toxicity tests may not be reliable, as throughout the experiment, due to increased homoaggregation, the nano-scale particles are no longer being tested.

2.5.2 The effect of n-TiO₂ on the photophysiology of *Nitzschia palea*

It was hypothesised that an increasing n-TiO₂ concentration would negatively impact the photophysiology of *N. palea*, causing reductions in all measured photosynthetic parameters. The only photosynthetic parameter that was negatively impacted by the presence of n-TiO₂ was the Fv/Fm which showed significant reductions, relative to the control, at 24 and 48 hours when exposed to 10 and 50 mg l⁻¹ n-TiO₂. The maximum PSII fluorescence in the dark-adapted state (Fv/Fm) is useful when inferring photosynthetic microalgal physiological status (Lombardi & Maldonado, 2011), and this parameter has been used as an end-point in many other studies evaluating the impact of ENPs on freshwater and marine algae (Chen *et al.*, 2012; Deng *et al.*, 2017; Marchello *et al.*, 2018; Middepogu *et al.*, 2018), whereas ETR_m, α , and E_k have rarely been used. At both 24 and 48 hours, Fv/Fm was lower in algae exposed to the 10 and 50 mg l⁻¹ n-TiO₂ treatment, relative to the control. At 72 hours, Fv/Fm showed a trend reversal relative to that observed at 24 and 48 hours. Significant increases in Fv/Fm , relative to the control, were recorded in the 0.5 and 5 mg l⁻¹ treatments. Similar findings were observed in the green alga *Chlamydomonas reinhardtii*, where exposure to n-TiO₂ (a mixture of anatase and rutile) (>1 mg l⁻¹) generated an initial decrease in Fv/Fm , but by 72 hours cell Fv/Fm values were higher in treatments compared

to the control (Chen *et al.*, 2012). Results obtained for this current thesis, however, do not concur with Deng *et al* (2017), who observed that the Fv/Fm of *P. tricornutum* was not affected after 48 hours of n-TiO₂ (anatase) exposure, but was significantly lower after 72 hours, relative to the control. Middepogu *et al* (2018) also observed a significant decrease in the Fv/Fm of *Chlorella pyrenoidosa* after 72 hours, relative to the control.

2.5.2.1 Temporal patterns

The decrease in Fv/Fm at 24 and 48 hours in the high n-TiO₂ treatments, compared with control values, could be explained by n-TiO₂ exposure causing the downregulation of genes involved in photosynthetic pathways (Middepogu *et al.*, 2018). The genes involved in the carbon fixation stage of photosynthesis in green alga, *C. pyrenoidosa*, have been shown to be downregulated in response to n-TiO₂ exposure (Middepogu *et al.*, 2018). Also, the internalization of reactive oxygen species (ROS) in algal cells has been shown to decrease concentrations of soluble proteins in *C. reinhardtii* (Chen *et al.*, 2012), which may cause inhibition of protein synthesis and therefore certain proteins involved in photosynthesis may not be produced, thus causing an overall decrease in photosynthetic activity.

At 72 hours, some n-TiO₂ treatments showed significantly higher Fv/Fm values compared to the controls. In addition to being an indicator of overall algal health, Fv/Fm is a sensitive indicator of sub-lethal effects, including nutrient depletion (Dijkman & Kromkamp, 2006). In healthy cells, Fv/Fm values are around 0.6 for green algae (Maxwell & Johnson, 2000) and slightly lower than that for diatoms (Dijkman & Kromkamp, 2006). The Fv/Fm for *N. palea* at 24 and 48 hours was 0.60 and 0.57 respectively, an expected value for healthy cells. At 72 hours, the Fv/Fm for *N. palea* was 0.40, an atypical value in healthy diatoms. This supports the idea that *N. palea* was potentially nutrient limited. There also may have been excess algal cells in the control samples, limiting light available to cells at the bottom of the biofilm. Therefore, cells lower in the biofilm, with reduced light exposure, may have shown lower Fv/Fm values.

Algae exposed to relatively low concentrations of n-TiO₂ may also be recovering. It

could be that low n-TiO₂ concentrations are stimulating low levels of ROS production, a level which is beneficial for algal growth and secondary metabolite accumulation (Kang *et al.*, 2014; He *et al.*, 2017). Levels of ROS can be decreased from a high to low concentration by the upregulation of an antioxidant enzyme group called superoxide dismutases (SOD), commonly referred to as "scavenger enzymes" as they help to scavenge excess ROS (Mosa *et al.*, 2018). This has been demonstrated in a green alga, *Scenedesmus obliquus*, where the upregulation of SOD was consistent with increased levels of ROS (Liu *et al.*, 2018).

2.5.3 Limitations and caveats of study

There were two main limitations in this study. Firstly, the starting cell concentration of *N. palea* was 10,000 cells/ml, which is a value based on the starting cell concentration of the OECD recommended diatom, *F. pelliculosa*. It may be possible, however, that the starting cell concentration for *N. palea* was too high, and because *N. palea* is a particularly fast growing species, a lower starting concentration may be necessary to prevent the control growth rate slowing over time. Secondly, an interesting observation in this study was the recovery in cell number of the high n-TiO₂ treatments after 72 hours of exposure. It would be beneficial to run the experiment for a longer period, e.g. 96 hours, to assess whether the final cell yield ends up being a similar value to that of the control sample.

2.5.4 Conclusion

In this study, I demonstrate for the first time that the diatom, *N. palea* was negatively affected by n-TiO₂ exposure, with regards to growth and photophysiology. Negative impacts were most pronounced after 24 hours, particularly with respect to growth inhibition and *Fv/Fm*. Decreasing levels of growth inhibition throughout the experiment may be due to the control sample growth rate slowing down, suggesting that a lower starting cell concentration may be beneficial for ENP toxicity testing with *N. palea*. This study confirms the short-term toxicity impacts of n-TiO₂ to benthic diatom *N. palea*. Due to the short-term susceptibility and easy identification of *N. palea* following n-TiO₂ exposure, this species may be a useful indicator species for rapid 24-hour toxicity tests of n-TiO₂s following OECD guidelines. However, due to transformational changes in the n-TiO₂s over longer 72-hour experiments,

revisions to OECD protocols for testing ENPs should be considered. Future studies should make use of shorter-term experiments for ENP toxicity testing, to reduce the amount of time needed for aggregation and sedimentation of the ENPs, which may alter the toxicity of ENPs to microalgae.

CHAPTER 3

The effects of titanium dioxide nanoparticles ($n\text{-TiO}_2$) on riverine biofilm communities in the field (Mill Stream, Tributary of River Frome, Dorset)



Watercolour of river by Tom Timberlake

3.1 Introduction

3.1.1 The roles of benthic biofilms in freshwater ecosystems

FRESHWATER benthic biofilms consist of a diverse community of phototrophic and heterotrophic microorganisms; benthic diatoms can be a dominant phototrophic component in these assemblages (Blinn *et al.*, 1980). In freshwaters, benthic biofilms are typically investigated in relatively shallow aquatic environments, affixed to natural or artificial substrata, such as stone, sediments or man-made materials. Secretions of extracellular polymeric substances (EPS) ensure the adhesion of microorganisms in a matrix-like structure, allowing the exchange of vital nutrients (Kurniawan *et al.*, 2015). In the benthic zone of a freshwater body, benthic diatoms are considered extremely important and have a central role in freshwater ecosystems. They provide many valuable ecosystem services, such as contributing to oxygen production (Kroll *et al.*, 2014), serving as a vital habitat and food source for aquatic invertebrates (Kroll *et al.*, 2014) and play a critical role in nutrient cycling. Biofilms can also help to alleviate toxic conditions by mopping up toxic compounds (Carvalho, 2018); EPS from the biofilms has been shown to bind heavy metals preventing entry to the biofilm (Teitzel & Parsek, 2003; Cheng *et al.*, 2018). Biofilms are regarded as an effective "community level monitoring" tool because they are relatively easy to sample, and provide a longer-term indication of the ecological status of the habitat.

3.1.2 The diatom fraction of freshwater biofilms

Within the biofilm, the diatoms can be grouped into ecological guilds depending on their growth morphologies. Passy (2007) defined three ecological guilds which include the low profile, high profile and the motile guild. Species that are classified in the "low profile guild" are ones that are of short stature, including prostrate and adnate diatoms, directly attached to the substrate at the bottom of the biofilm. These species are slow-moving, and do not tolerate high levels of nutrient pollution, but are relatively resistant to physical disturbances. Some of the genera include: *Achnanthes*, *Achnanthidium*, *Amphora*, and *Cocconeis*. Species that are classified in the "high profile guild" are larger, and reside in the upper-story of the biofilm. These species have a taller stature, with erect and stalked growth forms, and

are relatively tolerant to nutrient pollution, however they are more sensitive to physical disturbances (Passy, 2007; Marcel *et al.*, 2017). Some of the genera include: *Diatoma*, *Fragilaria*, *Gomphonema* and *Melosira*. Species that are classified in the "motile guild" have the ability to move, allowing the diatoms to optimize their position within the biofilm (Rimet & Bouchez, 2011). Some of the genera include: *Navicula*, *Nitzschia*, *Sellaphora* and *Surirella*. These ecological guilds have been used previously to assess nutrient and pollution stress in freshwater environments (Passy, 2007; Rimet & Bouchez, 2011; Marcel *et al.*, 2013).

Within the biofilm, species have varied individual tolerances to environmental pollutants. By sampling the community, an average tolerance value can be predicted, generating an integrated picture of the impact of a stressor, over a set time period (Guasch *et al.*, 2016). Much of the previous work on benthic biofilms has focused on assessing nutrient status (Kelly & Whitton, 1995; Kelly *et al.*, 2008). The increasing use of ENPs and their subsequent release into the environment has led to concerns about their impacts on freshwater biofilms. Given the importance of biofilms in freshwater ecosystems, it is essential that we better understand the impacts of stressors, such as ENPs. Due to the complexity of measuring concentrations of ENPs in freshwater environments, researching the use of artificial mesocosms to test the impacts of ENPs on freshwater biota in the benthos would be beneficial.

3.1.3 The use of artificial mesocosms to study biofilm functioning in freshwater environments

Due to the challenges posed by carrying out *in situ* measurements to determine the impacts of stressors on stream biofilms, a number of researchers have deployed artificial mesocosms. Artificial mesocosms have been deployed to evaluate the effects of anthropogenic pollutants, including herbicides (Seguin *et al.*, 2002; Pérez *et al.*, 2007; Rimet & Bouchez, 2011), insecticides (Finnegan *et al.*, 2018) and heavy metals (Smolyakov *et al.*, 2010; Shamshad *et al.*, 2016). The use of artificial mesocosms in field studies has several important advantages when compared to a fully natural system. When studying the effects of anthropogenic pollutants on freshwater biofilms, mesocosms allow a degree of control over the experiment, alleviating unmanageable, and often episodic factors that occur in the field,

such as high flooding, high winds, large invertebrate grazing, and the co-occurrence of other environmental contaminants (Sabater & Borrego, 2015).

3.1.4 The impact of titanium dioxide nanoparticles (n-TiO₂s) on freshwater biofilms

The growing industrial usage of ENPs will inevitably cause an increase in their concentrations in freshwater environments, entering directly from degraded consumer products (Bundschuh *et al.*, 2018) or indirectly in effluent from sewage treatment works (Vale *et al.*, 2016). Predicted environmental concentrations (PECs) for n-TiO₂ are 16 µg l⁻¹ in water and up to mg/kg concentrations in the sediment (Gottschalk *et al.*, 2009). It has been reported that the fate and behaviour of n-TiO₂s in freshwater biofilms was largely unknown (Navarro *et al.*, 2008). Since then, many authors have focused on the impacts of n-TiO₂s in single species, laboratory experiments, with an emphasis on impacts to planktonic species of algae (see Introduction in Chapter 2), and there are only limited published papers investigating n-TiO₂ effects on whole algal communities in mesocosm experiments.

It has been demonstrated that freshwater biofilms can efficiently receive, bind and accumulate n-TiO₂s (Battin *et al.*, 2009). Trials demonstrated that, in riverine mesocosms, the travel length of n-TiO₂s down a flume mesocosm was reduced on average 2.7 times, relative to mesocosms with no biofilms, due to increased n-TiO₂ accumulation in the biofilms (Battin *et al.*, 2009). This suggests biofilms can become a concentrated repository for n-TiO₂s in freshwater ecosystems. Some research into the impacts of n-TiO₂ on algal biofilm communities (laboratory/field based biofilms) has focused on long-term (28-78 days) exposure effects considering effects on whole aquatic food webs (Kulacki *et al.*, 2012; Jovanovic *et al.*, 2016; Wright *et al.*, 2018). Kulacki *et al.* (2012) investigated n-TiO₂ (1 mg l⁻¹) impacts on laboratory-based biofilms. Results indicated that the biofilm growth from algal monocultures and polycultures in mesocosms was not altered, but n-TiO₂ accumulation was higher in biofilms that held multiple species. Although no negative effects were observed, the flume mesocosms used in this study were an oversimplification of natural streams, and do not mimic natural environmental conditions that could alter the toxicity of n-TiO₂s. Jovanovic

et al (2016) investigated the effect of n-TiO₂s (0.025-0.25 mg l⁻¹) on multiple trophic levels in field-based assemblages located in outdoor mesocosms. They presented evidence that revealed that only the biomass of rotifers was negatively affected by n-TiO₂ exposure. Wright *et al* (2018) also measured the effects of n-TiO₂s at a higher concentration (0.05-5 mg l⁻¹) on whole aquatic trophic levels in field-based assemblages and found that n-TiO₂ (5 mg l⁻¹) negatively affected ash-free dry mass and phytoplankton chlorophyll *a* content and caused changes in the species composition of algal assemblages.

There are few studies investigating the impacts of n-TiO₂s on field-based biofilm assemblages, and from the literature, it is not clear whether the impacts are positive or negative. Field experiments are critical to our understanding of the effects of n-TiO₂s in natural freshwater environments, as it could be considered that laboratory studies, particularly single-species based studies, may bear no resemblance to field study results due to additional environmental complexities in the field and because whole communities are being investigated rather than just single species.

3.2 Aims of study

This field study was carried out to investigate the impacts of n-TiO₂ on the structure and functioning of freshwater biofilm communities. This was carried out by addressing the following aims: (i) to assess changes in algal biomass in response to n-TiO₂ exposure, using pigment and dry weight analysis; (ii) to assess changes in biofilm photophysiology in response to n-TiO₂ exposure and (iii) to identify any short-term changes in diatom species composition in response to n-TiO₂ exposure. The following specific hypotheses were posed:

(i) It was hypothesised that the biomass (total chlorophyll and dry mass) would be negatively impacted after n-TiO₂ exposure, and that higher concentrations of n-TiO₂ would cause greater negative impacts on the biomass of riverine biofilm assemblages.

(ii) It was hypothesised that n-TiO₂ exposure would negatively impact the photophysiology

of riverine biofilm assemblages over time, when compared to untreated control biofilms.

(iii) *It was hypothesised that n-TiO₂ exposure would directly impact the diatom species composition in riverine biofilm assemblages.*

3.3 Methods

3.3.1 Study site and environmental data

The experimental site was the Freshwater Biological Association (FBA) River Laboratories, in East Stoke, Dorset, UK (Coordinates: 50°40'47"N 2°11'05"W) (**Figure 3.1**). The field experiments were carried out over a 16-day period (06/06/18 - 22/06/18), including the 12-day biofilm colonisation phase. The site features several experimental channels (approx. 10 m long) for research on freshwater ecology. These channels are fed by the Mill Stream, a tributary of the River Frome. The River Frome (length: 48 km), which rises in the village of Evershot, is a chalk stream that flows into Pool Harbour at its confluence with the River Piddle. With its notable biodiversity, the Frome is considered a site for special scientific interest (SSSI) (Lazar *et al.*, 2010). The river's catchment is 414 km², predominantly composed of agricultural land (75%) (Poole Harbour Catchment Plan, 2014); the only major settlement adjoining the Frome is the town of Dorchester (population: 16,801 (2001)) (Bowes *et al.*, 2011). In the tourist season, the local population grows by 13% in Dorchester and 80% in Wareham (Wessex Water, 2012).

It has been reported that the River Frome did not meet Water Framework Directive (WFD) standards in 2014 by failing to reach a "good ecological status", which is likely due to agriculture and rural land management (Environmental Agency Catchment Data Explorer, 2014). Increases in nitrate levels have been measured, with concentrations rising from 2.4 mg l⁻¹ in the 1960s to 6.0 mg l⁻¹ in 2008-2009 (Bowes *et al.*, 2011). Annual soluble reactive phosphorus levels, however, have decreased from 190 µg l⁻¹ in 1989 to 49 µg l⁻¹ in 2007-2009 due to phosphate stripping being introduced at sewage treatment works (STWs)

(Bowes *et al.*, 2011). Whilst nutrients have been monitored regularly in the River Frome, to my knowledge, there is no published information about the release of ENPs in this area.

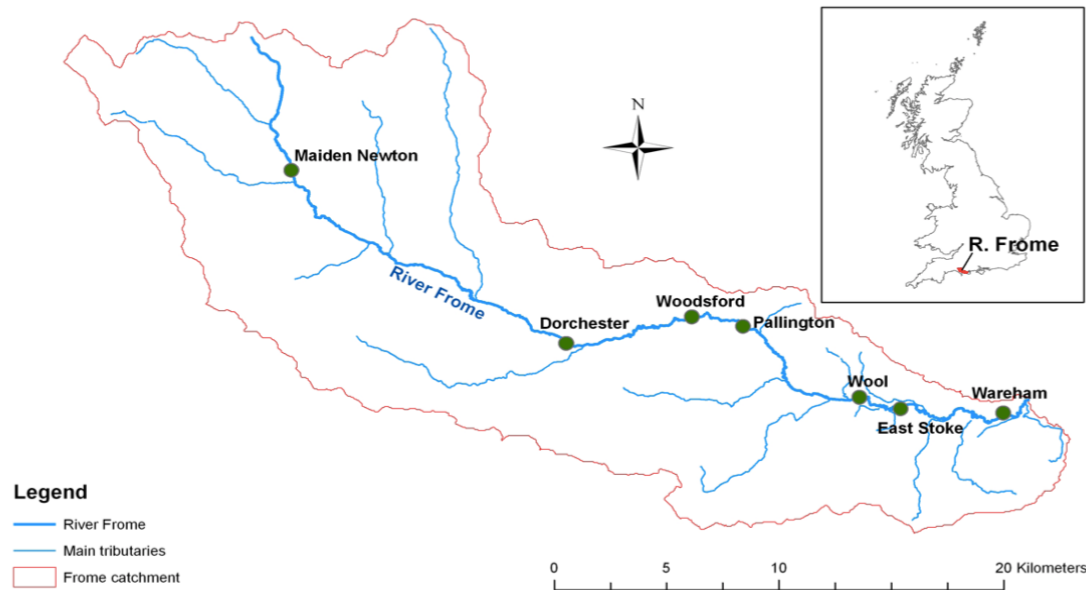


Figure 3.1: Map of the River Frome and the surrounding catchment areas. The Freshwater Biological Association (FBA) River Laboratory is situated at East Stoke, shown on the map. Image taken from Lazar *et al* (2010).

3.3.2 Experimental design

Tiles were chosen as an artificial substrate for establishing periphyton in this experiment, as they have been shown to promote rapid algal growth and have low surface variability, which prevents different algal growth trajectories (Lamberti & Resh, 1985). Unglazed and unpainted terracotta tiles (Terracotta natural quarry clay wall and floor tile, British Ceramic, Newton Abbot, UK) were used in this study. The tiles were placed in channels in the Mill Stream for an initial colonisation phase of 12 days, allowing biofilm communities to establish. Mesh (size: 1 mm) was attached to end of the channel to prevent excess detritus entering the channel and building up on the tiles. Plastic guttering channels (approx. 1 m long) were used as artificial outdoor mesocosms. The experimental system was set up drawing upon features used in the design published by Gold *et al* (2003). It comprised of a pair of plastic pipes (Verve Hose pipe, B&Q, UK) (pipe width: 25 mm) emerging from either end of the channel. Mesocosms were fed via plastic tubing, pumped (Blagdon Minipond Pump 700, Blagdon,

Dorking, UK) from a 30 l plastic reservoir, providing re-circulating river water either as controls (no added n-TiO₂) or treatments amended with dispersed n-TiO₂s (**Figure 3.2**). The river water was screened by passing it through a 250 µm mesh (Zooplankton net, Blades Scientific, Kent, UK) to remove larger material. Each channel was fed via an independent, recycled water supply at a constant flow rate. After the n-TiO₂s suspensions and river water were added to the mesocosms, the tiles, with established biofilms were transferred from the Mill Stream into the guttering channels, following a pre-incubation period.

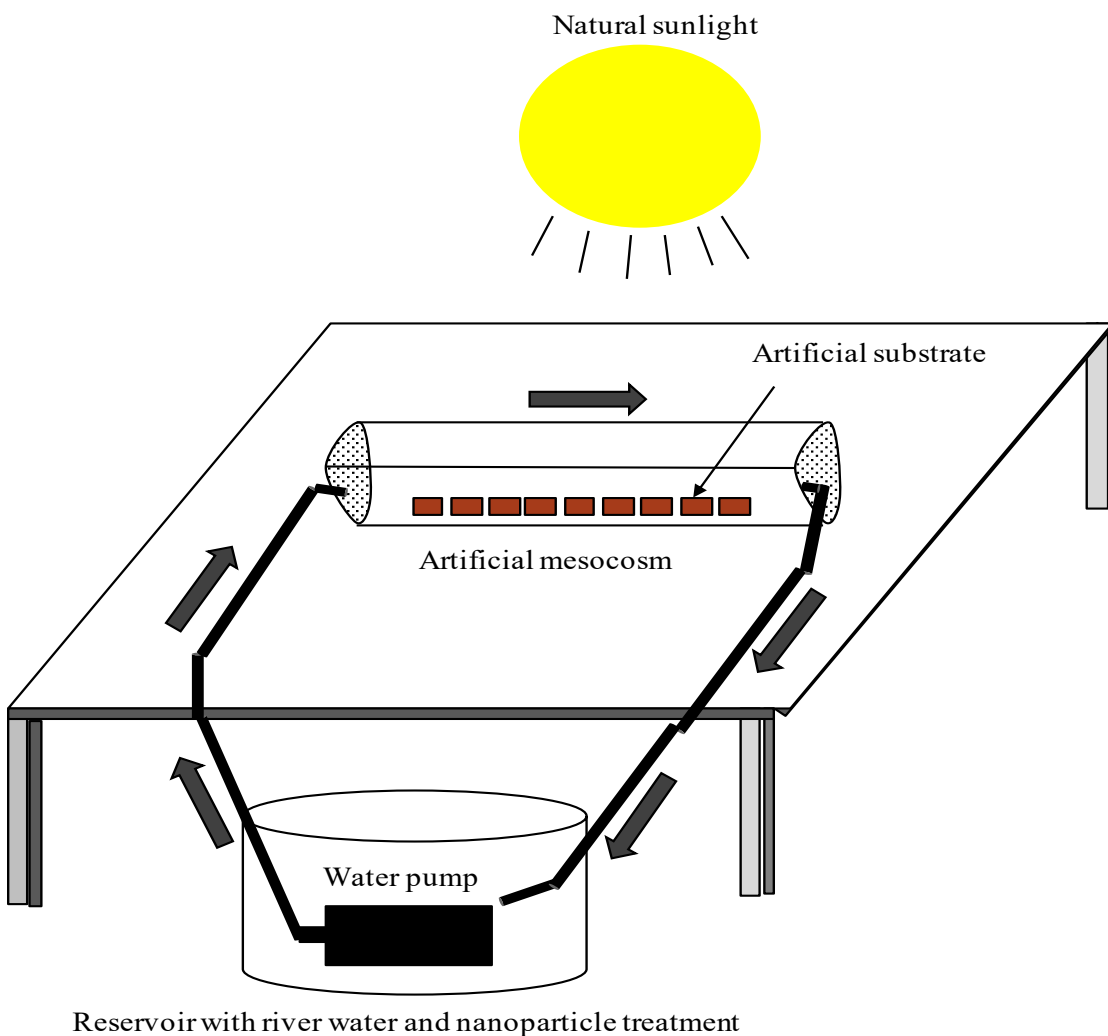


Figure 3.2: Artificial mesocosm set-up adapted from a design by Gold *et al.* (2003). Terracotta quarry tiles were placed in 1 m plastic guttering channels which were used as artificial outdoor streams. Three reservoirs were used, containing each treatment (untreated (no added n-TiO₂), 0.05 mg l⁻¹, 5 mg l⁻¹ n-TiO₂s). The grey arrows indicate the direction of water flow. Illustration completed on Powerpoint.

3.3.3 Experimental set-up

Nanomaterial suspensions were prepared immediately preceding the start of the experiment. Three artificial mesocosms were set up including one control (filtered river water and no added n-TiO₂) and two different n-TiO₂ treatments. Two concentrations of n-TiO₂ were prepared, defined as, low (0.05 mg l⁻¹) and high (5 mg l⁻¹) (see Chapter 2, section 2.3.3 for methods on nanoparticle preparation). These concentrations were chosen because the low concentration (0.05 mg l⁻¹) is an environmentally relevant concentration and the high concentration (5 mg l⁻¹) is representative of the n-TiO₂ concentration used for photocatalytic degradation of pharmaceuticals (Wright *et al.*, 2018), and is a concentration of n-TiO₂ found in wastewater treatment plants (Westerhoff *et al.*, 2011). A primary stock solution of 5000 mg l⁻¹ of n-TiO₂ was prepared in MilliQ water. The stock solution was then sonicated for 30 minutes to disperse the ENPs using a sonicator (Branson Ultrasonics, Danbury, USA). River water was collected from the Mill Stream and filtered through a plankton net (mesh size: 250 µm) to remove larger debris and macroinvertebrates. The n-TiO₂ stocks were added to the reservoirs containing filtered river water and well mixed to give final n-TiO₂ concentrations of 5 mg l⁻¹ and 0.05 mg l⁻¹. 14 l of each treatment solution was then added to mesocosms and left to age for 18 hours. The purpose of the aging process was to expose the n-TiO₂s to natural sunlight and ambient temperature before adding the colonised tiles (Seitz *et al.*, 2015).

Following 12 days of biofilm growth and an 18-hour n-TiO₂ ageing period, colonised tiles were transferred from the Mill Stream into the outdoor artificial mesocosms, which were set up adjacent to the Mill Stream. For each treatment, one channel was used; the tiles were colonised independently so each tile, within a single mesocosm can be considered a replicate for that treatment.

3.3.4 Mesocosm water properties

The temperature, pH, light irradiance levels and oxygen concentrations were measured in the mesocosm river water of each treatment channel every 24 hours over four days at a

standardised time point (14:00 hours). The pH was measured using a portable pH meter (H198185, Hanna Instruments, Rhode Island, US). The light irradiance was measured using a QRT1/PAR light sensor (Hansatech Instruments Ltd, Norfolk, UK). The oxygen levels were measured using a portable dissolved oxygen meter (HQ40D, Hach, Colorado, USA).

3.3.5 Biofilm sampling

Sampling of the freshwater biofilms was performed at 24 hours and 72 hours. Three colonised tiles were taken directly from the Mill Stream and sampled for initial measurements for biomass and photophysiology, immediately prior to the incubation of colonised tiles for the start of the outdoor mesocosm experiment. Each subsequent day, three tiles per treatment were sampled. To ensure random sampling of the tiles in any one stream, a random number generator was used. When tiles were removed, they were replaced with uncolonised tiles to avoid differences in the flow regime within the channels. Each biofilm was harvested on a tile over a standardised sampling area (25 cm²). The periphyton and any other associated material (sediments, twigs etc) was removed with a clean toothbrush into glass fibre filtered river water (Whatman GF/F, 4.2 mm diameter) and the volume of the harvested material was recorded; the slurry was then homogenized using a 2 ml syringe (0.8 mm needle, Monoject Kendall, Fisher Scientific, Leicestershire, UK). From this homogenised sample, 5 ml aliquots were taken and separated for dry mass measurement, PAM fluorometry, pigment extraction and preservation for species identification and cell enumeration.

3.3.6 Chlorophyll pigment extraction

Biofilm pigments were measured by filtering 5 ml of biofilm sample onto a filter (diameter = 47 mm, pore size = 0.45 µm) (GF/F; Whatmann, Maidstone, Kent, UK). The filter was tightly rolled, placed inside a 15 ml falcon tube and immediately stored in a freezer at -20 (°C). To extract pigments, 5 ml of 100% ethanol was added, and the sample was mixed thoroughly using a vortex for 30 seconds (VWR, Leicestershire, UK). The sample was then chilled in the fridge at 4 (°C) for 12 hours, before centrifugation at 3000 rpm (1811 RCF) for 10 minutes. The resulting supernatant was transferred to a 15 ml falcon tube and re-spun

to remove any remaining debris, which could cause undesired turbidity readings. The final supernatant was transferred to a 1 cm quartz glass cuvette and a full absorbance spectrum (400 - 800 nm) was measured using a WPA Biowave II spectrophotometer (Biochrom, Cambridge, UK). Total chlorophyll (mg l⁻¹) was calculated using an equation from Ritchie (2006) (**Equation 3.1**) and adjusted for surface area of colonisation (25 cm²). Concentrations of total chlorophyll were recorded as µg/cm². Individual chlorophyll pigments (*a*, *b*, and *c*) were also calculated to determine changes in pigment ratios at 24 and 72 hours (chlorophyll *a* = **Equation 3.2**; chlorophyll *b* = **Equation 3.3**; chlorophyll *c* = **Equation 3.4**).

$$\frac{((24.1209 \times A_{632}) + (11.2884 \times A_{649}) + (3.764 \times A_{665}) + (5.8338 \times A_{691})) \times sv}{V} / 100 \quad (3.1)$$

$$\frac{((0.0604 \times A_{632}) + (-4.5224 \times A_{649}) + (13.2969 \times A_{665}) + (-1.7453 \times A_{691})) \times sv}{V} / 100 \quad (3.2)$$

$$\frac{((-4.1982 \times A_{632}) + (25.7205 \times A_{649}) + (-7.4096 \times A_{665}) + (-2.7418 \times A_{691})) \times sv}{V} / 100 \quad (3.3)$$

$$\frac{((28.4593 \times A_{632}) + (-9.9944 \times A_{649}) + (-1.9344 \times A_{665}) + (-1.8093 \times A_{691})) \times sv}{V} / 100 \quad (3.4)$$

Where:

A_{632} : Absorbance value at 632 nm

A_{649} : Absorbance value at 649 nm

A_{665} : Absorbance value at 665 nm

A_{691} : Absorbance value at 691 nm

sv : Solvent volume (mls)

V : Volume of extract filtered (L)

3.3.7 Dry mass

Dry mass (DM) was quantified by filtering 5 ml of original biofilm slurry onto a pre-ovendried Whatmann filter (47 mm diameter; GF/F; Whatmann, Maidstone, Kent, UK) of known mass, where they were subsequently dried and mass determined. Sub-samples were frozen on site before transfer to Bristol University. The filters were oven-dried in a Heratherm incubator (Make: IMH100-S, Thermo Scientific, Germany) for 24 hours at 105 (°C), transferred to a desiccator and the mass determined after cooling. Measurements were carried out to four decimal places on a balance (Sartorius, Göttingen, Germany). Dry mass was recorded as mg/cm².

3.3.8 Pulse amplitude modulated (PAM) fluorometry

The photophysiology of the biofilms was evaluated using PAM. The measurements were taken at 24-hour intervals over a 72-hour period (0-72 hours) using the WATER-PAM fluorometer (see methods section 2.5.6 for instructions) with three replicates per treatment.

3.3.9 Diatom cleaning and species identification

Diatom frustules were cleaned, identified and counted to analyse species composition and diversity. The frustule cleaning process was based on a method described by Kelly *et al* (2008). From sub-samples (preserved with Lugol's iodine solution (1%)), 1 ml of the homogenised sample was transferred to a pyrex glass test tube and made up to 10 ml with deionised water, before being centrifuged for 10 minutes at 3000 rpm (1811 RCF). Supernatant was removed down to 1 ml. Samples were then digested in a fume hood by adding 2 ml of saturated potassium permanganate solution and 2 ml Hydrochloric acid

(HCl), (12N). Samples were placed in a rack in a water bath at 90 (°C) for 90 minutes in a fume hood. After turning to a pale straw colour, the test tubes were cooled to room temperature, then made up to 10 ml with deionised water and centrifuged for 10 minutes at 3000 rpm (1811 RCF). The supernatant was removed to leave 1 ml and the samples were vortexed for 30 seconds to ensure effective mixing. Test tubes were refilled with deionised water to 10 ml. This process was repeated 5 times to ensure complete acid removal. Before preparing slides for identification and enumeration, sample concentrations were assessed visually. If a sample appeared milky in colour it was deemed to be excessively concentrated and was therefore diluted with deionised water. The slides were prepared by placing 0.5 ml of sample on a coverslip on a large glass sheet, which was then left to dry for 24 hours. After drying, a hot plate was heated to 130 (°C). One drop of Naphrax was placed on a glass slide and inverted onto the cover slip; the slide and cover slip were then placed on to the hot plate for approx. 15 minutes. Using toothpicks, pressure was gently applied to the cover slip to remove gas bubbles which would otherwise impede species identification. After heating, the prepared slide was removed from the hot plate and left to cool. Samples were counted using a Leica DM LB2 microscope (Wetzlar, Germany) at a magnification of x1000, with reference to standard texts (Krammer & Lange-Bertalot 1986, 1997, 2000, 2004).

3.3.10 Statistical analysis

All statistical analysis was carried out using IBM SPSS Statistics 23 (IBM Corp., New York, USA). Homogeneity of variance was tested using Levene's test and normality of residuals was tested using the Kolmogorov-Smirnov test. Where data were non-normally distributed, it was logarithmically transformed. One-way ANOVA's were performed to examine differences between treatments at independent time points for dry mass, total chlorophyll and photophysiology. Two-way ANOVA's were performed to determine an interactive effect between n-TiO₂ treatment and type of chlorophyll pigment at independent time points. Where data were significant, *post-hoc* Bonferroni tests were applied to identify significant differences between treatments. Shannon-Weaver diversity scores were calculated to investigate differences between diatom species diversity. Using data obtained on the relative abundance of diatom species in riverine biofilm assemblages, species assemblages were ordinated us-

ing non-metric multidimensional scaling (NMDS) using a Bray-Curtis similarity measure (Community Analysis Package, PISCES). To identify which species were most influential in driving variation along informative NMDS axes, Spearman's rank correlations were carried out between the NMDS axis scores for each sample and the relative abundance scores based on diatom species composition of the cleaned frustules. Bonferroni corrections were used to account for multiple testing. To compare the composition of biofilm communities between samples, an analysis of similarities test (ANOSIM) was used. This is a non-parametric statistical test used to test whether similarity between groups is greater than or equal to the similarity within groups.

3.4 Results

3.4.1 Mesocosm water properties and local weather data

The temperature, pH, irradiance and oxygen concentration were measured over a four-day period in each of the treatment channels (**Table 3.1**). Amongst the treatment channels, no notable differences were observed in any of the measured parameters. Data from a local weather station (AccuWeather, June 2018) in Wareham (Dorset, UK) showed that there was excessively warm weather throughout the experiment. Data revealed an average air temperature of 22 (°C) (± 0.55 SE) was recorded from 06/06/2018 - 22/06/2018, which was 4.4 (°C) warmer than the average historical air temperature of that area (17.6 (°C)).

Table 3.1: Environmental parameters in stream mesocosm river water (temperature, pH, light irradiance and oxygen) in each treatment channel shown as a mean value (\pm standard error) over four days.

n-TiO ₂ treatment (mg l ⁻¹)	Temperature (°C)	pH	Light irradiance ($\mu\text{mol (photons) m}^{-2} \text{ s}^{-1}$)	Oxygen (mg l ⁻¹)
0	27.58 \pm 0.31	8.22 \pm 0.05	1549.25 \pm 45.27	7.88 \pm 0.21
0.05	28.73 \pm 0.64	8.29 \pm 0.08	1567.75 \pm 46.40	7.92 \pm 0.22
5	27.58 \pm 0.27	8.25 \pm 0.01	1484.50 \pm 121.2	7.79 \pm 0.20

3.4.2 Changes in the periphytic biomass of benthic biofilms following the application of n-TiO₂

3.4.2.1 The impact of n-TiO₂ on the total chlorophyll of riverine biofilm assemblages

The total chlorophyll content of the untreated and treated biofilms ($\mu\text{g}/\text{cm}^2$) was measured at 24 and 72 hours (**Figure 3.3**). Total chlorophyll was used as an endpoint in this field study as it is a useful indicator of the overall photosynthetic biomass of the biofilms.

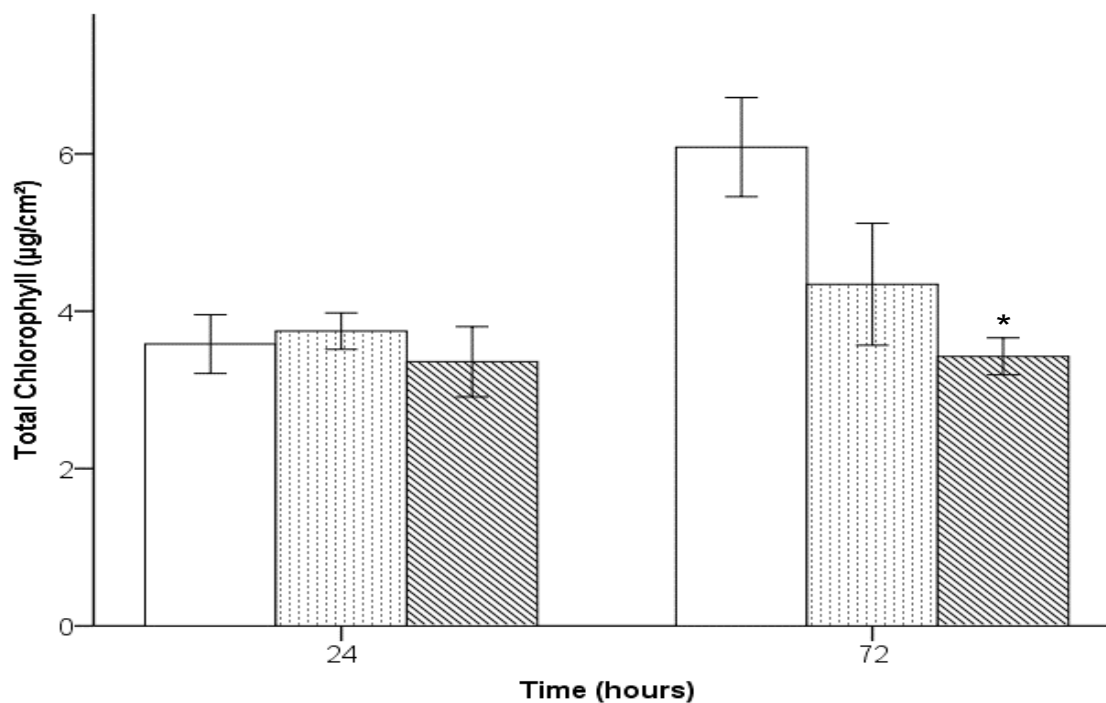


Figure 3.3: The total chlorophyll content ($\mu\text{g}/\text{cm}^2$) of riverine biofilm assemblages exposed to n-TiO₂ at 0 (control), 0.05 and 5 mg l^{-1} at 24 hours and 72 hours. The white bar = untreated (control), the dashed bar = 0.05 mg l^{-1} , and the striped bar = 5 mg l^{-1} . Error bars show mean \pm SE of three independent replicates. Significance, relative to the control at that time point, is shown at $p < 0.05$ (*) and $p < 0.01$ (**).

After 24 hours of n-TiO₂ exposure, the total chlorophyll of the biofilms ($\mu\text{g}/\text{cm}^2$) was 3.58, 3.75 and 3.36 ($\mu\text{g}/\text{cm}^2$) in the control, 0.05, and 5 mg l^{-1} samples respectively. There were no significant differences found between the total chlorophyll concentration in treatments ($F_{(2, 6)} = 0.29$, $p = 0.758$). To investigate whether there were any changes in different chlorophyll pigments between treatments, the composition of chlorophyll *a*, *b* and *c* was measured in each treatment (**Table 3.2**). No significant interaction effect was found between n-TiO₂ concentration and chlorophyll pigment ($F_{(4, 18)} = 0.56$, $p = 0.695$).

After 72 hours of n-TiO₂ exposure, the total chlorophyll of the biofilms was 6.09, 4.34 and 3.43 ($\mu\text{g}/\text{cm}^2$) in the control, 0.05 and 5 mg l^{-1} samples respectively. Growth in the biofilm from 24-72 hours was observed with a total chlorophyll increase of 70.1%, 15.8% and 2.1% in the control, 0.05 and 5 mg l^{-1} treatments, respectively. The total chlorophyll, relative to the control at this time point, was 29% lower in the 0.05 mg l^{-1} treatment and

significantly lower (44%) in the 5 mg l⁻¹ treatment ($F_{(2, 6)} = 5.20$, $p = < 0.001$).

To investigate whether there were any changes in the composition of different chlorophyll pigments between treatments, the composition of chlorophyll *a*, *b* and *c* was measured in each treatment (**Table 3.2**). A significant interaction effect was found between n-TiO₂ treatment and chlorophyll pigment ($F_{(4, 18)} = 4.36$, $p = 0.012$). The chlorophyll *a* and chlorophyll *c* concentrations were significantly lower in biofilms exposed to the 5 mg l⁻¹ treatment, relative to the control at 72 hours ($(F_{(2, 6)} = 5.41, p = 0.045)$; $(F_{(2, 6)} = 6.46, p = 0.032)$).

Table 3.2: The amount of each individual chlorophyll pigment (*a*, *b*, *c*) (µg/cm²) and the chlorophyll *a:b* and *a:c* ratios in the untreated and treated biofilms (0 (control), 0.05 5 mg l⁻¹) at 24 and 72 hours. Values show mean ± SE of three independent replicates. Significance, relative to the control at that time point is shown at $p < 0.05$ (*).

Time (hours)	n-TiO ₂ concentration (mg l ⁻¹)	Chlorophyll pigment (µg/cm ²)				
		<i>a</i>	<i>b</i>	<i>c</i>	<i>a:b</i>	<i>a:c</i>
24	0	1.11 ± 0.14	0.065 ± 0.01	0.19 ± 0.02	17.1	5.8
	0.05	1.30 ± 0.11	0.054 ± 0.01	0.22 ± 0.02	24.1	5.9
	5	1.28 ± 0.16	0.055 ± 0.01	0.21 ± 0.02	23.3	6.1
72	0	2.12 ± 0.22	0.11 ± 0.01	0.29 ± 0.05	19.3	7.3
	0.05	1.62 ± 0.27	0.087 ± 0.03	0.17 ± 0.01	18.6	9.5
	5	1.11 ± 0.15 (*)	0.051 ± 0.01	0.15 ± 0.02 (*)	21.8	7.4

3.4.2.2 The impact of n-TiO₂ on the dry mass of riverine biofilm assemblages

The dry mass of the untreated and treated biofilms (mg/cm²) was measured at 24 and 72 hours (**Figure 3.5**). Dry mass was used as an end-point in this study as it is another useful indicator of the biomass of the biofilms.

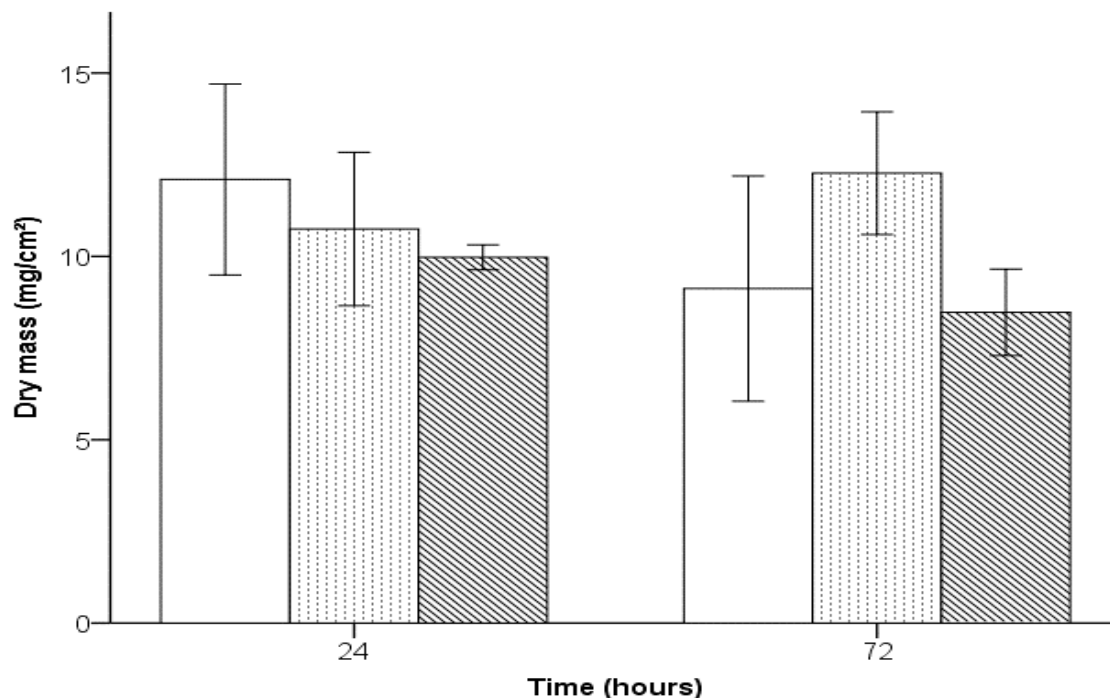


Figure 3.4: The dry mass (mg/cm²) of riverine biofilm assemblages exposed to n-TiO₂ at 0 (control), 0.05 and 5 mg l⁻¹ at 24 hours and 72 hours. The white bar = control (0 mg l⁻¹), the dashed bar = 0.05 mg l⁻¹, and the striped bar = 5 mg l⁻¹. Error bars show mean \pm SE of three independent replicates.

After 24 hours of n-TiO₂ exposure, the dry mass of the biofilms was 12.10, 10.75 and 9.97 (mg/cm²) in the control, 0.05 and 5 mg l⁻¹ samples respectively. The difference in dry mass between treatments was not found to be significant ($F_{(2, 6)} = 0.31$, $p = 0.746$).

After 72 hours, the dry mass of the biofilms (mg/cm²) was 9.12, 12.27 and 8.48 in the control, 0.05 and 5 mg l⁻¹ samples respectively. These differences between treatments were not found to be significant ($F_{(2, 6)} = 0.91$, $p = 0.453$).

3.4.3 Diatom species composition

The % relative abundance (RA) of diatom species found in the riverine biofilm assemblages is shown in **Table 3.3**, the 24 species with the highest RA are included in the table. Important species found in the benthic biofilms, defined as those with a >5% relative abundance (RA) included *Achnantheidium minutissimum*, *Encyonema minutum*, *Melosira*

varians, *Nitzschia dissipata* and small *Nitzschia* spp. The genus *Nitzschia* was grouped into categories depending on size (small, medium, large). Small species of *Nitzschia* had the highest relative abundance in the biofilm across all treatments (control = 33.16% (\pm 1.51% SE), 0.05 mg l⁻¹ = 33.30% (\pm 2.19% SE), 5 mg l⁻¹ = 27.97% (\pm 5.90% SE). At 72 hours, the diatom species composition and diversity within the Bacillariophyta (diatoms) was analysed. The Shannon-Weaver diversity score was 2.44 (\pm 0.075 SE), 2.42 (\pm 0.057 SE), and 2.50 (\pm 0.12 SE) for the 0, 0.05 and 5 mg l⁻¹ treatments respectively. No significant differences were found in diatom species diversity between treatments ($F_{(2, 6)} = 0.225$, $p = 0.805$). The NMDS plot summarising diatom assemblages on each slide showed clear separation in assemblage composition along Axis 2 between the 0 (control) with no added n-TiO₂s and the 5 mg l⁻¹ samples (**Figure 3.5**). However, an analysis of similarities test (ANOSIM) showed that differences in the assemblage composition between treatment groups were not significant ($R = -0.169$, $p = 1$). The diatom composition of the 0.05 mg l⁻¹ sample scores overlapped with both the control and the 5 mg l⁻¹ samples suggesting no clear differences in the assemblages at this concentration. The assemblages were separated along Axis 2, but showed greater overlap on Axis 1, suggesting Axis 2 is associated with the treatment effect. The stress value for the NMDS plot was 0.055 which suggests a good match between the data and the ordination distances, and therefore a good representation of the diatom assemblages. To investigate which species were most influential in driving assemblage differences observed along Axis 2, the RA of each species was correlated with Axis 2 values. The Spearman's Rank Correlation of each species' RA with Axis 2 showed that species most strongly associated with low Axis 2 scores were *Nitzschia fonticola* ($r_s = -0.898$, adj. $p = 0.024$), *Planothidium frequentissimum* ($r_s = -0.688$, adj. $p = 0.96$) and *Melosira varians* ($r_s = -0.594$, adj. $p = 1$). In contrast, the species most strongly associated with high axis 2 scores were *Nitzschia dissipata* ($r_s = 0.879$, adj. $p = 0.048$), *Achnanthidium minutissimum* ($r_s = 0.783$, adj. $p = 0.312$) and *Amphora pediculus* ($r_s = 0.717$, adj. $p = 0.72$). However, some of these species had very low RA (see **Table 3.3**) suggesting their influence on the community may not be as important.

Table 3.3: Species composition of diatom assemblages in riverine biofilm assemblages in the River Frome (Dorset, UK) after 72 hours. The mean RA of each species in each treatment (0, 0.05 and 5 mg l⁻¹) is shown alongside the SE. The Spearman's Rank correlation coefficient (r_s) of each species' RA with axis 2 values from the NMDS plot are shown in order of decreasing correlation. The p values are given alongside Bonferroni adjusted values (adj. p) to account for multiple testing.

Species	Mean Relative Abundance (%)						r_s	p	adj. p
	0	±SE	0.05	±SE	5	±SE			
<i>Nitzschia fonticola</i>	0.76	0.23	1.60	1.32	0.11	0.11	-0.898	0.001	0.024 *
<i>Nitzschia dissipata</i>	6.51	1.33	9.55	3.21	10.56	1.78	0.879	0.002	0.048 *
<i>Achnanthydium minutissimum</i>	8.85	1.50	10.04	1.35	13.23	1.27	0.783	0.013	0.312
<i>Amphora pediculus</i>	2.46	0.61	3.25	0.69	4.60	0.42	0.717	0.03	0.72
<i>Planothidium frequentissimum</i>	0.32	0.19	0.68	0.54	0.00	0.00	-0.688	0.04	0.96
<i>Nitzschia agg medium</i>	4.27	2.30	3.34	1.00	5.07	1.20	0.667	0.05	1
<i>Melosira varians</i>	13.81	2.66	10.86	0.94	8.76	0.74	-0.594	0.092	1
<i>Nitzschia agg small</i>	33.16	1.51	33.30	2.19	27.97	5.90	-0.45	0.224	1
<i>Cocconeis placentula</i>	0.63	0.32	0.56	0.43	0.34	0.20	-0.407	0.277	1
<i>Navicula cryptotenella</i>	0.99	0.50	0.67	0.67	0.44	0.44	-0.31	0.416	1
<i>Staurosirella pinnata</i>	0.65	0.65	0.77	0.77	0.11	0.11	-0.307	0.422	1
<i>Fragilaria capucina</i>	2.08	0.91	1.62	0.24	1.23	0.39	-0.233	0.546	1
<i>Nitzschia agg large</i>	4.07	0.70	4.04	0.81	3.46	1.34	-0.233	0.546	1
<i>Synedra ulna</i>	0.11	0.11	0.10	0.10	0.44	0.44	0.188	0.628	1
<i>Navicula gregaria</i>	1.85	0.92	1.20	0.40	0.90	0.49	-0.183	0.637	1
<i>Planothidium rostratum</i>	0.83	0.26	0.28	0.28	0.57	0.30	0.136	0.728	1
<i>Surirella brebissonii</i>	0.97	0.50	0.71	0.42	2.12	0.43	0.133	0.732	1
<i>Encyonema minuta</i>	4.54	1.56	3.40	1.50	5.38	0.47	-0.133	0.732	1
<i>Navicula reichardtiana</i>	1.05	0.36	2.77	1.18	1.81	0.93	-0.133	0.732	1
<i>Planothidium ellipticum</i>	0.33	0.19	0.31	0.17	1.01	0.38	0.126	0.748	1
<i>Navicula menisculus</i>	2.02	0.30	1.54	0.21	3.25	0.81	0.117	0.765	1
<i>Gomphonema parvulum</i>	3.83	0.62	3.03	0.86	1.91	0.80	-0.1	0.798	1
<i>Eolimna minima</i>	0.73	0.37	0.51	0.26	0.57	0.30	0.068	0.862	1
<i>Diatoma vulgare</i>	0.64	0.50	1.62	0.68	1.00	0.50	0.017	0.966	1

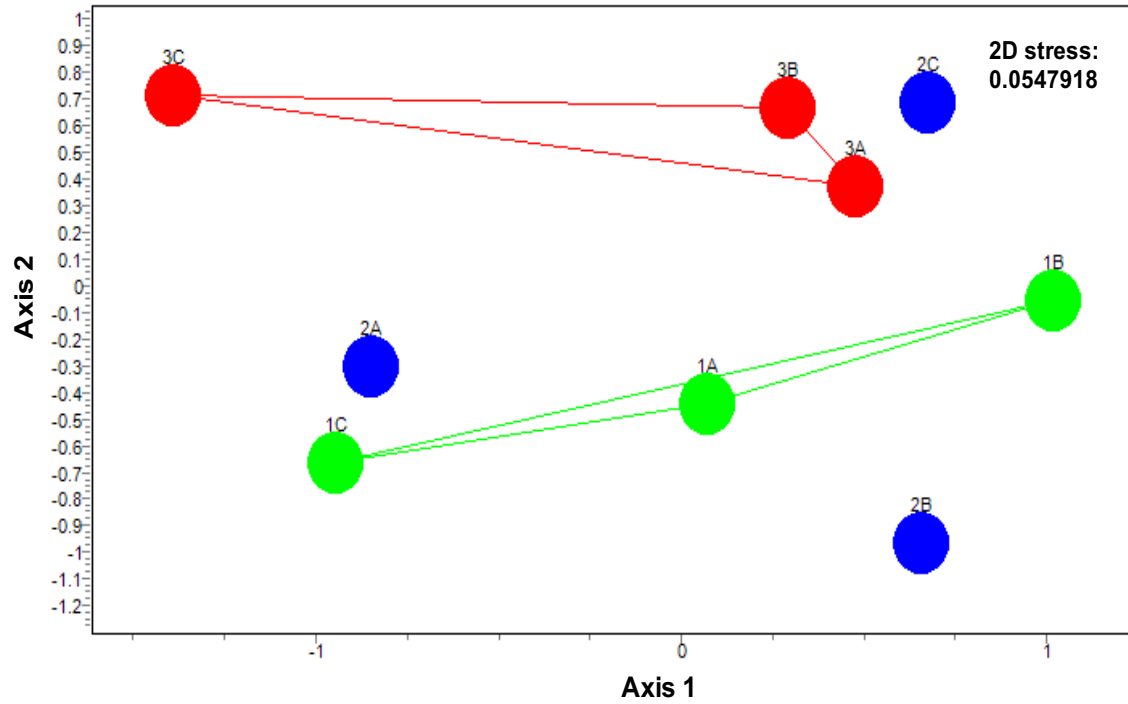


Figure 3.5: Axis 1 and Axis 2 of NMDS, based on RA of diatoms grown in riverine biofilm assemblages in the River Frome (Dorset, UK) after 72 hours. The colours indicate different treatments (green = control, blue = 0.05 mg l⁻¹, red = 5 mg l⁻¹) and the letters A, B and C indicate different replicate slides.

3.4.4 Changes in the photophysiology of riverine biofilms following n-TiO₂ exposure

3.4.4.1 The effect of n-TiO₂ on the rapid light curve of riverine biofilm assemblages

Using PAM fluorometry, RLCs were generated for each replicate of the untreated and treated biofilms at 24 hours (**Figure 3.6a**) and 72 hours (**Figure 3.6b**).

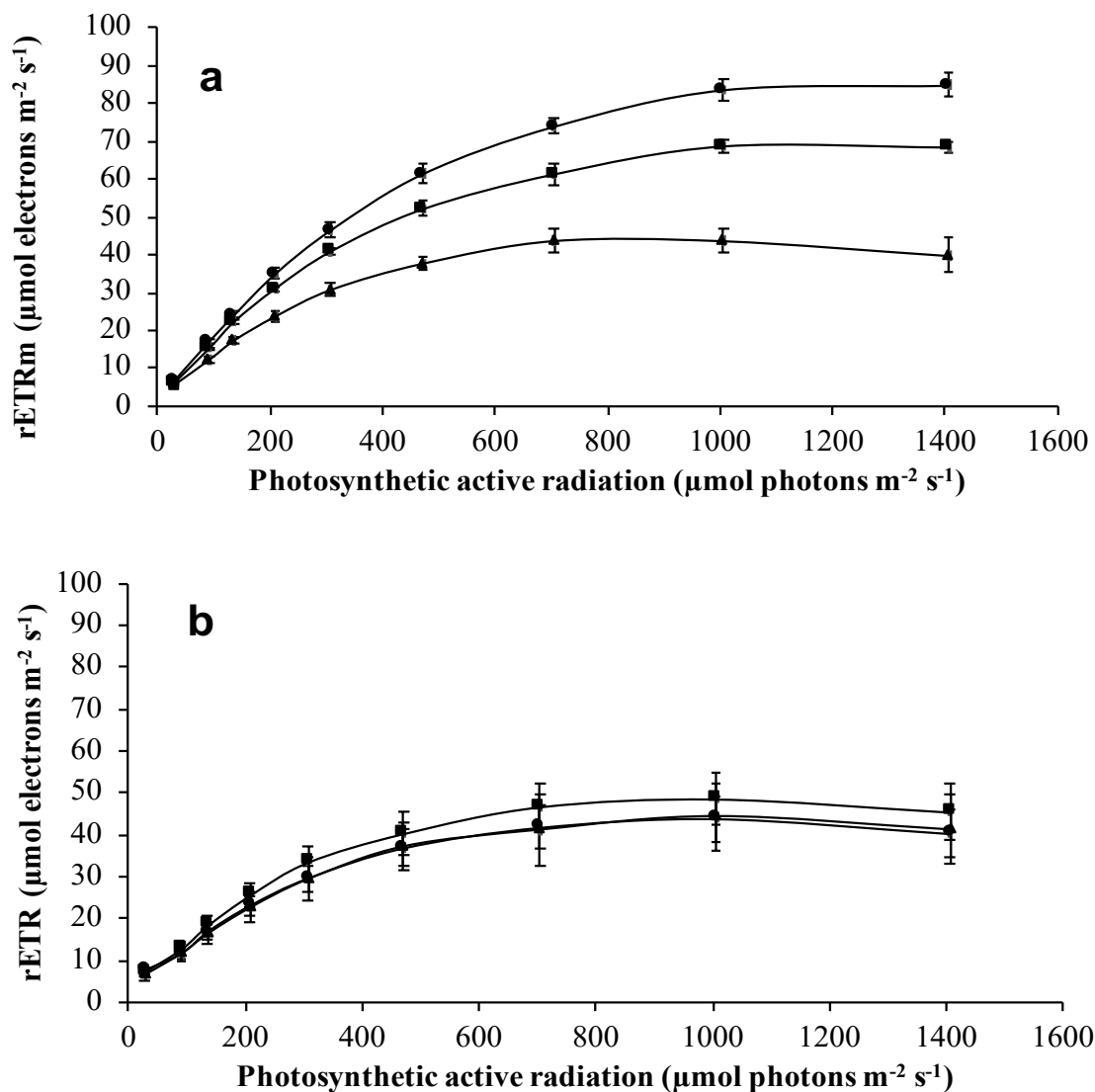


Figure 3.6: Rapid light curves (RLCs) produced from riverine biofilm assemblages at 24 hours (a) and 72 hours (b) to show the differences between the control, 0.05 mg l⁻¹ and 5 mg l⁻¹ samples. Control = closed circles, 0.05 mg l⁻¹ = closed squares, 5 mg l⁻¹ = closed triangles. Lines show means \pm SE of three independent replicates.

At 24 hours, an increasing n-TiO₂ concentration caused light saturation to occur at relatively lower PAR values, thus causing lower ETRm values. The slope of the light-limiting regions (α) was also lower with increasing n-TiO₂ concentration. At 72 hours, the light saturated at lower PAR values for untreated and treated samples relative to 24 hours. The value of (α) was also lower in all treatments relative to 24 hours. The RLCs at this time point showed similar profiles to each other.

3.4.4.2 The effects of n-TiO₂ on the maximum quantum yield of PSII in the dark-adapted state (Fv/Fm) of riverine biofilm assemblages

The effect of an increasing n-TiO₂ concentration on the Fv/Fm of the riverine biofilms at 24 and 72 hours is presented in **Figure 3.7**.

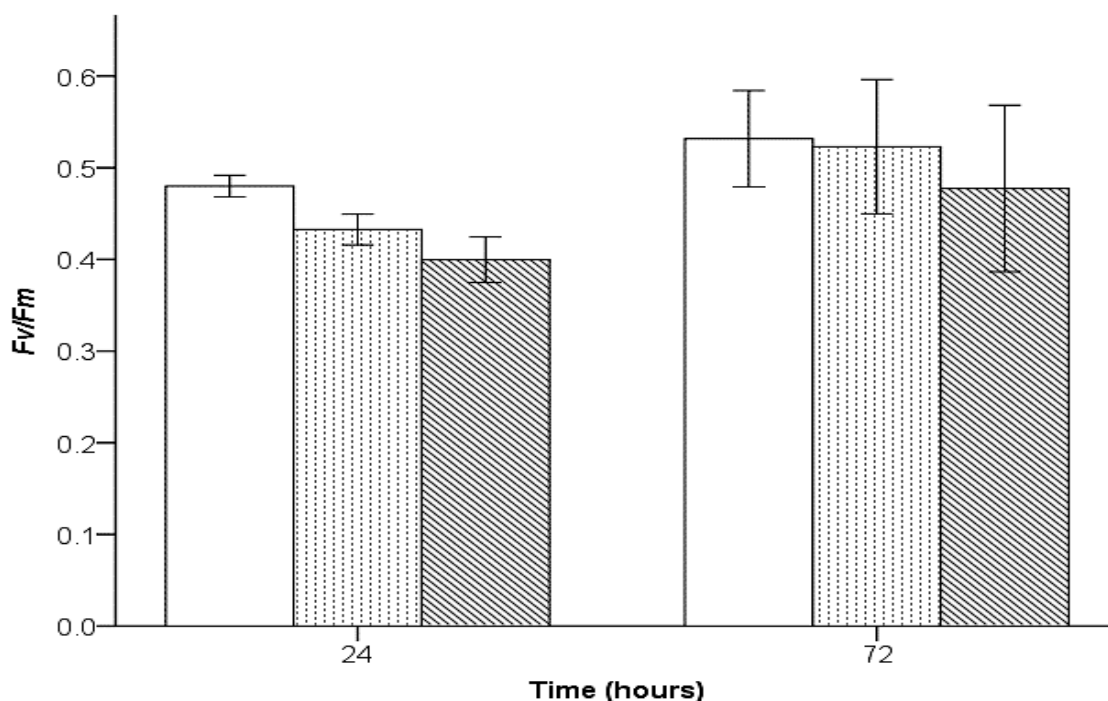


Figure 3.7: The effect of an increasing n-TiO₂ concentration on the maximum quantum yield of PSII in the dark-adapted state (Fv/Fm) in riverine biofilm assemblages at 24 hours and 72 hours. White bar = control, dotted bar = 0.05 mg l⁻¹ treatment, striped bar = 5 mg l⁻¹ treatment. Error bars show mean \pm SE of three independent replicates. Significance, relative to the control at each time point, is shown at $p < 0.05$ (*) and $p < 0.01$ (**).

After 24 hours of n-TiO₂ exposure, the Fv/Fm of the biofilms was 0.48, 0.43 and 0.40 in the control, 0.05 and 5 mg l⁻¹ treatments respectively. The Fv/Fm was 10% lower in the 0.05 mg l⁻¹ treatment and 17% lower in the 5 mg l⁻¹ treatment relative to the control at 24 hours, however, no significant differences were found between treatments ($F_{(2, 6)} = 4.70$, $p = 0.059$).

At 72 hours, the Fv/Fm of the biofilms was 0.53, 0.52 and 0.48 in the control, 0.05 and 5 mg l⁻¹ treatment respectively. The Fv/Fm increased in all treatments relative to 24 hours,

however, no clear trend was observed and no significant differences were found between treatments ($F_{(2, 6)} = 0.156$, $p = 0.859$).

3.4.4.3 The effects of n-TiO₂ on the maximum light-use coefficient for PSII (α) of riverine biofilm assemblages

The effect of an increasing n-TiO₂ concentration on the (α) of the biofilms at 24 and 72 hours is presented in **Figure 3.8**.

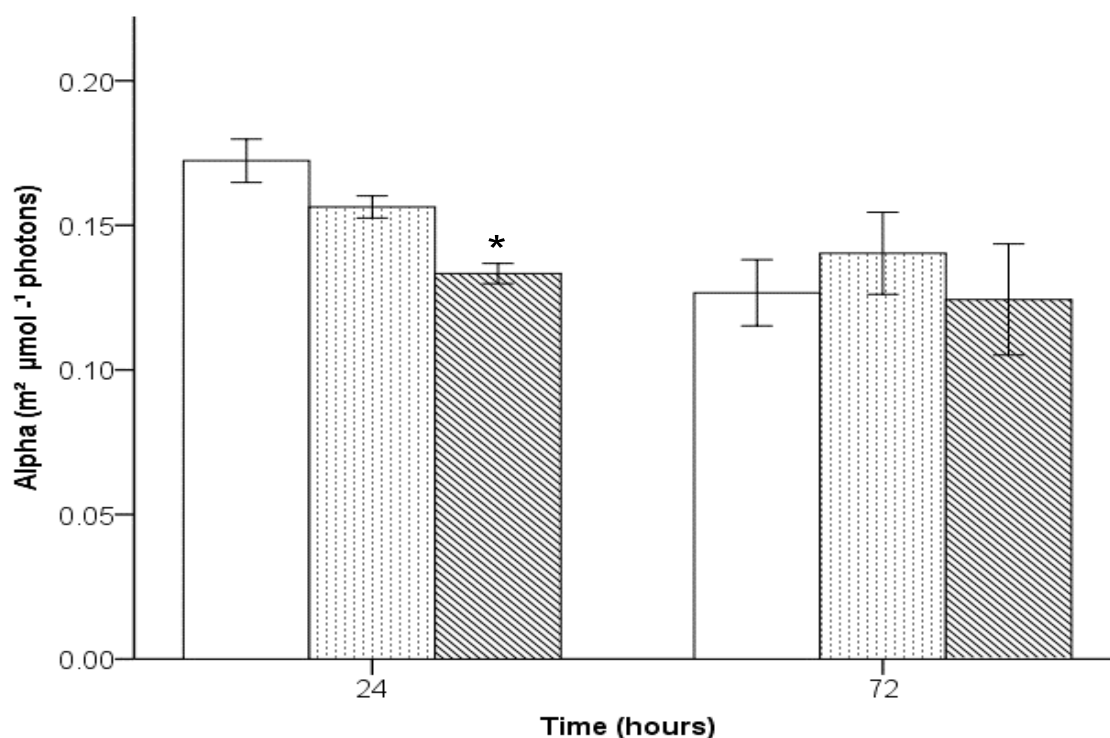


Figure 3.8: The effect of an increasing n-TiO₂ concentration on the maximum light use coefficient yield for PSII (α) in riverine biofilm assemblages at 24 hours and 72 hours. White bar = control, dotted bar = 0.05 mg l⁻¹ treatment, striped bar = 5 mg l⁻¹ treatment. Error bars show mean \pm SE of three independent replicates. Significance, relative to the control at each time point, is shown at $p = < 0.05$ (*) and $p = < 0.01$ (**).

After 24 hours of n-TiO₂ exposure, the (α) of the biofilms was 0.17, 0.16 and 0.13 in the control, 0.05 and 5 mg l⁻¹ treatments respectively. The value of (α) was 9% lower in the 0.05 mg l⁻¹ treatment and significantly lower (23%) in the 5 mg l⁻¹ treatment relative to the control at 24 hours ($F_{(2, 6)} = 13.84$, $p = < 0.001$).

After 72 hours, the (α) of the biofilms was 0.13, 0.14 and 0.12 in the control, 0.05 and 5 mg l⁻¹ treatments respectively. The value of (α) decreased in all treatments relative to their values at 24 hours. No clear trend was observed and no significant differences were found between treatments ($F_{(2, 6)} = 0.32$, $p = 0.739$).

3.4.4.4 The effects of n-TiO₂ on the maximum electron transport rate (rETR_m) of riverine biofilm assemblages

The effect of an increasing n-TiO₂ concentration on the rETR_m of the biofilms at 24 and 72 hours is presented in **Figure 3.9**.

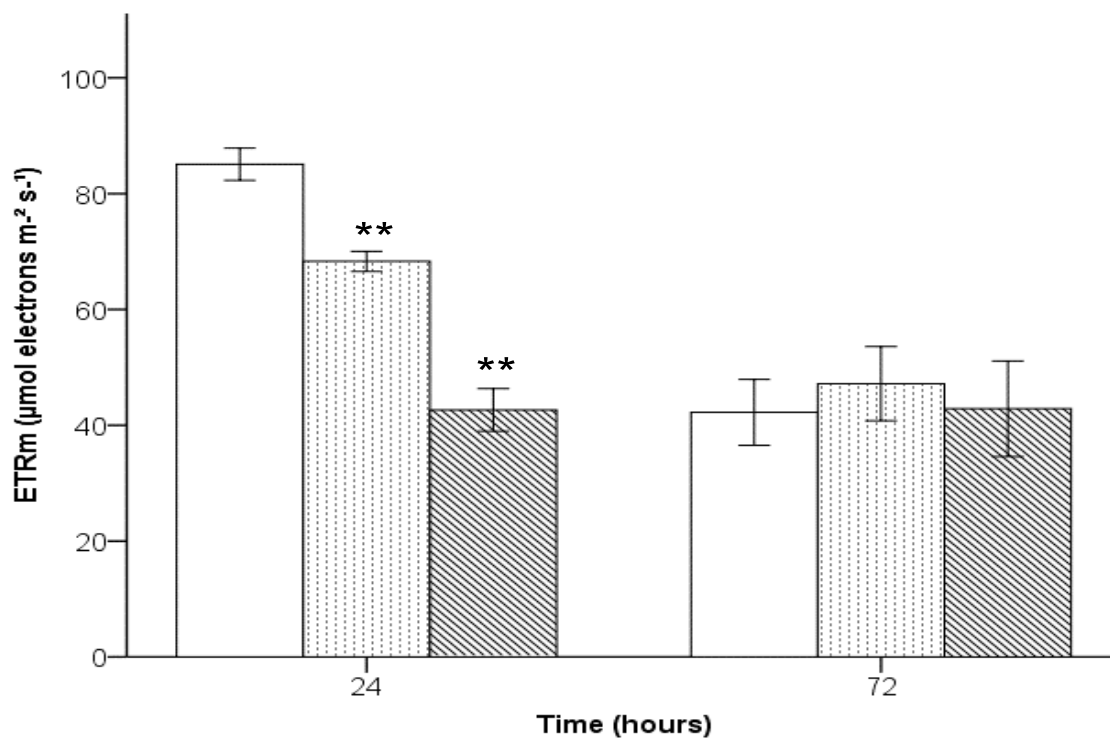


Figure 3.9: The effect of an increasing n-TiO₂ concentration on the maximum electron transport rate (ETR_m) in riverine biofilm assemblages at 24 hours and 72 hours. White bar = control, dotted bar = 0.05 mg l⁻¹ treatment, striped bar = 5 mg l⁻¹ treatment. Error bars show mean \pm SE of three independent replicates. Significance, relative to the control at each time point, is shown at $p < 0.05$ (*) and $p < 0.01$ (**).

After 24 hours of n-TiO₂ exposure, the rETR_m of the biofilms was 85, 68 and 43 in the control, 0.05 and 5 mg l⁻¹ treatments respectively. The rETR_m was significantly lower

(19.72%) in the 0.05 mg l⁻¹ treatment and significantly lower (49.88%) in the 5 mg l⁻¹ treatment relative to the control at 24 hours ($F_{(2, 6)} = 56.15$, $p < 0.001$).

After 72 hours, the rETR_m of the biofilms was 42, 47 and 43 in the control, 0.05 and 5 mg l⁻¹ treatments respectively. The ETR_m decreased from 85.08 at 24 hours to 42.23 (-50.36%) at 72 hours in the 5 mg l⁻¹ and the 0.05 mg l⁻¹ treatment decreased from 68.30 to 47.19 (-30.91%). The 5 mg l⁻¹ stayed relatively unchanged with no clear trend observed and no significant differences were found between treatments ($F_{(2, 6)} = 0.16$, $p = 0.860$).

3.4.4.5 The effects of n-TiO₂ on the light saturation coefficient (E_k) of riverine biofilm assemblages

The effect of an increasing n-TiO₂ concentration on the E_k of the biofilms at 24 and 72 hours is presented in **Figure 3.10**.

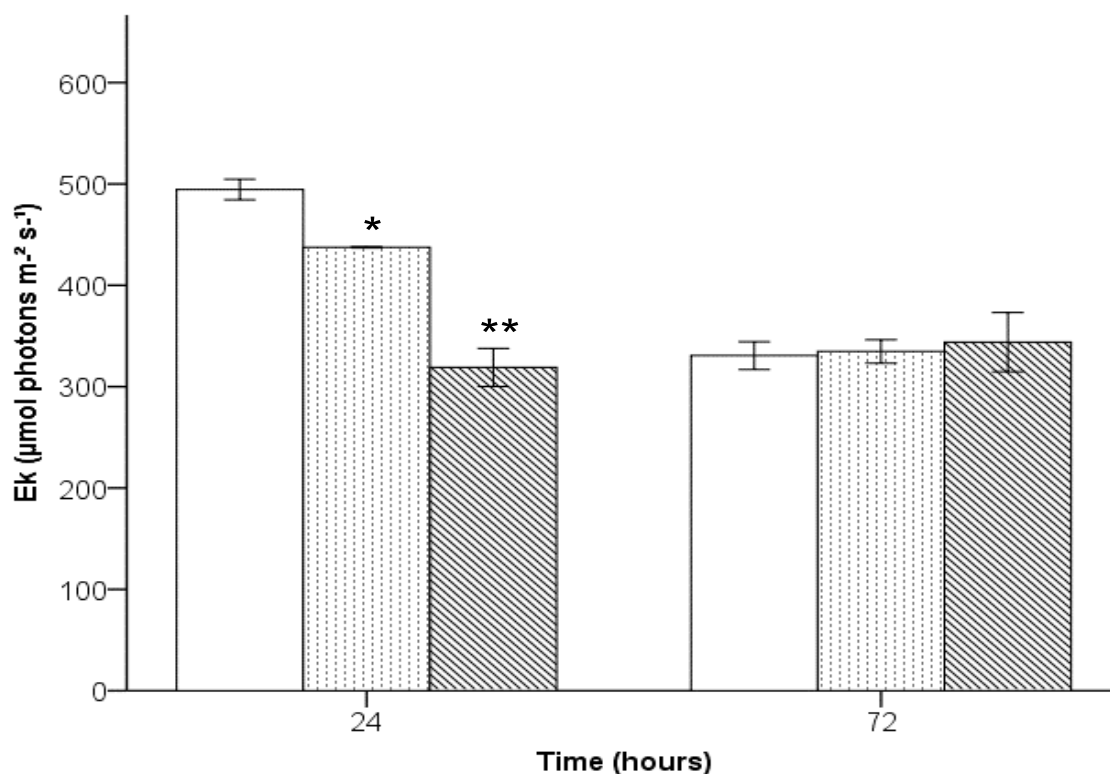


Figure 3.10: The effect of an increasing n-TiO₂ concentration on the light saturation coefficient (E_k) in riverine biofilm assemblages at 24 hours and 72 hours. White bar = control, dotted bar = 0.05 mg l⁻¹ treatment, striped bar = 5 mg l⁻¹ treatment. Error bars show mean \pm SE of three independent replicates. Significance, relative to the control at each time point, is shown at $p = < 0.05$ (*) and $p = < 0.01$

After 24 hours of n-TiO₂ exposure, the E_k of the biofilms was 494, 438 and 319 in the control, 0.05 and 5 mg l⁻¹ treatments respectively. The E_k of the biofilms was significantly lower (11.50%) in the 0.05 mg l⁻¹ treatment and significantly lower (35.49%) in the 5 mg l⁻¹ treatment relative to the control at 24 hours ($F_{(2, 6)} = 52.74$, $p = < 0.001$).

After 72 hours, the E_k of the control reduced from 494 at 24 hours to 331 (-33.12%), and the 0.05 mg l⁻¹ treatment reduced from 438 to 335 (-23.51%). The 5 mg l⁻¹ n-TiO₂ treatment increased from 318.99 to 374.58 (+17.11%). No clear trend was observed and no significant differences were found between treatments ($F_{(2, 6)} = 0.12$, $p = 0.891$).

3.4.5 Summary of results

- The total chlorophyll of the biofilms at 72 hours was significantly lower in biofilms exposed to 5 mg l⁻¹ n-TiO₂ treatment, relative to the control at that time point.
- At 72 hours, the concentration of chlorophyll *a* and chlorophyll *c* was significantly lower in biofilms exposed to the 5 mg l⁻¹ n-TiO₂ treatment, relative to the control at that time point.
- No changes in the dry mass of the biofilms were observed at 24 and 72 hours.
- No significant changes in the diatom assemblage of the biofilm were observed after 72 hours. However, subtle changes in the relative abundance of some species were observed between treatments.
- At 24 hours, the photophysiology of the biofilms was negatively impacted in biofilms exposed to the 0.05 and 5 mg l⁻¹ n-TiO₂ treatments. Significant lower values were observed in the (α), rETR_m, and E_k exposed to n-TiO₂, relative to the control.
- At 72 hours, the photophysiology of the biofilms showed no significant differences between untreated and treated biofilms.

3.5 Discussion

3.5.1 The effects of n-TiO₂ on the biomass of riverine biofilm assemblages

It was hypothesized that freshwater biofilm biomass (total chlorophyll and dry mass) would be negatively impacted after n-TiO₂ treatment, and that higher n-TiO₂ concentrations would have greater negative impacts on the biomass of riverine biofilms. The biofilm biomass, measured by total chlorophyll, was significantly lower, relative to the control, after 72 hours of exposure to the highest n-TiO₂ concentration (5 mg l⁻¹). More specifically, significantly lower concentrations, relative to the control, were found in chlorophyll *a* and chlorophyll *c*, but chlorophyll *b* did not significantly decrease. This result concurs with Wright *et al* (2018), who observed a chlorophyll *a* reduction when biofilms were exposed to 5 mg l⁻¹ n-TiO₂ and found no significant difference when biofilms were exposed to a lower

n-TiO₂ concentration (0.05 mg l⁻¹). In contrast, results from this study differ from findings of Jovanovic *et al* (2016), who reported that n-TiO₂ exposure (0.25 mg l⁻¹) had no impact on the concentration of chlorophyll *a* in biofilms. Interestingly, my study found no significant differences in dry mass between the untreated and treatment biofilms at either time point.

In this study, total chlorophyll increased by 70.1% in the control biofilms and 15.8% in the 0.05 mg l⁻¹ n-TiO₂ treatment from 24-72 hours. In the 5 mg l⁻¹ treatment, total chlorophyll increased by just 2.1%. While total chlorophyll did not decrease over time in the high n-TiO₂ concentration (5 mg l⁻¹), it was significantly lower than the total chlorophyll measured in the control at 72 hours. This may result from increased n-TiO₂ aggregation with EPS surrounding the biofilm (Battin *et al.*, 2009; Ferry *et al.*, 2009; Kroll *et al.*, 2014). Evidence has shown that algae secrete more EPS in the presence of n-TiO₂ and EPS secretion increases at higher n-TiO₂ concentrations (Gao *et al.*, 2018). These aggregations could shade the biofilms, reducing light availability for photosynthesis, and thus causing a reduction in photosynthetic pigments (Morelli *et al.*, 2018; Wright *et al.*, 2018).

Increases in community primary productivity, with simultaneous overall decrease in total chlorophyll, characterizes shifts from diatom-dominated biofilms to a green algae-dominated community (Guasch & Sabater, 1994; Sabater *et al.*, 2002). Chlorophyll *a* is the most abundant photosynthetic pigment and occurs in all algal taxa; changes in accessory pigments (e.g. chlorophyll *b* and chlorophyll *c*) concentrations can indicate changes in dominant populations of periphyton (Ledger & Hildrew, 1998). In the 5 mg l⁻¹ n-TiO₂ treatment of this study, a significant reduction, relative to the control, was recorded in chlorophylls *a* and *c*, but no significant differences were observed in chlorophyll *b* (**Table 3.2**), suggesting that n-TiO₂ exposure is potentially causing a shift to a community that is dominated by green algae, and diatoms may be leaving the biofilm.

3.5.2 The effects of n-TiO₂ on the diatom species composition of riverine biofilm assemblages

Short-term impacts on freshwater biofilm structure and function may alter the structure and functioning of multiple trophic levels in aquatic ecosystems (Fechner *et al.*, 2012). Biofilm establishment follows a "predictable microsuccession" with pioneer species including bacteria and low-profile diatom genera (e.g. *Achnanthes*, *Achnanthidium*, *Amphora*), followed by short-stalked taxa, and then longer, more erect and stalked species (Yallop & Kelly, 2006). Natural disturbances such as resource availability, velocity and temperature can induce changes in biofilm structure and functioning (Passy, 2007); anthropogenic pollutants may also have the potential to affect the biofilms. Biofilm contact with a particular toxicant, such as n-TiO₂, may exert a selection pressure that favours certain taxa in the biofilm (Sabater *et al.*, 2007). It was hypothesized that the diatom species composition of riverine biofilm assemblages would change after 72 hours in response to n-TiO₂ exposure. No significant differences in species diversity or community composition were found between the treated and untreated biofilms after 72-hour n-TiO₂ exposure. However subtle differences in diatom species composition were recorded between treatment biofilms. The NMDS plot revealed clear separation between samples in the control and 5 mg l⁻¹ treatment along NMDS Axis 2. High values of this axis were associated with species including *Nitzschia dissipata*, *Achnanthidium minutissimum* and *Amphora pediculus*, suggesting these species may be more tolerant to n-TiO₂ pollution. Whilst low axis values were associated with species including *Nitzschia fonticola*, *Planothidium frequentissimum* and *Melosira varians*, suggesting these are more susceptible species.

The ecological guild of a given diatom may determine how it will be impacted by anthropogenic stressors. This has been demonstrated in a lotic mesocosm experiment investigating changes in diatom community following herbicide and fungicide exposure. Results showed that diatoms classified in the low and motile guilds increased in herbicide-treated mesocosms, and the high profile guild diatoms showed the opposite trend, decreasing in herbicide-treated mesocosms (Rimet & Bouchez, 2011). In this study, the relative abun-

dance (%) of the diatoms *Achnanthes minutissimum* and *Amphora pediculus* was higher in the 5 mg l⁻¹ treatment compared to the control after 72 hours. Both *A. minutissimum* and *A. pediculus* are classified in the low-profile guild (Passy, 2007), which includes slow-moving taxa and species at the biofilm bottom, linked to the substrate. This could explain their slightly higher abundance in the high n-TiO₂ treatment, because they are less exposed to n-TiO₂s that do not penetrate past the surface of the biofilm, due to potential aggregation with the surrounding EPS. Also, *A. minutissimum* is an opportunistic species and is capable of rapidly colonising areas of the biofilm that have recently become exposed (Biggs *et al.*, 1998), therefore, it may be that other species left the biofilm and *A. minutissimum* rapidly colonised this new available niche in the biofilm. In contrast, the opposite result was recorded in the filamentous diatom species, *Melosira varians*, which decreased in relative abundance (%) at high n-TiO₂ concentrations (5 mg l⁻¹), relative to the control. This species has been previously shown to be highly sensitive to metal pollution (Medley & Clements, 1998). *M. varians* is classified in the high-profile guild (Passy, 2007); high-profile diatoms are located near top of the biofilm surface, increasing their risk of exposure to chemicals in the water column. *M. varians* is a tychoplanktonic species, meaning it can rise up and leave the biofilm. If the alga was stressed from n-TiO₂ exposure, it has the ability to detach from and leave the biofilm.

The most dominant genus across the biofilms was *Nitzschia*, with small species of *Nitzschia* making up 27-33% of the relative abundance recorded in the untreated and treated biofilms. *Nitzschia* is classified in the motile guild (Passy, 2007) and is considered a pollution-tolerant-genus (Khan, 1990). Motile guilds are particularly resistant to pollution stress because they are able to optimize their position in the biofilm and avoid external stress in the water column, such as high light, high flow rate, or anthropogenic pollutant stress (Chonova *et al.*, 2019). Motile diatoms also have a micro-habitat preference for thick matrices, which allows them to withstand higher levels of water contamination (Rimet & Bouchet, 2011). The ability of *Nitzschia* to adapt to changing environments due to movement may explain their abundance throughout the biofilm treatments.

3.5.3 The effects of n-TiO₂ on the photophysiology of riverine biofilm assemblages

It was hypothesized that the photophysiology of the biofilms would be negatively impacted in response to n-TiO₂ exposure, when compared to untreated biofilms. At 24 hours, as hypothesized, all photosynthetic parameters (Fv/Fm , $rETR_m$, (α) , and E_k) were lower, relative to the control at the low n-TiO₂ concentration (0.05 mg l⁻¹), and further decreased at the high n-TiO₂ concentration (5 mg l⁻¹). Interestingly, at 72 hours, no significant differences were found between treated and untreated biofilms in any of the measured photosynthetic parameters.

This initial negative impact at 24 hours in photophysiology could be due to an unfavourable environment created by the presence of n-TiO₂s at the biofilm surface. Motile species could be migrating downwards in n-TiO₂ treated biofilms, as an important adaptation for survival when presented with environmental stress (Du *et al.*, 2012). Therefore, when sampling the biofilms, the slurry of material removed from the slides, would contain algae from all levels within the biofilm, meaning the response measured would be from multiple algal taxa, some of which potentially spent more time in darker, lower parts of the biofilm. Lower irradiance levels have been shown to cause lower Fv/Fm values (Coelho *et al.*, 2011; Wu *et al.*, 2015). This phenomenon can be attributed to a behavioural response where vertical migration takes place and is thought to be a mechanism to allow organisms to follow gradients or avoid extreme stress, maximising their fitness and thereby conferring an evolutionary advantage (Consalvey *et al.*, 2004). For example, motile diatoms prevent photoinhibition using vertical migration (Kromkamp *et al.*, 1998; Frankenbach *et al.*, 2018).

At 72 hours, no differences were observed in biofilm photophysiology between treatments. The control treatment for (α) , ETR_m and E_k all reduced relative to what was observed at 24 hours. The decrease in photosynthetic parameters ((α) , ETR_m and E_k) in treated and untreated biofilms could be due to damage from high light and high temperature exposure. Light intensity in the field in this experiment was high ($>1000 \mu\text{mol (photons) m}^{-2} \text{ s}^{-1}$) and

this can drive photoinhibition, due to light-induced damage of the PSII reaction centre. The presence of UV irradiation may also be a reason for the decrease in photosynthetic parameters in untreated and treated biofilms. UV is unlikely to have increased n-TiO₂ photocatalytic activity, due to the crystalline phase used for this experiment, being rutile. Published research states that this phenomenon is only recorded from n-TiO₂s possessing the anatase crystalline form (Sayes *et al.*, 2006). Extended periods of UV exposure, however, could directly impair biofilm photophysiology (Agrawal, 1992; Bautista-Saraiva *et al.*, 2018) and elevated temperatures, which were present in this experiment, can complicate algal self-repair after damage from UV irradiation (Wong *et al.*, 2015). Interestingly, the F_v/F_m of the untreated and treated biofilms, although not significant, increased relative to the F_v/F_m at 24 hours. This could be due to the algae in the biofilms acclimating to high irradiance levels and adjusting their photosynthetic apparatus by converting the xanthophyll pigment diadinoxanthin (DD) to diatoxanthin (DT), which causes lower rETR_m (Serodio *et al.*, 2006).

3.5.4 Limitations and caveats of study

Firstly, throughout the duration of the experiment, the filtered river water (with or without added n-TiO₂) was topped up regularly in the artificial mesocosms to compensate for evaporation, due to high temperatures. This would potentially have allowed new algal taxa to colonise biofilms. These algae were kept in the shade before entering the mesocosm, so may have been slightly shade-adapted compared to algae already in the artificial mesocosms. Secondly, during the experiment, there were extreme weather conditions. Light levels were extremely high (1400-1600 $\mu\text{mol photons m}^{-2} \text{s}^{-1}$) and water temperature ranged from 27-29 (°C). The shallow and clear water of the artificial mesocosms may have not given much protection from high light irradiation. Therefore, a solution for future studies would be to provide a shading device, to prevent any photodamage that may occur. Lastly, the short time-scale of this experiment was beneficial, as it allowed for detection of negative impacts on biofilm photophysiology after n-TiO₂ exposure for 24 hours, which a lot of long-term studies may miss out on. By increasing this time-scale, the subtle differences observed in diatom species composition between treatments after 72 hours may start to show greater,

significant differences.

3.5.5 Conclusion

This chapter aimed to investigate n-TiO₂ impacts on the structure and functioning of riverine biofilm assemblages over a 72-hour period by assessing changes in biofilm biomass, photophysiology and diatom species composition following n-TiO₂ exposure. The results obtained revealed that n-TiO₂ exposure, at environmentally relevant concentrations (0.05 mg l⁻¹) and higher concentrations expected in sewage treatment effluent (5 mg l⁻¹) negatively impacted biofilm photophysiology after 24 hours. After 72 hours of n-TiO₂ exposure, however, all treatments showed photophysiological impairment, likely due to high light and high temperature exposure, which may have masked longer-lasting effects of n-TiO₂ toxicity. The biomass of the biofilm, as measured by total chlorophyll, did not grow in the 5 mg l⁻¹ treatment from 24-72 hours, and had significantly lower concentrations of total chlorophyll relative to the control at 72 hours. Although no significant differences were observed in diatom species composition between treatments, there were subtle changes in species, based on their ecological guild. This study has confirmed that n-TiO₂ exposure has an acute toxicity effect on riverine biofilm assemblages at environmentally relevant concentrations. Further short-term studies are needed to disentangle the toxicity mechanisms behind these negative impacts.

Synthesis and future recommendations

THIS synthesis contains four main sections. **Section 4.1** will make comparisons between my laboratory and field studies to see whether results were similar, and will determine whether *N. palea* is a good indicator species for n-TiO₂ toxicity in freshwater environments. **Section 4.2** will explore how the duration of the OECD toxicity test may be important, and how certain aspects of the test should be considered to avoid variations in response of the algae. **Section 4.3** will give recommendations for future toxicity testing of n-TiO₂s using outdoor artificial mesocosms in the field. **Section 4.4** will focus on the larger-scale impacts of n-TiO₂ pollution and wider impacts globally.

4.1 Do results from investigating n-TiO₂ impacts on a single species diatoms, *N. palea*, tell a similar story to the results from investigating the impacts of n-TiO₂ on whole riverine biofilm assemblages in the field?

Chapter 2 of this thesis investigated the impact of an increasing n-TiO₂ concentration on the growth and photophysiology of the single species benthic diatom, *N. palea*. Chapter 3 focused on n-TiO₂ impacts on riverine biofilm assemblages in field conditions, using the River Frome (Dorset, UK) as a study site. This section of the synthesis compares field and laboratory results, to determine whether they tell a similar story, and whether *N. palea* is a representative indicator species that can be used in laboratory toxicity testing to further our understanding of the impacts of n-TiO₂ exposure on field biofilms.

The lone method used in both the laboratory and field is pulse amplitude modulated (PAM) fluorometry; this was because whole community growth inhibition is not easily measured in the field, because there is a mixed community. For comparative purposes, the 24-hour values were used, as these are likely to be the most reliable, for reasons described in section 4.2 of this synthesis. In riverine biofilm assemblages in the field, exposure to the low nanoparticle concentration (0.05 mg l⁻¹) gave lower Fv/Fm values, decreasing by 9.86% relative to the control. Relatively higher concentrations of n-TiO₂ (5 mg l⁻¹) caused a 16.7% decrease in Fv/Fm relative to the control. In the laboratory study, exposure to 0.05 and 5 mg l⁻¹ n-TiO₂ caused smaller differences in Fv/Fm with values lower, by 5.14% and 5.26%, relative to the control. Larger significant reductions were seen in both the 10 and 50 mg l⁻¹ treatments (20.26% and 31.04%). Field biofilm rETR_m were lower, by 19.7% and by 49.87% in the 0.05 and 5 mg l⁻¹ treatment, relative to the control sample. The only reductions in laboratory rETR_m were recorded in the 10 (16.6%) and 50 mg l⁻¹ (26.6%) treatments. Results in the laboratory and the field do not tell a similar story; in the laboratory, relatively high n-TiO₂ concentrations were required to produce negative impacts on *N. palea* after 24 hours, whereas in riverine biofilms, negative impacts in photophysiology were seen at lower

concentrations (0.05 and 5 mg l⁻¹).

Key differences between the laboratory and field sites are likely to cause different responses to n-TiO₂ exposure, and the results obtained were expected to reflect this. Merely looking at the control Fv/Fm values (a crude indicator of photosynthetic health) at 24 hours, field values for the biofilms were already lower than those recorded in the laboratory for *N. palea* (field control $Fv/Fm = 0.48$, laboratory control $Fv/Fm = 0.60$). This difference is likely due to a multitude of factors characteristic of field conditions.

Firstly, field conditions differ entirely from those in the laboratory. In the field, UV irradiation is present, and during the experiment, water temperatures reached 27-29 (°C). Based on the published literature (Sayes *et al.*, 2006), we believe that UV exposure only causes photocatalytic activity in n-TiO₂s in the anatase crystalline phase, and not in the rutile phase. However, high UV irradiation in the field and elevated temperatures may be acute stressors for biofilm algal assemblages directly. High UV is known to reduce levels of algal photosynthetic pigments (Agrawal, 1992) and Fv/Fm has been observed to decrease in response to UV-A and UV-B exposure in microalgae (Lesser, 1996; Bautista-Saraiva *et al.*, 2018).

Secondly, in the laboratory, a single species was present (*N. palea*); the species used is motile, so is, therefore, able to move away from potential stress exerted by the nanoparticles. Accordingly, at low nanoparticle concentrations, *N. palea* would hypothetically have the capacity to escape the stressor. However, in field conditions, over 50 distinct taxa may be present in a biofilm; some will be able to move away, but some will be sessile, and unable to escape any stress from the n-TiO₂. Therefore, the whole community average tolerance value is likely to be less than that of *N. palea*.

By comparing field and laboratory results after 24-hour exposure, *N. palea* appears more tolerant to n-TiO₂ exposure than biofilm communities in the field. Arguably, because it is not as sensitive to n-TiO₂, it would not make a good model species, as a susceptible

taxon would be a better indicator. However, after 24 hours, *N. palea* produced a clear concentration-response pattern to increasing n-TiO₂ concentration. In addition, the current OECD-recommended diatom, *Fistulifera pelliculosa*, is not a good n-TiO₂ toxicity indicator, firstly because it is small in size and tends to clump together, complicating cell counts (Hana Masani, personal communication) and secondly, the only published study on n-TiO₂ impacts on *F. pelliculosa* found no impairment of biomass or *Fv/Fm* at up to 100 mg l⁻¹ n-TiO₂ after 72 hours (Joonas *et al.*, 2019). With this knowledge, *N. palea* would be a better indicator species than *F. pelliculosa*, and would be useful for rapid toxicity testing of n-TiO₂s (0-24 hours).

It is difficult to compare the *N. palea* susceptibility to n-TiO₂ with the OECD recommended green alga, *Raphidocelis subcapitata*, due to the varied responses in n-TiO₂ susceptibility recorded throughout the literature. Some studies found *R. subcapitata* to be highly impaired after 72 hours, with IC₅₀ values of 5.83 mg l⁻¹ and 2.53 mg l⁻¹ (Aruoja *et al.*, 2009; Lee & An, 2013). In contrast, others have shown much lower IC₅₀ values, indicating a much lower impact with values of 160 mg l⁻¹ and 113 mg l⁻¹ (Hartmann *et al.*, 2010; Metzler *et al.*, 2011). The differences in responses throughout the literature are likely caused by inter-laboratory methodological variation between studies; small differences in methodology are likely to result in large differences in response to n-TiO₂ exposure (Nyholm, 1985). This exemplifies the overwhelming necessity for a standardized ENP toxicity test for freshwater algae.

4.2 Problems with evaluating the impacts of ENPs using the OECD Freshwater Alga and Cyanobacteria Growth Inhibition Test

The OECD Freshwater Alga and Cyanobacteria Growth Inhibition Test guidelines state that toxicity experiments investigating the impacts of a hazardous substance on freshwater biota must be run for at least 72 hours. This test criterion was originally applied for testing

soluble toxicants, and requires the toxicant to dissolve in the aquatic medium. Titanium dioxide nanoparticles are insoluble in water and aquatic test media, and form suspensions when added to aquatic growth media (Hartmann *et al.*, 2010). Due to the physico-chemical properties of the nanoparticles and the chemical properties of the media in which they are immersed (e.g. high ionic strength), several time-dependent transformation processes, such as sedimentation and aggregation, will take place over the duration of the experiment. This complicates ENP toxicity testing, due to the unstable exposure conditions which will vary throughout the experiment, and it raises the question of whether actual 'nano-scale' properties are being tested for the majority of the incubation period. There may be a risk of underestimating toxicity due to increases in nanoparticle hydrodynamic diameter during the experiment (Cupi *et al.*, 2016). Rapid 0-24 hour toxicity tests, therefore, may be the most reliable for ENP toxicity testing, as they reduce the probability of time-dependent nanoparticle transformation changes and provide a reliable result before the nanoparticles have time to form aggregates, therefore becoming more like microparticles. Sorensen & Baun (2015) proposed carrying out 2-hour toxicity tests after ageing the nanoparticles in growth media for 24 hours as this method produced clear concentration-response patterns and as a result, reproducibility increased. Future studies evaluating ENP toxicity to freshwater algae should include time-course experiments to determine the point at which ENPs begin to aggregate in aquatic media and to determine ENP toxicity between 0-24 hours.

OECD guidelines recommend that algal cultures should receive continuous, uniform fluorescent illumination of cool white light throughout the duration of a toxicity test, with a light intensity ranging from 60-120 μmol (photons) $\text{m}^{-2} \text{s}^{-1}$. Some nanoparticle toxicity studies, published in the literature, have been compliant with these guidelines, whereas others used varying light-dark photoperiods. Continuous illumination may actually be an inferior option, as it is not a realistic reflection of field conditions. Outside the laboratory, algae are exposed to light and dark cycles, and continuous lighting may be an underlying cause of inaccurate nanoparticle toxicity estimates.

Keeping algae in varying experimental vessels for 72 hours is also a questionable practice,

and the type of exposure system used may affect ENP toxicity. Manier *et al* (2015) studied and compared three different exposure systems (Erlenmeyer flasks, 24-well microplates and cylindrical vials). Growth inhibition was substantially higher in the cylindrical vials (71%), relative to the controls, when compared with the 24-well microplates (49%) and Erlenmeyer flasks (33%). Visual observations in their study revealed the presence of large agglomerates in the microplates and flasks, which did not form in the vials, suggesting that in the systems where nanoparticles aggregated more, the negative impacts were less.

Despite the many and varied difficulties as documented above, laboratory tests are extremely important to ecotoxicological studies, and do provide fast, cheap and sensitive test results for measuring toxicity of selected substances in environmentally relevant organisms. However, it is recommended that current guidelines for ENP toxicity testing should be reconsidered, due to the time-dependent transformational changes that the ENPs undergo. A shorter test may mitigate a substantial amount of the variability in ENP toxicity results; while shortening exposure time does not increase environmental relevance as such, it offers more control during testing, and may aid researchers in ranking different ENP toxicities.

4.3 Future recommendations for testing the impacts of n-TiO₂s in the field

In a realistic environmental scenario, the amount of n-TiO₂ that algae in water bodies are exposed to is likely to be seasonally-dependent. Algae are likely to experience substantially increased nanoparticle concentrations in the summer months due to increased sunscreen use, with more people swimming in water bodies. In winter, n-TiO₂ exposure will be lower. More studies are therefore required to better understand post n-TiO₂ exposure algal recovery. This could be done in outdoor mesocosms in the field; after a set period of n-TiO₂ exposure, biofilms could be translocated to a new channel with identical conditions to the control biofilms, and long term changes in biofilm growth and photophysiology could be measured. It is also suggested that future tests should also evaluate the effects of n-TiO₂ to other members of the periphytic community, such as cyanobacteria, and also on the grazers that

feed on periphyton to see whether n-TiO₂ toxicity is biomagnified up the food chain to higher trophic levels.

4.4 The larger scale impacts of n-TiO₂ pollution on the world's water bodies

Pollution of n-TiO₂s may be having large-scale negative impacts globally. Coastal tourism has rapidly increased in the last decade (Tovar-Sanchez *et al.*, 2013); higher numbers of people visiting these areas therefore means the amount of sunscreen being used is also increasing. Most of the common sunscreens on our shelves contain minerals such as titanium dioxide and zinc oxide in the nano-scale form (n-TiO₂ & n-ZnO), which are used as UV filters (Smijs & Pavel, 2011). Every year, it is predicted that approximately 14,000 tons of sunscreen end up in waterways (Downs *et al.*, 2016), sourced from humans, covered in sunscreen, swimming in the ocean. Conservative estimates for a Mediterranean beach reveal that during a summer day, 4 kg of n-TiO₂s could be released into the water, increasing hydrogen peroxide (H₂O₂) concentration to 270 nM/day (Sanchez-Quiles & Tovar-Sanchez, 2014). This mass pollution of sunscreen into our waters has led to concerns about the impacts of nanoparticle pollution on coral reefs in the ocean. Corals live in symbiosis with dinoflagellate algae (zooxanthellae). The algae absorb sunlight and photosynthesise, creating nutrients that feed the coral. Exposure to n-TiO₂ in the Caribbean mountainous star coral (*Montastraea faveolata*) at 0.1 and 10 mg l⁻¹ caused significant algal expulsion in all the colonies (Jovanovic & Guzman, 2014). Without algae, corals are left bleached and pale, deprived of their main source of food. Although climate change seems to be the primary cause of coral bleaching (Baker *et al.*, 2008), oceanic sunscreen pollution of oceans may speed up the bleaching process. Sanchez-Quiles & Tovar-Sanchez (2014) demonstrated that photoexcitation of n-TiO₂s and ZnO nanoparticles under solar radiation produced significant amounts of H₂O₂, a strong bleach which generates high levels of stress on algae. Commercial companies are already latching onto this media hype and developing "non-nano sunscreens". The particle size of n-TiO₂s and ZnO used in these new developing products are between 100-130 nm, which lies slightly outside the defined range of a nanoparticle (1-100 nm). As

such, this is not only false advertising, but also may not mitigate nanoparticle pollution effects at all. Another potentially significant concern is the impact of sunscreen pollution on marine diatoms. Several studies have reported negative effects of n-TiO₂ on marine diatoms (Miller *et al.*, 2010; Tovar-Sanchez *et al.*, 2013; Galletti *et al.*, 2016). As marine microalgae represent the first level of the trophic chain, mass pollution of n-TiO₂ could have negative cascading effects on the entire ecosystem. Somewhere between a fifth and a quarter of all photosynthesis on the planet is carried out by diatoms, meaning that as much as a 25% of Earth's oxygen is sourced by these microscopic marine cells. By fixing carbon, or converting it from CO₂ into sugar, diatoms help reduce atmospheric CO₂, so diatom activity reduces global warming effects (Galletti *et al.*, 2016). If n-TiO₂ concentrations get too high, and begin to impair marine diatoms, the concentration of greenhouse gases in our atmosphere may increase, having extreme negative consequences on global warming and climate change.

Glossary and Abbreviations

Glossary

Anatase: crystalline phase of titanium dioxide nanoparticles, providing high photocatalytic activity in commercial products, such as sunscreens

Brookite: crystalline phase of titanium dioxide nanoparticles, not typically used in commercial products

Fine particles: particles with a size range spanning 100 nm - 3µm

Heteroaggregation: aggregation of dissimilar particle (e.g. NP-algal cell aggregation)

Homoaggregation: aggregation of similar particles (e.g. NP-NP aggregation)

Nanoparticles: particles with a size range of 1-100 nm, possessing three outer dimensions at the nanoscale

Photocatalysis: acceleration of a chemical reaction when a catalyst is present

Point zero charge: when the electrical charge density on the surface is zero

Rutile: crystalline phase of titanium dioxide nanoparticles, typically used in paint as a white pigment

Steric hindrance: the termination of a chemical reaction caused by a molecule's structure

Zeta potential: the potential difference across an electric double layer usually between a solid surface and a liquid

Abbreviations

Alpha: the theoretical maximum light utilization coefficient

DARLEQ: diatoms for assessing river and lake ecological quality

DM: dry mass

DOM: dissolved organic matter

EC₅₀: the concentration which induces a response halfway between the baseline and maximum after a specified exposure time

E_k: the light saturation coefficient

ENP: engineered nanoparticle

EPA: environmental protection agency

EPS: extracellular polymeric substances

ETR_m: the maximum electron transport rate

FA: fulvic acids

FBA: freshwater biological association

FDA: food and drug administration

***F_v*/*F_m*:** the maximum quantum yield of PSII in the dark-adapted state

GI: growth inhibition

HA: humic acids

IC₂₀: the concentration at which 20% of the population growth is inhibited

IC₅₀: the concentration at which 50% of the population growth is inhibited

IS: ionic strength

NM: nanomaterial

NOM: natural organic matter

NP: nanoparticle

n-TiO₂: titanium dioxide nanoparticle

OECD: organization for economic cooperation and development

PAM: pulse amplitude modulated fluorometry

PAR: photosynthetic active radiation

PEC: predicted environmental concentration

PSII: photosystem two

PZC: point zero charge

RCF: relative centrifugal force

RLC: rapid light curve

ROS: reactive oxygen species

RPM: revolutions per minute

SEM: scanning electron microscope/microscopy

SSSI: site for special scientific interest

STW: sewage treatment works

TDI: trophic diatom index

WFD: water framework directive

WPMN: working party of manufactured nanomaterials

References

- Agrawal, S. B. (1992). Effects of supplemental U.V.-B radiation on photosynthetic pigment, protein and glutathione contents in green algae. *Environmental and Experimental Botany*, **32**, 137-143.
- Al-Harashsheh, M., Batiha, M., Kraishan, S. and Al-Zoubi, H. (2014). Precipitation treatment of effluent acidic wastewater from phosphate-containing fertilizer industry: Characterization of solid and liquid products. *Separation and Purification Technology*, **123**, 190-199.
- Aruoja, V., Dubourguier, H. C., Kasemets, K. and Kahru, A. (2009). Toxicity of nanoparticles of CuO, ZnO, and TiO₂ to micro algae *Pseudokirchneriella subcapitata*. *Science of The Total Environment*, **407**, 1461-1468.
- Baker, A. C., Glynn, P. W. and Riegl, B. (2008). Climate change and coral reef bleaching: An ecological assessment of long-term impacts, recovery trends and future outlook. *Estuarine, Coastal and Shelf Science*, **80**, 435-471.
- Bakshi, S., He, Z. L. and Harris, W. G. (2015). Natural nanoparticles: implications for environment and human health. *Critical Reviews in Environmental Science and Technology*, **45**, 861-904.
- Barbagallo, R. P., Oxborough, K., Pallett, K. E. and Baker, N. R. (2003). Rapid, noninvasive screening for perturbations of metabolism and plant growth using chlorophyll fluorescence imaging. *Plant Physiology*, **132**, 485-493.
- Battin, T., Kammer, F., Weilhartner, A., Ottofuelling, S. and Hofmann, T. (2009). Nanostructured TiO₂: transport behaviour and effects on aquatic microbial communities under environmental conditions. *Environmental Science & Technology*, **43**, 8098-8104.
- Bautista-Saraiva, A., Bonomi-Barufi, J., Figueroa, F. and Necchi, O. (2018). UV-radiation effects on photosynthesis, photosynthetic pigments and UV-absorbing substances in three species of tropical lotic macroalgae. *Theoretical and Experimental Plant Physiology*, **30**, 181-192.
- Bennion, H., Kelly, M., Juggins, S., Yallop, M., Burgess, A., Jamieson, J. and Krokowski, J. (2014). Assessment of ecological status in UK lakes using benthic diatoms. *Freshwater Science*, **33**, 639-654.
- Berg, J. M., Romoser, A., Banerjee, N., Zebda, R. and Sayes, C. M. (2009). The relationship between pH and zeta potential of 30 nm metal oxide nanoparticle suspensions relevant to in vitro toxicological evaluations. *Nanotoxicology*, **3**, 276-283.
- Bessa da Silva, M., Abrantes, N., Noqueira, V., Goncalves, F. and Pereira, R. (2016). TiO₂ nanoparticles for the remediation of eutrophic shallow freshwater systems: efficiency and impacts on aquatic biota under a microcosm experiment. *Aquatic Toxicology*, **178**, 58-71.

Biggs, B. J. F., Stevenson, R. J. and Lowe, R. L. (1998). A habitat matrix conceptual model for stream periphyton. *Archiv fur Hydrobiologie*, **143**, 25-56.

Blinn, D. W., Fredericksen, A. and Korte, V. Colonization rates and community structure of diatoms on three different rock substrata in a lotic system. *British Phycological Journal*, **15**, 303-310.

Bour, A., Mouchet, F., Verneuil, L., Evariste, L., Silvestre, J., Pinelli, E. and Gauthier, L. (2015). Toxicity of CeO₂ nanoparticles at different trophic levels? Effects on diatoms, chironomids and amphibians. *Chemosphere*, **120**, 230-236.

Bour, A., Mouchet, F., Cadarsi, S., Sylvestre, J., Verneuil, L., Baque, D., Chauvet, E., Bonzom, J. M., Pagnout, C. and Clivot, H. (2016). Toxicity of CeO₂ nanoparticles on freshwater experimental trophic chain: a study in environmentally relevant conditions through the use of mesocosms. *Nanotoxicology*, **10**, 245-255.

Bowes, M. J., Smith, J. T., Neal, C., Leach, D. V., Scarlett, P. M., Wickham, H. D., Harman, S. A., Armstrong, L. K., Davy-Bowker, J., Haft, M. and Davies, C. E. (2011). Changes in water quality of the River Frome (UK) from 1965-2009: is phosphorus mitigation finally working?. *Science Of The Total Environment*, **409**, 3418-3430.

Bundschuh, M., Seitz, F., Rosenfeldt, R. and Schulz, R. (2016). Effects of nanoparticles in fresh waters: risks, mechanisms and interactions. *Freshwater Biology*, **61**, 2185-2196.

Bundschuh, M., Filser, J., Luderwald, S., McKee, M. S., Metreveli, G., Schaumann, G. E., Schulz, R. and Wagner, S. (2018). Nanoparticles in the environment: where do we come from, where do we go to?. *Environmental Sciences Europe*, **30**, 6.

Camuel, A., Guieysse, B., Alcantara, C. and Bechet, Q. (2017). Fast algal eco-toxicity assessment: influence of light intensity and exposure time on *Chlorella vulgaris* inhibition by atrazine and DCMU. *Ecotoxicology and Environmental Safety*, **140**, 141-147.

Carvalho, C. (2018). Marine Biofilms: A Successful Microbial Strategy With Economic Implications. *Frontiers in Marine Science*, **5**, <https://doi.org/10.3389/fmars.2018.00126>.

Cassaignon, S., Koelsch, M. and Jolivet, J. (2007). From TiCl₃ to TiO₂ nanoparticles (anatase, brookite and rutile): thermohydrolysis and oxidation in aqueous medium. *Journal of Physics and Chemistry of Solids*, **68**, 695-700.

Chen, L., Zhou, L., Liu, Y., Deng, S., Wu, H. and Wang, G. (2012). Toxicological effects of nanometer titanium dioxide (nano-TiO₂) on *Chlamydomonas reinhardtii*. *Ecotoxicology and Environmental Safety*, **84**, 155-162.

Chen, X., Mao, X., Cao, Y. and Yang, X. (2013). Use of siliceous algae as biological monitors of heavy metal pollution in three lakes in a mining city, southeast China. *Oceanological and Hydrobiological Studies*, **42**, 233-242.

Cherchi, C., Chernenko, T., Diem, M. and Gu, A. Z. (2011). Impact of nano titanium dioxide exposure on cellular structure of *Anabaena variabilis* and evidence of internalization. *Environmental Toxicology and Chemistry*, **30**, 861-869.

Chonova, T., Kurmayer, R., Rimet, F., Labanowski, J., Vasselon, V., Keck, F., Illmer, P. and Bouchez, A. (2019). Benthic diatom communities in alpine river impacted by waste water treatment effluent as revealed using DNA metabarcoding. *Frontiers in Microbiology*, **10**, <https://doi.org/10.3389/fmicb.2019.00653>.

Cleuvers, M., Altenburger, R. and Ratte, H. (2002). Combination effect of light and toxicity in algal tests. *Journal of Environmental Quality*, **31**, 539-547.

Cleuvers, M. and Weyers, A. (2003). Algal growth inhibition test: does shading of coloured substances really matter?. *Water Research*, **37**, 2718-2722.

Coelho, H., Viera, S. and Serodio, J. (2011). Endogenous versus environmental control of vertical migration by intertidal benthic microalgae. *European Journal of Phycology*, **30**, 271-281.

Consalvey, M., Paterson, D. M. and Underwood, G. J. C. (2004). The ups and downs of life in a benthic biofilm: migration of benthic diatoms. *Diatom Research*, **19**, 181-202.

Consalvey, M., Perkins, R., Paterson, D. and Underwood, G. (2005). PAM fluorescence: a beginners guide for benthic diatomists. *Diatom Research*, **20**, 1-22.

Cosgrove, J. and Borowitzka, M. (2006). Applying pulse amplitude modulation (PAM) fluorometry to microalgae suspensions: stirring potentially impacts fluorescence. *Photosynthesis Research*, **88**, 343-350.

Crane, M., Handy, R. D., Garrod, J. and Owen, R. (2008). Ecotoxicity test methods and environmental hazard assessment for engineered nanoparticles. *Ecotoxicology*, **17**, 421-437.

Cupi, D., Hartmann, N. B. and Baun, A. (2016). Influence of pH and media composition on suspension stability of silver, zinc oxide, and titanium dioxide nanoparticles and immobilization of *Daphnia magna* under guideline testing conditions. *Ecotoxicology and Environmental Safety*, **127**, 144-152.

Danielsson, K., Gallego-Urrea, J., Hasselov, M., Gustafsson, S. and Jonsson, C. (2017). Influence of organic molecules on the aggregation of TiO₂ nanoparticles in acidic conditions. *Journal of Nanoparticle Research*, **19**, 133-138.

Debenest, T., Silvestre, J., Coste, M., Delmas, F. and Pinelli, E. (2008). Herbicide effects on freshwater benthic diatoms: induction of nucleus alterations and silica cell wall abnormalities. *Aquatic Toxicology*, **88**, 88-94.

Decho, A. W. and Gutierrez, T. (2017). Microbial extracellular polymeric substances (EPSs) in ocean systems. *Frontiers in Microbiology*, **8**, 922-927.

- De Jong, W. H. and Borm, P. J. A. (2008). Drug delivery and nanoparticles: applications and hazards. *International Journal of Nanomedicine*, **3**, 133-149.
- De Schampheleere, K. and Janssen, C. (2004). Comparison of the effect of different pH buffering techniques on the toxicity of copper and zinc to *Daphnia magna* and *Pseudokirchneriella subcapitata*. *Ecotoxicology*, **13**, 697-705.
- Deng, X. Y., Cheng, J., Hu, X. L., Wang, L., Li, D. and Gao, K. (2017). Biological effects of TiO₂ and CeO₂ nanoparticles on the growth, photosynthetic activity, and cellular components of a marine diatom *Phaeodactylum tricornutum*. *Science of The Total Environment*, **575**, 87-96.
- Dijkman, N. A. and Kromkamp, J. C. (2006). Photosynthetic characteristics of phytoplankton in the Scheldt estuary: community and single-cell fluorescence measurements. *European Journal of Phycology*, **41**, 425-434.
- Downs, C. A., Kramarsky-Winter, E., Segal, R., Fauth, J., Knutson, S., Bronstein, O., Ciner, F. R., Jeger, R., Lichtenfeld, Y., Woodley, C. M., Pennington, P., Cadenas, K., Kushmaro, A. and Loya, Y. (2016). Toxicopathological effects of the sunscreen UV filter, oxybenzone (benzophenone-3), on coral planulae and cultured primary cells and its environmental contamination in Hawaii and the U.S. Virgin Islands. *Archives of Environmental Contamination and Toxicology*, **70**, 265-288.
- Doyle, J., Palumbo, V., Huey, B. and Ward, J. (2014). Behaviour of titanium dioxide nanoparticles in three aqueous media samples: agglomeration and implications for benthic deposition. *Water, Air & Soil Pollution*, **225**, 2106-2110.
- Du, G., Li, W., Li, H. and Chung, I. K. (2012). Migratory responses of benthic diatoms to light and temperature monitored by chlorophyll fluorescence. *Journal of Plant Biology*, **55**, 159-164.
- Dunphy-Guzman, K., Finnegan, M. and Banfield, J. (2006). Influence of surface potential on aggregation and transport of titania nanoparticles. *Environmental Science & Technology*, **40**, 7688-7693.
- Fechner, L. C., Gourlay-France, C., Bourgeault, A. and Tusseau-Vuillemin, M. H. (2012). Diffuse urban pollution increases metal tolerance of natural heterotrophic biofilms. *Environmental Pollution*, **162**, 311-318.
- Ferry, J., Craig, P., Hexel, C., Sisco, P., Frey, R., Pennington, P., Fulton, M., Scott, I., Decho, A., Kashiwada, S., Murphy, C. and Shaw, T. (2009). Transfer of gold nanoparticles from the water column to the estuarine food web. *Nature Nanotechnology*, **4**, 441-444.
- Finnegan, M., Emburey, S., Hommen, U., Baxter, L., Hoekstra, P., Hanson, M., Thompson, H. and Hamer, M. (2018). A freshwater mesocosm study into the effects of the neonicotinoid insecticide thiamethoxam at multiple trophic levels. *Environmental Pollution*, **242**, 1444-1457.

- Fu, L., Hamzeh, M., Dodard, S., Zhao, Y. and Sunahara, G. (2015). Effects of TiO₂ nanoparticles on ROS production and growth inhibition using freshwater green algae pre-exposed to UV irradiation. *Environmental Toxicology and Pharmacology*, **39**, 1074-1080.
- Frankenbach, S., Schmidt, W., Frommlet, J. and Serodio, J. (2018). Photoinactivation, repair and the motility-physiology trade-off in microphytobenthos. *Marine Ecology Progress Series*, **601**, 41-57.
- French, R., Jacobson, A., Kim, B., Isley, S., Penn, R. and Baveye, P. (2009). Influence of ionic strength, pH, and cation valence on aggregation kinetics of titanium dioxide nanoparticles. *Environmental Science & Technology*, **43**, 1354-1359.
- Galletti, A., Seo, S., Joo, S. H., Su, C. and Blackwelder, P. L. (2016). Effects of titanium dioxide nanoparticles derived from consumer products on the marine diatom *Thalassiosira pseudonana*. *Environmental Science and Pollution Research*, **23**, 21113-21122.
- Gao, X., Zhou, K., Zhang, L., Yang, K. and Lin, D. (2018). Distinct effects of soluble and bound exopolymeric substances on algal bioaccumulation and toxicity of anatase and rutile TiO₂ nanoparticles. *Environmental Science: Nano*, **5**, 720-729.
- Gatoo, M. A., Naseem, S., Arfat, M. Y., Mahmood Dar, A., Qasim, K. and Zubair, S. (2014). Physicochemical properties of nanomaterials: implication in associated toxic manifestations. *BioMed Research International*, **2014**, <http://dx.doi.org/10.1155/2014/498420>.
- Gold, C., Feurtet-Mazel, A., Coste, M. and Boudou, A. (2003). Effects of cadmium stress on periphytic diatom communities in indoor artificial streams. *Freshwater Biology*, **48**, 316-328.
- González, A., Fernández-Rojo, L., Leflaive, J., Pokrovsky, O. and Rols, J. (2016). Response of three biofilm-forming benthic microorganisms to Ag nanoparticles and Ag⁺: the diatom *Nitzschia palea*, the green alga *Uronema confervicolum* and the cyanobacteria *Leptolyngbya* sp. *Environmental Science and Pollution Research*, **23**, 22136-22150.
- Goto, N., Kawamura, T., Mitamura, O. and Terai, H. (1999). Importance of extracellular organic carbon production in the total primary production by tidal-flat diatoms in comparison to phytoplankton. *Marine Ecology Progress Series*, **190**, 289-295.
- Gottschalk, F., Sonderer, T., Scholz, R. W. and Nowack, B. (2009). Modeled environmental concentrations of engineered nanomaterials (TiO₂, ZnO, Ag, CNT, Fullerenes) for different regions. *Environmental Science & Technology*, **43**, 9216-9222.
- Gottschalk, F. and Nowack, B. (2011). The release of engineered nanomaterials to the environment. *Journal of Environmental Monitoring*, **13**, 1145-1155.
- Guasch, H. and Sabater, S. (1994). Primary production of epilithic communities in undisturbed Mediterranean streams. *SIL Proceedings, 1922-2010*, **25**, 1761-1764.
- Guasch, H. and Sabater, S. (2002). Light history influences the sensitivity to atrazine in periphytic algae. *Journal of Phycology*, **34**, 233-241.

- Guasch, H., Artigas, J., Bonet, B., Bonnineau, C., Canals, O., Corcoll, N., Foulquier, A., Lopez-Doval, J. C., Kim-Tiam, S., Morin, S., Navarro, E., Pesce, S., Proja, S., Salvado, H. and Serra, A. (2016). 'The use of biofilms to assess the effects of chemicals on freshwater ecosystems', in Romani, A., Guasch, H. and Balaguer, M. D. *Aquatic Biofilms: Ecology, Water Quality and Wastewater Treatment*. Poole: Caister Academic Press, pp. 125-144.
- Gutierrez, T., Biller, D. V., Shimmield, T. and Green, D. H. (2012). Metal binding properties of the EPS produced by *Halomonas* sp. TG39 and its potential in enhancing trace element bioavailability to eukaryotic phytoplankton. *Biometals*, **25**, 1185-1194.
- Hall, S., Bradley, T., Moore, J. T., Kuykindall, T. and Minella, L. (2009). Acute and chronic toxicity of nano-scale TiO₂ particles to freshwater fish, cladocerans, and green algae, and effects of organic and inorganic substrate on TiO₂ toxicity. *Nanotoxicology*, **3**, 91-97.
- Han, B. P., Virtanen, M., Koponen, J. and Straskraba, M. (2000). Effect of photoinhibition on algal photosynthesis: a dynamic model. *Journal of Plankton Research*, **22**, 865-885.
- Handy, R. D., von der Kammer, F., Lead, J. R., Hassellöv, M., Owen, R. and Crane, M. (2008). The ecotoxicology and chemistry of manufactured nanoparticles. *Ecotoxicology*, **17**, 287-314.
- Handy, R. D., Cornelis, G., Fernandes, T., Tsyusko, O., Decho, A. and Sabo-Attwood, T. (2012). Ecotoxicity test methods for engineered nanomaterials: practical experiences and recommendations from the bench. *Environmental Toxicology and Chemistry*, **35**, 15-31.
- Hartmann, N. B., Von der Kammer, F., Hofmann, T., Baalousha, M., Ottofuelling, S. and Baun, A. (2010). Algal testing of titanium dioxide nanoparticles ? testing considerations, inhibitory effects and modification of cadmium bioavailability. *Toxicology*, **269**, 190-197.
- Hartmann, N. B., Engelbrekt, C., Zhang, J., Ulstrup, J., Kusk, K. O. and Baun, A. (2013). The challenges of testing metal and metal oxide nanoparticles in algal bioassays: titanium dioxide and gold nanoparticles as case studies. *Nanotoxicology*, **7**, 1082-1094.
- Hartmann, N. B., Jensen, K. A., Baun, A., Rasmussen, K., Rauscher, H., Tantra, R., Cupi, D., Gilliland, D., Pianella, F. and Sintes, J. R. (2015). Techniques and protocols for dispersing nanoparticle powders in aqueous media - is there a rationale for harmonization?. *Journal of Toxicology and Environmental Health Part B*, **18**, 1-28.
- He, G., Chen, R., Lu, S., Jiang, C., Liu, H. and Wang, C. (2015). Dominating role of ionic strength in the sedimentation of nano-TiO₂ in aquatic environments. *Journal of Nanomaterials*, **2015**, 1-10.
- He, M., Yan, Y., Pei, F., Wu, M., Gebreluel, T., Zou, S. and Whang, C. (2017). Improvement on lipid production by *Scenedesmus obliquus* triggered by low dose exposure to nanoparticles. *Scientific Reports*, **7**, <http://dx.doi.org/10.1038/s41598-017-15667-0>.
- Herlory, O., Bonzom, J. and Gilbin, R. (2013). Sensitivity evaluation of the green alga

Chlamydomonas reinhardtii to uranium by pulse amplitude modulated (PAM) fluorometry. *Aquatic Toxicology*, **140-141**, 288-294.

Hjorth, R., Skjolding, L. M., Sorensen, S. N. and Baun, A. (2017). Regulatory adequacy of aquatic ecotoxicity testing of nanomaterials. *NanoImpact*, **8**, 28-37.

Hough, Z. J., Walters, H. S. and Bechtold, H. A. (2017). Titanium dioxide (TiO₂) nanoparticles more strongly affect bacteria compared to algae in stream ecosystems. *Journal of Student Research*, **6**, 103-108.

Hund-Rinke, K. and Simon, M. (2006). Ecotoxic effect of photocatalytic active nanoparticles (TiO₂) on algae and daphnids. *Environmental Science and Pollution Research*, **13**, 225-232.

Hund-Rinke, K. and Wenzel, A. (2010). TiO₂ nanoparticles - relationship between dispersion preparation method and ecotoxicity in the algal growth test. *Environmental Sciences Europe*, **22**, 517-528.

Hund-Rinke, K., Baun, A., Cupi, D., Fernandes, T. F., Handy, R., Kinross, J. H. Navas, J. M., Peijnenburg, W., Schlich, K., Shaw, B. J. and Scott-Fordsmand, J. J. (2016). Regulatory ecotoxicity testing of nanomaterials ? proposed modifications of OECD test guidelines based on laboratory experience with silver and titanium dioxide nanoparticles. **10**, 1442-1447.

Hu, J., Wang, J., Liu, S., Zhang, Z., Zhang, H., Cai, X., Pan, J. and Liu, J. (2018). Effect of TiO₂ nanoparticle aggregation on marine microalga *Isochrysis galbana*. *Journal of Environmental Sciences*, **66**, 208-215.

Ikuma, K., Decho, A. and Lau, B. (2015). When nanoparticles meet biofilms ? interactions guiding the environmental fate and accumulation of nanoparticles. *Frontiers in Microbiology*, **6**, <http://dx.doi.org/10.3389/fmicb.2015.00591>.

Iswarya, V., Bhuvaneshwari, M., Alex, S. A., Iyer, S., Chaudhuri, G., Chandrasekaran, P. T., Bhalerao, G. M., Chakravarty, S., Raichur, A. M., Chandrasekaran, N. and Mukherjee, A. (2015). Combined toxicity of two crystalline phases (anatase and rutile) of titania nanoparticles towards freshwater microalgae: *Chlorella sp.* *Aquatic Toxicology*, **161**, 154-169.

Ivask, A., Kurvet, I., Kasemets, K., Blinova, I., Aruoja, V., Suppi, S., Vija, H., Kakinen, A., Titma, T., Heinlaan, M., Visnapuu, M., Koller, D., Kisand, V. and Kahru, A. (2014). Size-dependent toxicity of silver nanoparticles to bacteria, yeast, algae, crustaceans and mammalian cells in vitro. *PLoS ONE*, **9** (7), <http://dx.doi.org/10.1371/journal.pone.0102108>.

Jeevanandam, J., Barhoum, A., Chan, Y. S., Dufresne, A. and Danquah, M. K. (2018). Review on nanoparticles and nanostructured materials: history, sources, toxicity and regulations. *Beilstein Journal of Nanotechnology*, **9**, 1050-1074.

Jesline, A., John, A., Narayanan, P., Vani, C. and Murugan, S. (2014). Antimicrobial activity of zinc and titanium dioxide nanoparticles against bio-film producing methicillin-resistant

- Staphylococcus aureus*. *Applied Nanoscience*, **5**, 157-162.
- Ji, J., Long, Z. and Lin, D. (2011). Toxicity of oxide nanoparticles to the green algae *Chlorella* sp. *Chemical Engineering Journal*, **170**, 525-530.
- Jia, K., Sun, C., Wang, Y., Li, X., Mu, W. and Fan, Y. (2019). Effect of TiO₂ nanoparticles and multiwall carbon nanotubes on the freshwater diatom *Nitzschia frustulum*: evaluation of growth, cellular components and morphology. *Chemistry and Ecology*, **35**, 69-85.
- Joonas, E., Aruoja, V., Olli, K. and Kahru, A. (2019). Environmental safety data on CuO and TiO₂ nanoparticles for multiple algal species in natural water: filling the data gaps for risk assessment. *Science of The Total Environment*, **647**, 973-980.
- Jovanovic, B. and Guzman, H. M. (2014). Effects of titanium dioxide (TiO₂) nanoparticles on Caribbean reef-building coral (*Montastraea faveolata*). *Environmental Toxicology and Chemistry*, **33**, 1346-1353.
- Jovanovic, B., Bezirci, G., Cagan, A., Coppens, J., Levi, E., Oluz, Z., Tuncel, E., Duran, H. and Beklioglu, M. (2016). Food web effects of titanium dioxide nanoparticles in an outdoor freshwater mesocosm experiment. *Nanotoxicology*, **10**, 902-912.
- Juggins, S., Kelly, M., Allott, T., Kelly-Quinn, M. and Monteith, D. (2016). A Water Framework Directive-compatible metric for assessing acidification in UK and Irish rivers using diatoms. *Science of The Total Environment*, **568**, 671-678.
- Ju-Nam, Y. and Lead, J. (2008). Manufactured nanoparticles: an overview of their chemistry, interactions and potential environmental implications. *Science of The Total Environment*, **400**, 396-414.
- Kang, N. K., Lee, B., Choi, G., Moon, M., Park, M. S., Lim, J. and Yang, J. (2014). Enhancing lipid productivity of *Chlorella vulgaris* using oxidative stress by TiO₂ nanoparticles. *Korean Journal of Chemical Engineering*, **31**, 861-867.
- Keller, A., Wang, H., Zhou, D., Lenihan, H., Cherr, G., Cardinale, B., Miller, R. and Ji, Z. (2010). Stability and aggregation of metal oxide nanoparticles in natural aqueous matrices. *Environmental Science & Technology*, **44**, 1962-1967.
- Kelly, M. G. & Whitton, B. A. (1995). The trophic diatom index: a new index for monitoring eutrophication in rivers. *Journal of Applied Phycology*, **7**, 433-444.
- Kelly, M., Juggins, S., Guthrie, R., Pritchard, S., Jamieson, J., Rippey, B., Hirst, H. and Yallop, M. (2008). Assessment of ecological status in U.K. rivers using diatoms. *Freshwater Biology*, **53**, 403-422.
- Kernazhitsky, L., Shymanovska, V., Gavrilko, T., Naumov, V., Fedorenko, L., Kshnyakin, V. and Baran, J. (2014). Room temperature photoluminescence of anatase and rutile TiO₂ powders. *Journal of Luminescence*, **146**, 199-204.

Kessler, R. (2011). Engineered nanoparticles in consumer products: understanding a new ingredient. *Environmental Health Perspectives*, **119**, 120-125.

Khan, I. (1990). Assessment of water pollution using diatom community structure and species distribution - a case study in a tropical river basin. *Internationale Revue der gesamten Hydrobiologie und Hydrographie*, **75**, 317-338.

Khan, I., Saeed, K., Khan, I. (2017). Nanoparticles: properties, applications and toxicities. *Arabian Journal of Chemistry*, **5**, 1-23.

Kim Tiam, S., Lavoie, I., Doose, C., Hamilton, P. and Fortin, C. (2018). Morphological, physiological and molecular responses of *Nitzschia palea* under cadmium stress. *Ecotoxicology*, **27**, 675-688.

Klaine, S. J., Alvarez, P. J. J., Batley, G. E., Fernandes, T. F., Handy, R. D., Lyon, D. Y. (2008). Nanomaterials in the environment: behaviour, fate, bioavailability, and effects. *Environmental Toxicology and Chemistry*, **27**, 1825-1851.

Kolkwitz, R. & Marsson, M. (1908). Ökologie der pflanzlichen Saprobien. *Berichte der Deutschen Botanischen Gesellschaft*, **26 (7)**, <https://doi.org/10.1111/j.1438-8677.1908.tb06722.x>.

Krammer, K. and Lange-Bertalot, H. (1986) *Die Süßwasserflora von Mitteleuropa 2: Bacillariophyceae. 1 Teil: Naviculaceae*. Gustav Fischer-Verlag, Stuttgart. 876 pp.

Krammer, K. and Lange-Bertalot, H. (1997) *Die Süßwasserflora von Mitteleuropa, II:2. Bacillariophyceae. Teil 2: Bacillariaceae, Epithemiaceae, Surirellaceae. 2te Auflage, mit einem neuen Anhang*. Gustav Fischer Verlag, Stuttgart. 594 pp.

Krammer, K. and Lange-Bertalot, H. (2000) *Die Süßwasserflora von Mitteleuropa 2: Bacillariophyceae. 3 Teil: Centrales, Fragilariaceae, Eunotiaceae*, 2nd edn. Gustav Fischer Verlag, Stuttgart.

Krammer, K. and Lange-Bertalot, H. (2004) *Süßwasserflora von Mitteleuropa 2, Bacillariophyceae. Teil 4: Achnanthaceae. Kritische Ergänzungen zu Achnanthes s.l., Navicula s.str., Gomphonema*. Spektrum Akademischer Verlag/Gustav Fischer, Heidelberg. 468 pp.

Kroll, A., Behra, R., Kaegi, R. and Sigg, L. (2014). Extracellular polymeric substances (EPS) of freshwater biofilms stabilize and modify CeO₂ and Ag nanoparticles. *PLoS ONE*, **9**, <https://doi.org/10.1371/journal.pone.0110709>.

Kromkamp, J., Barranguet, C. and Peene, J. (1998). Determination of microphytobenthos PSII quantum efficiency and photosynthetic activity by means of variable chlorophyll fluorescence. *Marine Ecology Progress Series*, **162**, 45-55.

Krug, H., F. and Wick, P. (2011). Nanotoxicology: an interdisciplinary challenge. *Angew Chem Int Ed Engl*, **50**, 1260-1278.

Kulacki, K. and Cardinale, B. (2012). Effects of nano-titanium dioxide on freshwater algal

population dynamics. *PLoS ONE*, **7**, <http://doi.org/10.1371/journal.pone.0047130>.

Kulacki, K., Cardinale, B., Keller, A., Bier, R. and Dickson, H. (2012). How do stream organisms respond to, and influence, the concentration of titanium dioxide nanoparticles? A mesocosm study with algae and herbivores. *Environmental Toxicology and Chemistry*, **31**, 2414-2422.

Kurniawan, A., Hiraki, A., Fukuda, Y. and Yamamoto, T. (2015). Nutrient ions during biofilm forming process. *Procedia Environmental Sciences*, **28**, 252-257.

Lamberti, G. and Resh, V. (1985). Comparability of introduced tiles and natural substrates for sampling lotic bacteria, algae and macro invertebrates. *Freshwater Biology*, **15**, 21-30.

Laux, P., Tentschert, J., Riebeling, C., Braeuning, A., Creutzenberg, O., Epp, A., Fessard, V., Haas, K., Haase, A., Hund-Rinke, K., Jakubowski, N., Kearns, P., Lampen, A., Rauscher, H., Schoonjans, R., Stormer, A., Thielmann, A., Muhle, U. and Luch, A. (2018). Nanomaterials: certain aspects of application, risk assessment and risk communication. *Archives of Toxicology*, **92**, 121-141.

Lavoie, I., Morin, S., Laderriere, V. and Fortin, C. (2018). Freshwater diatoms as indicators of combined long-term mining and urban stressors in Junction Creek (Ontario, Canada). *Environments*, **5**, <http://doi.org/10.3390/environments5020030>.

Lazar, A. N., Wade, A. J., Whitehead, P. G. and Heppell, C. M. (2010). Modelling fixed plant and algal dynamics in rivers. Proceedings of the British Hydrological Society Third International Symposium: Role of Hydrology in Managing Consequences of a Changing Global Environment, pp 1-8.

Ledger, M. E. and Hildrew, A. G. (1998). Temporal and spatial variation in the epilithic biofilm of an acid stream. *Freshwater Biology*, **40**, 655-670.

Lee, W. and An, Y. (2013). Effects on zinc oxide and titanium dioxide nanoparticles on green algae under visible, UVA, and UVB irradiations: no evidence of enhanced algal toxicity under UV pre-irradiation. *Chemosphere*, **91**, 536-544.

Leguay, S., Lavoie, I., Levy, J. L. and Fortin, C. (2015). Using biofilms for monitoring metal contamination in lotic ecosystems: the protective effects of hardness and pH on metal bioaccumulation. *Environmental Toxicology and Chemistry*, **35**, 1489-1501.

Lesser, M. (1996). Elevated temperatures and ultraviolet radiation cause oxidative stress and inhibit photosynthesis in symbiotic dinoflagellates. *Limnology & Oceanography*, **41**, 271-283.

Li, L., Zheng, B. and Li, L. (2010). Biomonitoring and bioindicators used for river ecosystems: definitions, approaches and trends. *Procedia Environmental Sciences*, **2**, 1510-1524.

Li, S., Wallis, L., Ma, H. and Diamond, S. (2014). Phototoxicity of TiO₂ nanoparticles to a freshwater benthic amphipod: are benthic systems at risk?. *Science of The Total Environment*, **466-467**, 800-808.

- Li, F., Liang, Z., Zheng, X., Zhao, W., Wu, M. and Wang, Z. (2015). Toxicity of nano-TiO₂ on algae and the site of reactive oxygen species production. *Aquatic Toxicology*, **158**, 1-13.
- Li, L., Sillanpaa, M. and Risto, M. (2016). Influences of water properties on the aggregation and deposition of engineered titanium dioxide nanoparticles in natural waters. *Environmental Pollution*, **219**, 132-138.
- Li, S., Wang, C., Qin, H., Li, Y., Zheng, J., Peng, C. and Li, D. (2016). Influence of phosphorus availability on the community structure and physiology of cultured biofilms. *Journal of Environmental Sciences*, **42**, 19-31.
- Lin, D., Drew Story, S., Walker, S., Huang, Q. and Cai, P. (2016). Influence of extracellular polymeric substances on the aggregation kinetics of TiO₂ nanoparticles. *Water Research*, **104**, 381-388.
- Lin, D., Story, S., Walker, S., Huang, Q., Liang, W. and Cai, P. (2017). Role of pH and ionic strength in the aggregation of TiO₂ nanoparticles in the presence of extracellular polymeric substances from *Bacillus subtilis*. *Environmental Pollution*, **228**, 35-42.
- Liu, D., Liu, H., Wang, S., Chen, J. and Xia, Y. (2018). The toxicity of ionic liquid 1-decylpyridinium bromide to the algae *Scenedesmus obliquus*: Growth inhibition, phototoxicity, and oxidative stress. *Science of The Total Environment*, **622-623**, 1572-1580.
- Lombardi, A. T. and Maldonado, M. T. (2011). The effects of copper on the photosynthetic response of *Phaeocystis cordata*. *Photosynthesis Research*, **108**, 77-87.
- Luo, Z., Wang, Z., Xu, B., Sarakiotis, I. L., Du Laing, G. and Yan, C. (2014). Measurement and characterization of engineered titanium dioxide nanoparticles in the environment. *Journal of Zhejiang University Science A*, **15**, 593-605.
- Luo, M., Huang, Y., Zhu, M., Tang, Y., Ren, T., Ren, J., Wang, H. and Li, F. (2018). Properties of different natural organic matter influence the adsorption and aggregation behaviour of TiO₂ nanoparticles. *Journal of Saudi Chemical Society*, **22**, 146-154.
- Lupi, F., Fernandes, H. and Sa-Correia, I. (1998). Increase of copper toxicity to growth of *Chlorella vulgaris* with increase of light intensity. *Microbial Ecology*, **35**, 193-198.
- Mahmoud, W., Rastogi, T. and Kummerer, K. (2017). Application of titanium dioxide nanoparticles as a photocatalyst for the removal of micropollutants such as pharmaceuticals from water. *Current Opinion in Green and Sustainable Chemistry*, **6**, 1-10.
- Manier, N., Le Manch, S., Bado-Nilles, A. and Pascal, P. (2015). Effect of two TiO₂ nanoparticles on the growth of unicellular green algae using the OECD 201 test guideline: influence of the exposure system. *Toxicological & Environmental Chemistry*, **98**, 860-876.
- Marcel, R., Berthon, V., Castets, V., Rimet, F., Thiers, A., Frédéric, L. and Bruno, F. (2017). Modelling diatom life forms and ecological guilds for river biomonitoring. *Knowledge and*

Management of Aquatic Ecosystems, **418**, 15.

Marchello, A. E., Barreto, D. M. and Lombardi, A. T. (2018). Effects of titanium dioxide nanoparticles in different metabolic pathways in the freshwater microalga *Chlorella sorokiniana* (Trebouxiophyceae). *Water, Air, & Soil Pollution*, **229**, <https://doi.org/10.1007/s11270-018-3705-5>.

Matouke, M. M., Elewa, D. T. and Abdullahi, K. (2018). Binary effect of titanium dioxide nanoparticles (nTiO₂) and phosphorus on microalgae (*Chlorella ?Ellipsoides* Gerneck, 1907). *Aquatic Toxicology*, **198**, 40-48.

Maurer-Jones, M. A., Gunsolus, I. L., Murphy, C. J. and Haynes, C. L. (2013). Toxicity of engineered nanoparticles in the environment. *Analytical Chemistry*, **85**, 3036-3049.

Maxwell, K. and Johnson, G. N. (2000). Chlorophyll fluorescence - a practical guide. *Journal of Experimental Botany*, **51**, 659-668.

Medley, C. N. and Clements, W. H. (1998). Responses of diatom communities to heavy metals in streams: the influence of longitudinal variation. *Ecological Applications*, **8**, 631-644.

Menard, A., Drobne, D. and Jemec, A. (2011). Ecotoxicity of nanosized TiO₂. Review of in vivo data. *Environmental Pollution*, **159**, 677-684.

Mensch, A., Hernandez, R., Kuether, J., Torelli, M., Feng, Z., Hamers, R. and Pederson, J. (2017). Natural organic matter concentration impacts the interaction of functionalized diamond nanoparticles with model and actual bacterial membranes. *Environmental Science & Technology*, **51**, 11075-11084.

Metzler, D. M., Li, M., Erdem, A. and Huang, C. P. (2011). Responses of algae to photocatalytic nano-TiO₂ particles with an emphasis on the effect of particle size. *Chemical Engineering Journal*, **170**, 538-546.

Metzler, D. M., Erdem, A., Tseng, Y. H. and Huang, C. P. (2012). Responses of algal cells to engineered nanoparticles measured as algal cell population, chlorophyll a, and lipid peroxidation: effect of particle size and type. *Journal of Nanotechnology*, **2012**, <http://dx.doi.org/10.1155/2012/237284>.

Metzler, D., Erdem, A. and Huang, C. (2018). Influence of algae age and population on the response to TiO₂ nanoparticles. *International Journal of Environmental Research and Public Health*, **15** (4), <http://dx.doi.org/10.3390/ijerph15040585>.

Mezni, A., Alghool, S., Sellami, B., Saber, B. N. and Altalhi, T. (2018). Titanium dioxide nanoparticles: synthesis, characterisations and aquatic ecotoxicity effects. *Chemistry and Ecology*, **34**, 288-299.

Middepogu, A., Hou, J., Gao, X. and Lin, D. (2018). Effect and mechanism of TiO₂ nanoparticles on the photosynthesis of *Chlorella pyrenoidosa*. *Ecotoxicology and Environmental Safety*, **161**, 497-506.

- Miller, R. J., Lenihan, H. S., Muller, E. B., Tseng, N., Hanna, S. K. and Keller, A. A. (2010). Impacts of metal oxide nanoparticles on marine phytoplankton. *Environmental Science & Technology*, **44**, 7329-7334.
- Miller, R. J., Bennett, S., Keller, A. A., Pease, S. and Lenihan, H. S. (2012). TiO₂ nanoparticles are phototoxic to marine phytoplankton. *PLoS ONE*, **7**, <https://doi.org/10.1371/journal.pone.0030321>.
- Mishra, M., Arukha, A. P., Bashir, T., Yadav, D. and Prasad, G. B. K. S. (2017). All new faces of diatoms: potential source of nanomaterials and beyond. *Frontiers in Microbiology*, **8**, <http://dx.doi.org/10.3389/fmicb.2017.01239>.
- Mitra, A. and Mukhopadhyay, S. (2016). Biofilm mediated decontamination of pollutants from the environment. *AIMS Bioengineering*, **3**, 44-59.
- Morelli, E., Gabellieri, E., Bonomini, A., Tognotti, D., Grassi, G. and Corsi, I. (2018). TiO₂ nanoparticles in seawater: aggregation and interactions with the green alga *Dunaliella tertiolecta*. *Ecotoxicology and Environmental Safety*, **148**, 184-193.
- Moreno-Garrido, I., Lubían, L. M. and Soares, A. M. V. M. (2000). Influence of cellular density on determination of EC₅₀ in microalgal growth inhibition tests. *Ecotoxicology and Environmental Safety*, **47**, 112-116.
- Moreno-Garrido, I., Hampel, M., Lubían, L. and Blasco, J. (2003). Sediment toxicity tests using benthic marine microalgae *Cylindrotheca closterium* (Ehremberg) Lewin and Reimann (Bacillariophyceae). *Ecotoxicology and Environmental Safety*, **54**, 290-295.
- Moreno-Garrido, I., Pérez, S. and Blasco, J. (2015). Toxicity of silver and gold nanoparticles on marine microalgae. *Marine Environmental Research*, **111**, 60-73.
- Morin, S., Duong, T. T., Dabrin, A., Coynel, A., Herlory, O., Baudrimont, M., Delmas, F., Durrieu, G., Schafer, J., Winterton, P., Blanc, G. and Coste, M. (2008). Long-term survey of heavy-metal pollution, biofilm contamination and diatom community structure in the Riou Mort watershed, South-West France. *Environmental Pollution*, **151**, 532-542.
- Mosa, K. A., El-Naggar, M., Ramamoorthy, K., Alawadhi, H., Elnaggar, A., Wartanian, S., Ibrahim, E. and Hani, H. (2018). Copper nanoparticles induced genotoxicity, oxidative stress, and changes in superoxide dismutase (SOD) gene expression in cucumber (*Cucumis sativus*) Plants, **9**, <https://doi.org/10.3389/fpls.2018.00872>.
- Mueller, N. and Nowack, B. (2008). Exposure modeling of engineered nanoparticles in the environment. *Environmental Science & Technology*, **42**, 4447-4453.
- Murchie, E. and Lawson, T. (2013). Chlorophyll fluorescence analysis: a guide to good practice and understanding some new applications. *Journal of Experimental Botany*, **64**, 3983-3998.
- Nam, S., Kwak, J. and An, Y. (2018). Quantification of silver nanoparticle toxicity to algae

in soil via photosynthetic and flow-cytometric analyses. *Scientific Reports*, **8**, <http://dx.doi/10.1038/s41598-017-18680-5>.

Navarro, E., Baun, A., Behra, R., Hartmann, N., Filser, J., Miao, A., Quigg, A., Santschi, P. and Sigg, L. (2008). Environmental behaviour and ecotoxicity of engineered nanoparticles to algae, plants, and fungi. *Ecotoxicology*, **17**, 372-386.

Nyholm, N. (1985). Response variable in algal growth inhibition tests - Biomass or growth rate?. *Water Research*, **19**, 273-279.

OECD TG 201. (2011). Freshwater Alga and Cyanobacteria Growth Inhibition Test. Available from: <https://www.oecd-ilibrary.org/environment/test-no-201-alga-growth-inhibition-test9789264069923-en>. Accessed: 3rd February 2019.

OECD. (2018). Draft guidance document on aquatic and sediment toxicological testing of nanomaterials. Available from: <https://www.oecd.org/env/ehs/testing/DraftGD%20Aquatic%20publicsite.pdf>. Accessed: 28th March 2019.

Ozkaleli, M. and Erdem, A. (2018). Biototoxicity of TiO₂ nanoparticles on *Raphidocelis subcapitata* microalgae exemplified by membrane deformation. *International Journal of Environmental Research and Public Health*, **15**, <http://dx.doi/10.3390/ijerph15030416>.

Passy, S. I. (2007). Diatom ecological guilds display distinct and predictable behaviour along nutrient and disturbance gradients in running waters. *Aquatic Botany*, **86**, 171-178.

Perdue, E. and Ritchie, J. (2003). Surface and Ground Water, Weathering, and Soils, Treatise on Geochemistry. In: Drever, J. I., Holland, H. D., Turekian, K. K. (Eds.), Elsevier-Pergamon, Oxford, 273-318.

Pérez, G. L., Torremorell, A., Mugni, H., Rodríguez, P., Solange Vera, M., do Nascimento, M., Allende, L., Bustingorry, J., Escaray, R., Ferraro, M., Izaguirre, I., Pizarro, H., Bonetto, C., Morris, D. P. and Zagarese, H. (2007). Effects of the herbicide Roundup on freshwater microbial communities: a mesocosm study. *Ecological Applications*, **17**, 2310-2322.

Perkins, R., Mouget, J., Lefebvre, S. and Lavaud, J. (2006). Light response curve methodology and possible implications in the application of chlorophyll fluorescence to benthic diatoms. *Marine Biology*, **149**, 703-712.

Piccino, F., Gottschalk, F. and Seeger, S. (2012). Industrial production quantities and uses of ten engineered nanomaterials in Europe and the world. *Journal of Nanoparticle Research*, **14**, <http://dx.doi/10.1007/s11051-012-1109-9>.

Raj, S., Jose, S., Sumod, U. S. and Sabitha, M. (2012). Nanotechnology in cosmetics: opportunities and challenges. *Journal of Pharmacy and Bioallied Sciences*, **4**, 186-193.

Rasmussen, K., Gonzalez, M., Kearns, P., Sintes, J. R., Rossi, F. and Sayre, P. (2016). Review of achievements of the OECD Working Party of Manufactured Nanomaterials? Testing and Assessment Programme. From exploratory testing to test guidelines. *Regulatory Toxi-*

cology and Pharmacology, **74**, 147-160.

Rimet, F., Ector, L., Cauchie, H. and Hoffmann, L. (2009). Changes in diatom-dominated biofilms during simulated improvements in water quality: implications for diatom-based monitoring in rivers. *European Journal of Phycology*, **44**, 567-577.

Rimet, F. and Bouchez, A. (2011). Use of diatom life-forms and ecological guilds to assess pesticide contamination in rivers: lotic mesocosm approaches. *Ecological Indicators*, **11**, 489-499.

Ritchie, R. (2006). Consistent sets of spectrophotometric chlorophyll equations for acetone, methanol and ethanol solvents. *Photosynthesis Research*, **89**, 27-41.

Romani, A. and Sabater, S. (2001). Structure and activity of rock and sand biofilms in a Mediterranean stream. *Ecology*, **82**, 3232-3245.

Romer, I., Gavin, A. J., White, T. A., Merrifield, R. C., Chipman, J. K., Viant, M. R. and Lead, J. R. (2013). The critical importance of defined media conditions in *Daphnia magna* nanotoxicity studies. *Toxicology Letters*, **223**, 103-108.

Sabater, S., Guasch, H., Romani, A. and Muñoz, I. (2002). The effect of biological factors on the efficiency of river biofilms in improving water quality. *Hydrobiologia*, **469**, 149-156.

Sabater, S., Guasch, H., Ricart, M., Romani, A., Vidal, G., Klunder, C. and Schmitt-Jansen, M. (2007). Monitoring the effect of chemicals on biological communities. The biofilm as an interface. *Analytical and Bioanalytical Chemistry*, **387**, 1425-1434.

Sabater S. and Borrego C. (2015) Application of microcosm and mesocosm experiments to pollutant effects in biofilms. In: McGenity T., Timmis K., Nogales B. (eds) Hydrocarbon and Lipid Microbiology Protocols. Springer Protocols Handbooks. Springer, Berlin, Heidelberg.

Sabater, S., Timoner, X., Borrego, C. and Acuna, V. (2016). Stream biofilm responses to flow intermittency: from cells to ecosystems. *Frontiers in Environmental Science*, **4**, <http://doi.org/10.3389/fenvs.2016.00014>.

Sadiq, I., Dalai, S., Chandrasekaran, N. and Mukherjee, A. (2011). Ecotoxicity study of titania (TiO₂) NPs on two microalgae species: *Scenedesmus sp.* and *Chlorella sp.* *Ecotoxicology and Environmental Safety*, **74**, 1180-1187.

Sanchez-Quiles, D. and Tovar-Sanchez, A. (2014). Sunscreens as a source of hydrogen peroxide production in coastal waters. *Environmental Science & Technology*, **48**, 9037-9042.

Sayes, C., Wahi, R., Kurian, P., Liu, Y., West, J., Ausman, K., Warheit, D. and Colvin, V. (2006). Correlating nanoscale titania structure with toxicity: a cytotoxicity and inflammatory response study with human dermal fibroblasts and human lung epithelial cells. *Toxicological Sciences*, **92**, 174-185.

Schoeman, F. R., Archibald, R. E. M. and Barlow, D. J. (1976). Structural observations and notes on the freshwater diatom *Navicula pelliculosa* (Brebisson ex Kützing) Hilse. *British Phycological Journal*, **11**, 251-263.

Seguin, F., Le Bihan, F., Leboulanger, C. and Berard, A. (2002). A risk assessment of pollution: induction of atrazine tolerance in phytoplankton communities in freshwater outdoor mesocosms, using chlorophyll fluorescence as an endpoint. *Water Research*, **36**, 3227-3236.

Seitz, F., Luderwald, S., Rosenfeldt, R., Schulz, R. and Bundschuh, M. (2015). Aging of TiO₂ Nanoparticles transiently increases their toxicity to the pelagic microcrustacean *Daphnia magna*. *PLOS ONE*, **10**, <http://doi.org/10.1371/journal.pone.0126021>.

Sekar, R., Nair, K. V. K., Rao, V. N. R. and Venugopalan, V. P. (2002). Nutrient dynamics and successional changes in a lentic freshwater biofilm. *Freshwater Biology*, **47**, 1365-2427.

Sendra, M., Moreno-Garrido, I., Yeste, M., Gatica, J. and Blasco, J. (2017). Toxicity of TiO₂, in nanoparticle or bulk form to freshwater and marine micro algae under visible light and UV-A radiation. *Environmental Pollution*, **227**, 39-48.

Serodio, J., Vieira, S., Cruz, S. and Coelho, H. (2006). Rapid light-response curves of chlorophyll fluorescence in microalgae: relationship to steady-state light curves and non-photochemical quenching in benthic diatom-dominated assemblages. *Photosynthesis Research*, **90**, 29-43.

Shah, S. N. A., Shah, Z., Hussain, M. and Khan, M. (2017). Hazardous effects of titanium dioxide nanoparticles in ecosystem. *Bioinorganic Chemistry and Applications*, **2017**, <http://doi.org/10.1155/2017/4101735>.

Shamshad, I., Khan, S., Waqas, M., Asma, M., Nawab, J., Gul, N., Raiz, A. and Li, G. (2016). Heavy metal uptake capacity of fresh water algae (*Oedogonium westii*) from aqueous solution: A mesocosm research. *International Journal of Phytoremediation*, **18**, 393-398.

Sharma, V. (2009). Aggregation and toxicity of titanium dioxide nanoparticles in aquatic environment? A Review. *Journal of Environmental Science and Health*, **44**, 1485-1495.

Sharma, P., Jha, A., Dubey, R. and Pessarakli, M. (2012). Reactive oxygen species, oxidative damage, and antioxidative defense mechanism in plants under stressful conditions. *Journal of Botany*, **2012**, 1-26.

Shevlin, D., O'Brien, N. and Cummins, E. (2018). Silver engineered nanoparticles in freshwater systems ? likely fate and behaviour through natural attenuation processes. *Science of the Total Environment*, **621**, 1033-1046.

Shi, H., Magaye, R., Castranova, V. and Zhao, J. (2013). Titanium dioxide nanoparticles: a review of current toxicological data. *Particle and Fibre Toxicology*, **10**, <http://doi.org/10.1186/1743-8977-10-15>.

Sládeček, V. (1986). Diatoms as indicators of organic pollution. *Acta hydrochimica et hydrobiologica*, **14**, <http://doi.org/10.1002/aheh.19860140519>.

Smijs, T. G. and Pavel, S. Titanium dioxide and zinc oxide nanoparticles in sunscreens: focus on their safety and effectiveness. *Nanotechnology, Science and Applications*, **4**, 95-112.

Smolyakov, B., Ryzhikh, A. and Romanov, R. (2010). The fate of Cu, Zn, and Cd in the initial stage of water system contamination: the effect of phytoplankton activity. *Journal of hazardous materials*, **184**, 819-825.

Smulders, S., Luyts, K., Brabants, G., Landuyt, K., Kirschhock, C., Smolders, E., Golan-ski, L., Vanoirbeek, J. and Hoet, P. (2014). Toxicity of nanoparticles embedded in paints compared with pristine nanoparticles in mice. *Toxicological Sciences*, **114**, 132-140.

Sorensen, S. N. and Baun, A. (2015). Controlling silver nanoparticle exposure in algal toxicity testing - a matter of timing. *Nanotoxicology*, **9**, 201-209.

Suman, T. Y., Rajasree, S. R. R. and Kirubakaran, R. (2015). Evaluation of zinc oxide nanoparticles toxicity on marine alga *Chlorella vulgaris* through flow cytometric, cytotoxicity and oxidative stress analysis. *Ecotoxicology and Environmental Safety*, **113**, 23-30.

Sutherland, I. W. (2001). Biofilm exopolysaccharides: a strong and sticky framework. *Microbiology*, **147**, <http://doi.org/10.1099/00221287-147-1-3>.

Tang, Z. and Cheng, T. (2018). Stability and aggregation of nanoscale titanium dioxide particle (nTiO₂): effect of cation valence, humic acid, and clay colloids. *Chemosphere*, **192**, 51-58.

Tang, Y., Xin, H., Yang, F. and Long, X. (2018a). A historical review and bibliometric analysis of nanoparticles toxicity on algae. *Journal of Nanoparticle Research*, **20**, <https://doi.org/10.1007/s11051-018-4196-4>.

Tang, J., Zhu, N., Zhu, Y., Zamir, S. M. and Wu, Y. (2018b). Sustainable pollutant removal by periphytic biofilm via microbial composition shifts induced by uneven distribution of CeO₂ nanoparticles. *Bioresource Technology*, **248**, 75-81.

Teitzel, G. and Parsek, M. (2003). Heavy metal resistance of biofilm and planktonic *Pseudomonas aeruginosa*. *Applied and Environmental Microbiology*, **69**, 2313-2320.

Tella, M., Auffan, M., Brousset, L., Morel, E., Proux, O., Chaneac, C., Angeletti, B., Pailles, C., Artells, E., Santaella, C., Rose, J., Thiery, A. and Bottero, J. Y. (2015). Chronic dosing of a simulated pond ecosystem in indoor aquatic mesocosms: fate and transport of CeO₂ nanoparticles. *Environmental Science: Nano*, **2**, 653-663.

Tovar-Sanchez, A., Sanchez-Quiles, D., Basterretxea, G., Benede, J. L., Chisvert, A., Salvador, A., Moreno-Garrido, I. and Blasco, J. (2013). Sunscreen products as emerging pollutants to coastal waters. *PLoS One*, **8**, <http://doi.org/10.1371/journal.pone.0065451>.

United States Environmental Protection Agency. Reviewing New Chemicals under the Toxic Substances Control Act (TSCA). Available at: <https://www.epa.gov/reviewing-new-chemicals-under-toxic-substances-control-act-tsca/control-nanoscale-materials-under>. Accessed: March 28th 2019.

U.S. Environmental Protection Agency. (1994). Short-term methods for estimating the chronic toxicity of effluents and receiving water to freshwater organisms. EPA 600/7-91-002. Washington, DC.

Vale, G., Mehennaoui, K., Cambier, S., Libralato, G., Jomini, S. and Domingos, R. (2016). Manufactured nanoparticles in the aquatic environment-biochemical responses on freshwater organisms: A critical overview. *Aquatic Toxicology*, **170**, 162-174.

Vance, M., Kuiken, T., Vejerano, E., McGinnis, S., Hochella, M., Rejeski, D. and Hull, M. (2015). Nanotechnology in the real world: redeveloping the nanomaterial consumer products inventory. *Beilstein Journal of Nanotechnology*, **6**, 1769-1780.

Van Driel, B., Kooyman, P., van den Berg, K., Schmidt-Ott, A. and Dik, K. (2016). A quick assessment of the photocatalytic activity of TiO₂ pigments ? From lab to conservation studio!. *Microchemical Journal*, **126**, 162-171.

Verneuil, L., Silvestre, J., Mouchet, F., Flahaut, E., Boutonnet, J., Bourdiol, F., Bortolamiol, T., Baqué, D., Gauthier, L. and Pinelli, E. (2015). Multi-walled carbon nanotubes, natural organic matter, and the benthic diatom *Nitzschia palea*: "A sticky story". *Nanotoxicology*, **9**, 219-229.

Villeneuve, A., Montuelle, B. and Bouchez, A. (2011). Effects of flow regime and pesticides on periphytic communities: evolution and role of biodiversity. *Aquatic Toxicology*, **102**, 123-133.

Wang, J., Zhang, X., Chen, Y., Sommerfeld, M. and Hu, Q. (2008). Toxicity assessment of manufactured nanomaterials using the unicellular green alga *Chlamydomonas reinhardtii*. *Chemosphere*, **73**, 1121-1128.

Wang, Y., Zhu, X., Lao, Y., Lv, X., Tao, Y., Huang, B., Wang, J., Zhou, J. and Cai, Z. (2016). TiO₂ nanoparticles in the marine environment: physical effects responsible for the toxicity on algae *Phaeodactylum tricornutum*. *Science of The Total Environment*, **565**, 818-826.

Wang, Z., Luo, Z. and Yan, Y. (2018). Dispersion and sedimentation of titanium dioxide nanoparticles in freshwater algae and daphnia aquatic culture media in the presence of arsenate. *Journal of Experimental Nanoscience*, **13**, 119-129.

Warheit, D. B. and Brown, S. C. (2019). What is the impact of surface modifications and particle size on commercial titanium dioxide particle samples?. A review of in vivo pulmonary and oral toxicity studies. *Toxicology Letters*, **302**, 42-59.

Westerhoff, P., Song, G., Hristovski, K. and Kiser, M. (2011). Occurrence and removal of

titanium at full scale wastewater treatment plants: implications for TiO₂ nanomaterials. *Journal of Environmental Monitoring*, **13**, <http://doi.org/10.1039/c1em10017c>.

Wong, C. Y., Teoh, M. L., Phang, S., Lim, P. and Beardall, J. (2015). Interactive effects of temperature and UV radiation on photosynthesis of *Chlorella* strains from polar, temperate and tropical environments: differential impacts on damage and repair. *PLoS ONE*, **10**, <https://doi.org/10.1371/journal.pone.0139469>.

Wright, M., Matson, C., Baker, L., Castellon, B., Watkins, P. and King, R. (2018). Titanium dioxide nanoparticle exposure reduces algal biomass and alters algal assemblage composition in wastewater effluent-dominated stream mesocosms. *Science of The Total Environment*, **626**, 357-365.

Wu, H., Jiang, H., Liu, C. and Deng, Y. (2015). Growth, pigment composition, chlorophyll fluorescence and antioxidant defenses in the red alga *Gracilaria lemaneiformis* (Gracilariaceae, Rhodophyta) under light stress. *South African Journal of Botany*, **100**, 27-32.

Xia, B., Chen, B., Sun, X., Qu, K., Ma, F. and Du, M. (2015). Interaction of TiO₂ nanoparticles with the marine microalga *Nitzschia closterium*: Growth inhibition, oxidative stress and internalization. *Science of The Total Environment*, **508**, 525-533.

Xu, H., Pan, J., Zhang, H. and Yang, L. (2016). Interactions of metal oxide nanoparticles with extracellular polymeric substances (EPS) of algal aggregates in an eutrophic ecosystem. *Ecological Engineering*, **94**, 464-470.

Xu, F. (2018). Review of analytical studies on TiO₂ nanoparticles and particle aggregation, coagulation, flocculation, sedimentation, stabilization. *Chemosphere*, **212**, 662-677.

Yallop, M. and Kelly, M. (2006). From pattern to process: understanding stream phyto-benthic assemblages and implications for determining ecological status. *Nova Hedwigia*, **130**, 357-372.

Zhang, Y., Leu, Y., Aitken, R. J. and Riediker, M. (2015). Inventory of engineered nanoparticle-containing consumer products available in the Singapore retail market and likelihood of release into the aquatic environment. *International Journal of Environmental Research*, **12**, 8717-8743.

Zhang, C., Lohwacharin, J. and Takizawa, S. (2017). Properties of residual titanium dioxide nanoparticles after extended periods of mixing and settling in synthetic and natural waters. *Scientific Reports*, **7** (1), <http://doi.org/10.1038/s41598-017-09699-9>.

Zhu, M., Wang, H., Keller, A., Wang, T. and Li, F. (2014). The effect of humic acid on the aggregation of titanium dioxide nanoparticles under different pH and ionic strengths. *Science of The Total Environment*, **487**, 375-380.